European air quality maps of PM and ozone for 2013 and their uncertainty

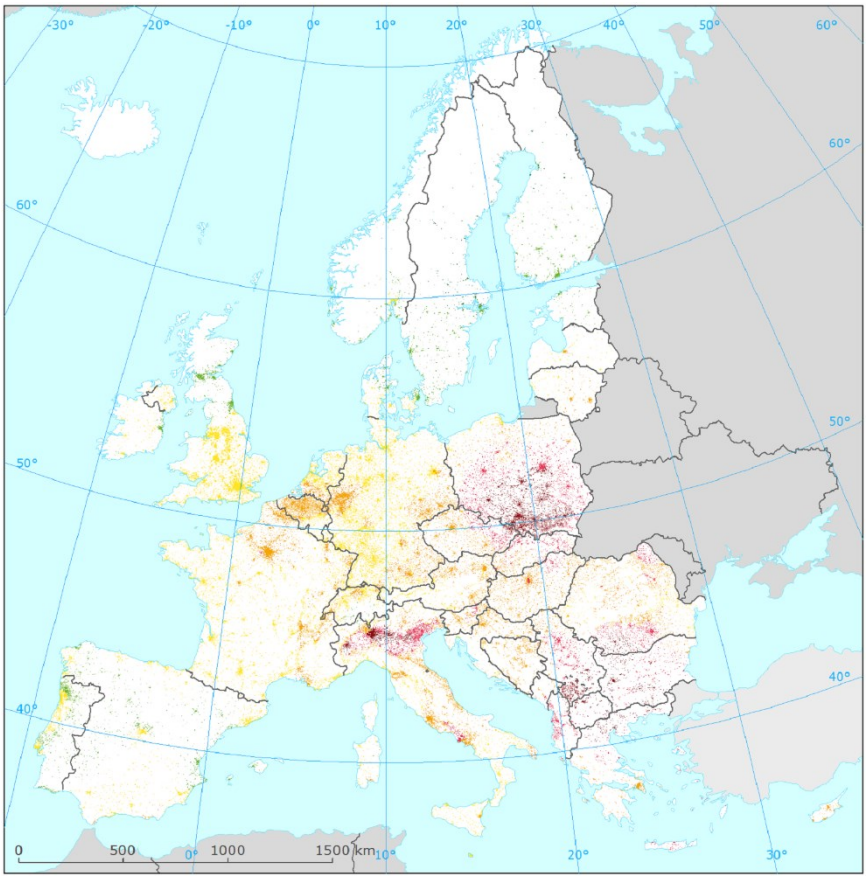

ETC/ACM Technical Paper 2015/5
March 2016

Jan Horálek, Peter de Smet, Pavel Kurfürst,
Frank de Leeuw, Nina Benešová

European Topic Centre
on Air Pollution and
Climate Change Mitigation

The European Topic Centre on Air Pollution and Climate Change Mitigation (ETC/ACM)
is a consortium of European institutes under contract of the European Environment Agency
RIVM Aether CHMI CSIC EMISIA INERIS NILU ÖKO-Institut ÖKO-Recherche PBL UAB UBA-V VITO 4Sfera

Front page picture:
Urban background concentration map of $PM_{2.5}$ annual average for the year 2013. Spatially interpolated concentration field in the urban areas. Units: µg.m^{-3}. (Figure A1.3 of this paper.)

Author affiliation:
Jan Horálek, Pavel Kurfürst, Nina Benešová: Czech Hydrometeorological Institute (CHMI), Prague, Czech Republic
Peter de Smet, Frank de Leeuw: National Institute for Public Health and the Environment (RIVM), Bilthoven, The Netherlands

Refer to this document as:
Horálek J, De Smet P, Kurfürst P, De Leeuw F, Benešová N (2016). European air quality maps of PM and ozone for 2013 and their uncertainty. ETC/ACM Technical paper 2015/5. http://acm.eionet.europa.eu/reports/ETCACM_TP_2015_5_AQMaps2013

DISCLAIMER

ETC/ACM Technical Paper 2015/5
European Topic Centre on Air and Climate Change Mitigation
PO Box 1
3720 BA Bilthoven
The Netherlands
Phone +31 30 2748562
Fax +31 30 2744433
Email etcacm@rivm.nl
Website http://acm.eionet.europa.eu/

Contents

1 Introduction

This paper provides an update of European air quality concentration maps, probabilities of exceeding relevant thresholds and population exposure estimates for 2013. The analysis is based on interpolation of annual statistics of monitoring data from 2013, reported by EEA member and cooperating countries in 2014. The paper presents mapping results and includes an uncertainty analysis of the interpolated maps, adopting the latest methodological developments of Horálek et al. (2007, 2008, 2010, 2013, 2014a, 2015), De Smet et al. (2009, 2010, 2011, 2012) and Denby et al. (2011b, 2011c).

We again consider in this paper PM_{10}, $PM_{2.5}$ and ozone as being the most relevant pollutants for annual updating. The analysis method for the year 2013 was similar to that for the previous years. In this paper, we summarise the updates applied to the 2013 data.

The mapping method is based primarily on air quality measurements. It combines monitoring data, chemical transport model results and other supplementary data (altitude, meteorology). The method is a linear regression model followed by kriging of the residuals produced from that model (residual kriging).

The maps of health related indicators of PM_{10}, $PM_{2.5}$ and ozone are created for the rural and urban background areas separately on a grid at 10x10 km resolution. Subsequently to this, the rural and urban background maps are merged into one combined air quality indicator map using a population density grid at 1x1 km resolution. We also derive the population exposure estimates on basis of this 1 x 1 km grid resolution, as it accounts better for the smaller urbanisations in the European context that are not resolved at the 10 x 10 km grid resolution. At the European scale, we present the final combined maps at 1x1 km grid resolution on aggregated maps at 10x10 km grid resolution. The maps of vegetation related ozone indicators are on a grid at 2x2 km resolution, based on rural background measurements and serve as input to EEA core indicator CSI005.

Next to the annual indicator maps, we present in tables the population exposure to PM_{10}, $PM_{2.5}$ and ozone and the exposure of vegetation to ozone. Tables of population exposure are prepared using combined final maps and the population density map of 1x1 km grid resolution. The tables of the vegetation exposure are prepared with a 2x2 km grid resolution based on the Corine Land Cover 2006.

For all the maps, we include a quantitative estimate of their interpolation uncertainty, using cross-validation parameters and scatter-plots. In addition, the paper contains the maps with probability estimates of limit/target value exceedances.

Apart of the maps and exposure tables for 2013, we present the inter-annual difference maps and the exposure tables showing the evolution of population-weighted concentration in the last nine years.

Chapter 2 describes briefly the used methodology. Chapter 3 documents the updated input data. Chapters 4, 5 and 6 present the calculations, the mapping, the exposure estimates and the uncertainty results for PM_{10}, $PM_{2.5}$ and ozone respectively. Chapter 7 summarizes the conclusions on exposure estimates and the interpolation uncertainties involved with the mapping of the air pollutant indicators. Annex 1 presents separate urban background maps for urbanised areas only, aimed to better visualise the urban background concentration levels, without the influence of the dominating pattern of extended rural areas.

Dealing with the annual indicator data, one should take into account the data coverage. For the x-th highest values (i.e. for the PM_{10} indicator 36^{th} highest daily mean and for the ozone indicator 26^{th} highest daily maximum 8-hour mean), no correction for missing data has been applied so far. The most straightforward way to solve the missing data issue in these cases is to use the percentiles instead of the x-th highest values. The maps and tables for the percentile indicators are presented in Annex 2.

According to the current mapping procedure, the interpolated maps for year Y-2 are available by end of November of year Y. Typically, the critical factor on its timing is the availability of the EMEP model results for year Y-2 by August/September of year Y only. However, the preliminary version of the EMEP model for year Y-2 based on emission for year Y-3 is available just in autumn of year Y-1. Potential use of such a model version in the mapping would enable the maps are ready just around June of year Y, in time to be included in EEAs' annual Air Quality reports. Annex 3 examines the possible use of such a version of the EMEP model results in the mapping.

2 Used methodology

2.1 Mapping method

Previous technical papers prepared by the ETC/ACM, resp. ETC/ACC (Technical Papers 2014/4, 2013/13, 2012/12, 2011/11, 2011/5, 2010/10, 2010/9, 2009/16, 2009/9, 2008/8, 2007/7, 2006/6, 2005/8, 2005/7) discuss methodological developments and details on spatial interpolations and their uncertainties. No changes took place in the methodology in comparison with the five preceding reports (Horálek et al., 2015 and references cited therein), respectively with the $PM_{2.5}$ mapping methodology paper (Denby et al., 2011c). In this chapter a summary on the currently applied method is given. The evaluation of this mapping method using FAIRMODE Delta tool is presented in Horálek et al. (2016).

2.1.1 Pseudo $PM_{2.5}$ station data estimation

To supplement measured $PM_{2.5}$ data, in the mapping procedure we also use data from so-called *pseudo $PM_{2.5}$ stations*. These data are the estimates of $PM_{2.5}$ concentrations at the locations of PM_{10} stations with no $PM_{2.5}$ measurement. These estimates are based on measured PM_{10} data and different supplementary data, using linear regression:

$$\hat{Z}_{PM2.5}(s) = c + b.Z_{PM10}(s) + a_1.X_1(s) + ... + a_n.X_n(s) + \varepsilon(s) \quad (2.1)$$

where $\hat{Z}_{PM2.5}(s)$ is the estimated value of $PM_{2.5}$ at the station s,
$Z_{PM10}(s)$ is the measured value of PM_{10} at the station s,
$X_1(s), ..., X_n(s)$ are the values of other supplementary variables at the station s,
$c, b, a_1, ..., a_n$ are the parameters of the linear regression model calculated based on the data at the points of measuring stations with both $PM_{2.5}$ and PM_{10} measurements,
n is the number of other supplementary variables used in the linear regression model (apart from PM_{10}).

When applying this estimation method, rural and urban/suburban background stations are handled together. For details, see Denby et al. (2011c).

2.1.2 Interpolation

The mapping method used is a linear regression model followed by kriging of the residuals produced from that model (residual kriging). Interpolation is therefore carried out according to the relation:

$$\hat{Z}(s_0) = c + a_1.X_1(s_0) + a_2.X_2(s_0) + ... + a_n.X_n(s_0) + \eta(s_0) \quad (2.2)$$

where $\hat{Z}(s_0)$ is the estimated value of the air pollution indicator at the point s_o,
$X_1(s_0), X_2(s_0), ..., X_n(s_0)$ are the n number of individual supplementary variables at the point s_o
$c, a_1, a_2, ..., a_n$ are the $n+1$ parameters of the linear regression model calculated based on the data at the points of measurement,
$\eta(s_0)$ is the spatial interpolation of the residuals of the linear regression model at the point s_o calculated based on the residuals at the points of measurement.

For different pollutants and area types (rural, urban), different supplementary data are used, depending on their improvement to the fit of the regression. Ordinary kriging is used to interpolate the residuals:

$$\hat{R}(s_0) = \sum_{i=1}^{N} \lambda_i R(s_i), \ \sum_{i=1}^{N} \lambda_i = 1, \quad (2.3)$$

where $R(s_i)$ are the residuals in the points of the measuring stations s_i,
$\lambda_1, ..., \lambda_N$ are the weights estimated based on variogram,
N is the number of the stations used in the interpolation.

The variogram (as a measure of a spatial correlation) is estimated using a spherical function (with parameters *nugget, sill, range*). For details, see Horálek et al. (2007), Section 2.3.5 and Cressie (1993).

For $PM_{2.5}$, both measurement data and the estimated data from the pseudo $PM_{2.5}$ stations are used.

For the PM_{10} and $PM_{2.5}$ indicators we apply, prior to linear regression and interpolation, a logarithmic transformation to measurement and EMEP model concentrations. In the case of $PM_{2.5}$ rural map creation, population density is also log-transformed. After interpolation, we apply a back-transformation. For details, see De Smet et al. (2011) and Denby et al. (2008). In the case of urban background $PM_{2.5}$ map, we do not use any supplementary data – we apply just lognormal kriging.

For the vegetation related indicators (AOT40 for crops and forests) we only construct rural maps based on rural background stations, based on the assumption that no vegetation is located in urban areas. For the health related indicators, we construct the rural and urban background maps separately and then we merge them.

2.1.3 Merging of rural and urban background maps

Health related indicator maps are constructed (using linear regression with kriging of its residuals) for the rural and urban background areas separately on a grid at 10x10 km resolution. The rural map is based on rural background stations and the urban background map on urban and suburban background stations. Subsequent to this, the rural and urban background maps are merged into one combined air quality indicator map using a European-wide population density grid at 1x1 km resolution. For the 1x1 km grid cells with a population density less than a defined value of α_1, we select the rural map value and for grid cells with a population density greater than a defined value α_2, we select the urban background map value. For areas with population density within the interval (α_1, α_2) a weighting function of α_1 and α_2 is applied (for details and the setting of the parameters α_1 and α_2, see Horálek et al., 2010, 2007 and 2005). This applies to the grid cells where the estimated rural value is lower (PM_{10} and $PM_{2.5}$) or higher (ozone), than the estimated urban background map value. In the exceptional cases when this criterion does not hold, we apply a joint urban/rural map (created using all background stations regardless their type), as far as its value lies in between the rural and urban background map value. For details, see De Smet et al. (2011).

Summarising, the separate rural, urban and joint urban/rural maps are constructed at a resolution of 10x10 km; their merging however takes place on basis of the 1x1 km resolution population density grid, resulting in a final combined pollutant indicator map on this 1x1 km resolution grid. This map is used for the population exposure estimates. We refer to the applied chain of optimised combinations of spatial resolutions, the process of *interpolation -> merging -> exposure estimate*, as the '10-1-1' (in km). For presentational purposes of European map illustrations, a spatial aggregation to 10x10 km resolution is sufficient and as such applied in this paper.

In all calculations and map presentations the EEA standard projection and datum defined as EEA ETRS89-LAEA5210 is used. The interpolation and mapping domain consists of the areas of all EEA member and cooperating countries, as far as they fall into the EEA map extent *Map_1c* (EEA, 2011). The mapping domain covers the whole Europe apart from Belarus, Moldova, Ukraine and the European parts of Russia and Kazakhstan.

For further details and discussion on subjects briefly addressed in this section, refer to De Smet et al. (2011), chapter 2.

2.2 Calculation of population and vegetation exposure

Population and vegetation exposure estimates are based on the interpolated concentration maps, population density data and land cover data.

2.2.1 Population exposure

Population exposure for individual countries and for Europe as a whole is calculated from the air quality maps and population density data, both at 1x1 km resolution. For each concentration class, the total population per country as well as the European-wide total is determined. In addition, we express per-country and European-wide exposure as the population-weighted concentration, i.e. the average concentration weighted according to the population in a grid cell:

$$\hat{c} = \frac{\sum_{i=1}^{N} c_i p_i}{\sum_{i=1}^{N} p_i} \tag{2.4}$$

where $\hat{c}$ is the population-weighted average concentration in the country or in the whole Europe,
p_i is the population in the i^{th} grid cell,
c_i is the concentration in the i^{th} grid cell,
N is the number of grid cells in the country or in Europe as a whole.

2.2.2 Vegetation exposure

Vegetation exposure for individual countries and for Europe as a whole is calculated based on the air quality maps and land cover data, both in 2x2 km grid resolution. For each concentration class, the total vegetation area per country as well as European-wide is determined.

2.3 Methods for uncertainty analysis

The uncertainty estimation of the European map is based on cross-validation. The cross-validation method computes the quality of the spatial interpolation for each measurement point from all available information except from the point in question, i.e. it withholds one data point and then makes a prediction at the spatial location of that point. This procedure is repeated for all measurement points in the available set. The predicted and measured values at these points are plotted in the form of a scatter plot. With help of statistical indicators the quality of the predictions is demonstrated objectively. The advantage of the nature of this cross-validation technique is that it enables evaluation of the quality of the predicted values at locations without measurements, as long as they are within the area covered by the measurements.

In addition, we make a simple comparison between the point measurements and interpolated values of the 10x10 km grid (or the 2x2 km grid in the case of AOT40). Where the 10x10 km grid is used, the grid value is the averaged result of the 1x1 km interpolations in each 10 x 10 km grid area. The interpolated value within a grid cell will only approximate the predicted value(s) at the station(s) lying within that cell.

Another method to estimate uncertainties is based on geostatistical theory: together with the prediction, the prediction standard error is computed at all the grid cells, which represents in fact the interpolation uncertainty map (see Cressie, 1993 for a detailed discussion). Based on the concentration and the uncertainty map, the exceedance probability map is created (Section 2.3.3).

2.3.1 Cross-validation

The results of cross-validation are described by the statistical indicators and scatter plots. The main indicator used is root mean squared error (RMSE) and additional is bias (mean prediction error, MPE):

$$RMSE = \sqrt{\frac{1}{N}\sum_{i=1}^{N}(\hat{Z}(s_i) - Z(s_i))^2} \tag{2.5}$$

$$bias(MPE) = \frac{1}{N}\sum_{i=1}^{N}(\hat{Z}(s_i) - Z(s_i)) \tag{2.6}$$

where $Z(s_i)$ is the air quality indicator value derived from the measured concentration at the i^{th} point, $i = 1, \ldots, N$,
$\hat{Z}(s_i)$ is the air quality estimated indicator value at the i^{th} point using other information, without the indicator value derived from the measured concentration at the i^{th} point,
N is the number of the measuring points.

Next to the RMSE expressed in the absolute units, one could express this uncertainty in relative terms by relating the RMSE to the mean of the air pollution indicator value for all stations:

$$RRMSE = \frac{RMSE}{\bar{Z}}.100 \qquad (2.7)$$

where $RRMSE$ is the relative RMSE, expressed in percent,

$\bar{Z}$ is the arithmetic average of the indicator values $Z(s_1), \ldots, Z(s_N)$, as derived from measurement concentrations at the station points $i = 1, \ldots, N$.

Other indicators are R^2 and the regression equation parameters *slope* and *intercept*, following from the scatter plot between the predicted (using cross-validation) and the observed concentrations

RMSE should be as small as possible, bias (MPE) should be as close to zero as possible, R^2 should be as close to *1* as possible, slope *a* should be as close to *1* as possible, and intercept *c* should be as close to zero as possible (in the regression equation $y = a.x + c$).

In the cross-validation of $PM_{2.5}$, only stations with measured $PM_{2.5}$ data are used (not the pseudo $PM_{2.5}$ stations).

2.3.2 Comparison of the point measured and interpolated grid values

The comparison of measured and predicted grid values is described by the linear regression equation and its parameters and statistical values. The comparison is executed separately for rural and urban background maps. In the case of $PM_{2.5}$, only the stations with actual measured $PM_{2.5}$ data are used (not the pseudo $PM_{2.5}$ stations).

The point observation – point cross-validation prediction analysis (Section 2.3.1) describes interpolation performance at point locations when there is no observation (as it follows the leave-one-out approach). In this case, the smoothing effect of the interpolation is most prevalent.

The point observation – grid prediction approach indicates performance of the value for the 10x10 km (resp. 1x1 km or 2x2 km) grid cell with respect to the observations that are located within that cell. As such, some variability is due to smoothing but it also includes smoothing due to spatial averaging into the 10x10 km (resp. 1x1 km or 2x2 km) grid cells. Therefore, the point-grid approach tells us how well our interpolated and aggregated values approximate the measurements at the actual stations locations. Whereas, the point-point approach tells us how well our interpolated values estimate the indicator when there are no measurements at a location (under the constrained that it is within the area covered by measurements).

2.3.3 Exceedance probability mapping

The maps with the probability of exceedance (PoE) of a specific threshold value (e.g. limit or target value) are constructed using the concentration and uncertainty maps:

$$PoE(x) = 1 - \Phi\left(\frac{LV - C_c(x)}{\delta_c(x)}\right) \qquad (2.6)$$

where $PoE(x)$ is the probability of limit/target value (*LV/TV*) exceedance in the grid cell *x*,

$\Phi(\,)$ is the cumulative distribution function of the normal distribution,

LV is the limit or target value of the relevant indicator,

$C_c(x)$ is the interpolated concentration in the grid cell *x*,

$\delta_c(x)$ is the standard error of the estimation in the grid cell *x*.

The standard error of the probability map of the combined (rural and urban background) map is calculated from the standard errors of the separate rural and urban background maps; see Horálek et al. (2008), Section 2.3 and De Smet et al. (2011), Chapter 2. The maps with the probability of threshold value exceedance (PoE) are constructed in 10 x 10 km grid resolution.

3 Input data

The types of input data in this paper are not different from that of Horálek et al. (2015). The air quality, meteorological and where possible, the supplementary data has been updated. No further changes in selecting and processing of the input data have been implemented. For readability of this paper, we reproduce here the list of the input data. The key data is the air quality measurements at the monitoring stations extracted from AirBase, including geographical coordinates (*latitude*, *longitude*). The supplementary data cover the whole mapping domain and are converted into the EEA reference projection ETRS89-LAEA5210 on a 10 x 10 km grid resolution. The data for the AOT40 maps, however, we converted – like last year – into a 2 x 2 km resolution to allow accurate land cover exposure estimates to be prepared for use in Core Set Indicator 005 of the EEA.

3.1 Air quality monitoring data

Air quality station monitoring data for the relevant year are extracted from the Air Quality e-Reporting database, from so-called 'frozen set', EEA (2015a). The set was supplemented by 104 Italian stations (of different types), which were uploaded to the Air Quality e-Reporting database at a later stage and were provided internally by the EEA in the file 'Airbase_format_stat_subselect.txt'. Next to this, this data set is supplemented by several rural stations from the database EBAS (NILU, 2015) not reported to the Air Quality e-Reporting database. Only data from stations classified by the Air Quality e-Reporting database and/or EBAS of the type *background* for the areas *rural*, *suburban* and *urban* are used. *Industrial* and *traffic* station types are not considered; they represent local scale concentration levels not applicable at the mapping resolution employed. The following substances and their indicators are considered:

PM_{10} – annual average [µg.m^{-3}], year 2013
– 36th highest daily average value [µg.m^{-3}], year 2013
– 90.4th percentile of daily average values [µg.m^{-3}], year 2013

$PM_{2.5}$ – annual average [µg.m^{-3}], year 2013

Ozone – 26th highest daily maximum 8-hour average value [µg.m^{-3}], year 2013
– 93.2nd percentile of daily maximum 8-hour average values [µg.m^{-3}], year 2013
– SOMO35 [µg.m^{-3}.day], year 2013
– AOT40 for agricultural crops [µg.m^{-3}.hour], year 2013
– AOT40 for forests [µg.m^{-3}.hour], year 2013

SOMO35 is the annual sum of the differences between maximum daily 8-hour concentrations above 70 µg.m^{-3} (i.e. 35 ppb) and 70 µg.m^{-3}. AOT40 is the sum of the differences between hourly concentrations greater than 80 µg.m^{-3} (i.e. 40 ppb) and 80 µg.m^{-3}, using only observations between 7:00 and 19:00 UTC, calculated over the three months from May to July (AOT40 for agricultural crops), respectively over the six months from April to September (AOT40 for forests). Note that the term *vegetation* as used in the Air Quality Directive 2008/50/EC is not further defined. Nevertheless, the target value used in the directive is the same as the critical load used in the Mapping Manual (UNECE, 2004) for "agricultural crops", so we have interpreted the term *vegetation* in the AQ directive as agricultural crops. Therefore, the exposure of *agricultural crops* has been evaluated here on basis of the AOT40 for vegetation as defined in the AQ directive. Further, we call this indicator "AOT40 for crops".

Only the stations with annual data coverage of at least 75 percent are used. In the case of SOMO35 and AOT40 indicators, the correction for the missing data is applied according to the equation

$$I_{corr} = I \cdot \frac{N}{N_{\max}} \tag{3.1}$$

where I_{corr} is the corrected indicator (SOMO35, AOT40 for crops or AOT40 for forests),
I is the value of the given indicator without any correction,
N is the number of the daily data for the given station,
N_{max} is the maximum number of the days applicable for the given indicator.

For the indicators relevant to human health (i.e. PM_{10}, $PM_{2.5}$ and for ozone the 26th highest daily maximum 8-hour average and SOMO35) data from *rural*, *urban* and *suburban background* stations are considered. For the indicators relevant to vegetation damage (both AOT40 parameters for ozone) only *rural background* stations are considered. In the case of existing data (with sufficient annual coverage) from two or more different measurement devices in the same station, the average of such data is used.

We excluded the stations from French overseas areas (departments), Svalbard, Azores, Madeira and Canary Islands. These areas outside the EEA map extent *Map_1c* (EEA, 2011) were excluded from the interpolation and mapping domain. To reach a more extended spatial coverage by measurement data we use, in addition to the AirBase data, ten additional rural background stations for PM_{10} and five for $PM_{2.5}$ from the EBAS database (NILU, 2015). Table 3.1 shows the number of the measurement stations selected for the individual pollutants and their respective indicators. Compared to 2012, the number of rural background stations selected for 2013 decreased by approximately 7 % for PM_{10} stations, increased by about 6 % for $PM_{2.5}$ stations and decreased by approximately 1 – 6 % for ozone. The number of the urban/suburban background stations decreased by approximately 16 % for PM_{10}, by approximately 3 % for $PM_{2.5}$, and by about 1 % for ozone. The decrease in the number of the urban/suburban PM_{10} stations is influenced by the lack of the Turkish stations in 2013.

Table 3.1 Number of stations selected for individual indicators and areas– rural background stations used for rural areas, urban and suburban background stations used for urban background areas in 2013 mapping.

	PM_{10}		$PM_{2.5}$	ozone			
	annual average	36th daily maximum	annual average	26th highest daily max. 8h	SOMO35	AOT40 for crops	AOT40 for forests
rural	311	308	147	499	485	494	492
urban	1007	1002	454	979	962		

For $PM_{2.5}$ mapping an additional 185 rural background and 646 urban/suburban background PM_{10} stations (at locations without $PM_{2.5}$ measurement) were also used for the purpose of calculating the pseudo $PM_{2.5}$ station data.

Due to a lack of stations in Turkey, no proper interpolation results could be presented for this country for all the indicators. Therefore, we excluded Turkey from the production process of the maps and exposure tables of this paper.

3.2 EMEP MSC-W model output

The chemical dispersion model used was the EMEP MSC-W (formerly called Unified EMEP) model (version rv4.7), which is an Eulerian model with a resolution of circa 50x50 km. Information from this model was converted to 10x10 km grid resolution (for health related indicators), resp. into the 2x2 km grid resolution (for vegetation related indicators) for the interpolation process.

As per the previous year, we received the EMEP data in the form of daily means for PM_{10} and $PM_{2.5}$ and hourly means for ozone. We aggregated these primary data to the same set of parameters as we have for the air quality observations:

PM_{10} – annual average [$\mu g.m^{-3}$], year 2013 (aggregated from daily means)
– 36th highest daily average value [$\mu g.m^{-3}$], year 2013 (aggregated from daily means)

$PM_{2.5}$ – annual average [$\mu g.m^{-3}$], year 2013 (aggregated from daily means)

Ozone – 26th highest daily maximum 8-hour average value [$\mu g.m^{-3}$], year 2013 (aggregated from hourly means)
– SOMO35 [$\mu g.m^{-3}.day$], year 2013 (aggregated from hourly means)
– AOT40 for crops [$\mu g.m^{-3}.hour$], year 2013 (aggregated from hourly means)
– AOT40 for forests [$\mu g.m^{-3}.hour$], year 2013 (aggregated from hourly means)

Due to the complete temporal data coverage of the modelled data, the PM_{10} indicator 90.4th percentile of daily means is identical with the 36th highest daily mean and the ozone indicator 93.2nd percentile of daily maximum 8-hour means is identical with the 26th highest daily maximum 8-hour mean.

Simpson et al. (2012, 2013) and https://wiki.met.no/emep/page1/emepmscw_opensource (web site of Norwegian Meteorological Institute) describe the model in more detail. Emissions for the relevant year (Mareckova et al., 2015) are used and the model is driven by ECMWF meteorology for the relevant year. EMEP (2015) provides details on the EMEP modelling for 2013.

In the routine mapping procedure, model results based on 2013 meteorology and 2013 emission data are used. In addition, the mapping procedure is applied on model results (version rv4.5) based on 2013 meteorology but 2012 emission data (Mareckova et al., 2014). See for details EMEP (2014). Results of this sensitivity calculation are presented in Annex 3.

In the original format of the model results, a point represents the centre of a grid cell (in 50x50 km resolution). The data are imported into *ArcGIS* as a point shapefile and converted into ETRS89-LAEA5210 projection, subsequently converted into a 100x100 m resolution raster grid and spatially aggregated into the reference EEA 10x10 km grid (for health related indicators), resp. into the 2x2 km grid (for vegetation related indicators).

3.3 Altitude

We use the altitude data field (in meters) of *Global Multi-resolution Terrain Elevation Data 2010 (GMTED2010)*, with an original grid resolution of 15x15 arcseconds (some 463x463 m at 60N). Source: U.S. Geological Survey Earth Resources Observation and Science, see Danielson et al. (2011). We converted the field into the ETRS 1989 LAEA projection. (The resolution after projection was in 449.2x449.2 m). In the following step, we resampled the raster dataset to 100x100 m resolution and shifted it to the extent of EEA reference grid. As a final step, the dataset was spatially aggregated into 2x2 km and 10x10 km resolutions.

3.4 Meteorological parameters

Actual meteorological surface layer parameters we extracted from the *Meteorological Archival and Retrieval System (MARS)* of the *ECMWF (European Centre for Medium-range Weather Forecasts)*. Currently we use the following ECMWF variables (details specified in Horálek et al. 2007, Section 4.5) on a 0.25x0.25 degrees (about 28x28 km at 60N) resolution as supplementary data in the regressions:

Wind speed – annual average [$m.s^{-1}$], year 2013
Surface solar radiation – annual average of daily sum [$MWs.m^{-2}$], year 2013

The data are imported into *ArcGIS* as a point shapefile. Each point represents the centre of a grid cell. The shapefile is converted into ETRS89-LAEA5210 projection, converted into a 100x100 m resolution raster grid and spatially aggregated into the reference EEA 10x10 km grid, resp. into the 2x2 km grid.

3.5 Population density and population totals

Population density (in $inhbs.km^{-2}$, census 2011) is based on *Geostat 2011* grid dataset, Eurostat (2014). The dataset is in 1x1 km resolution, in the EEA reference grid.

For regions, which are not included in the Geostat 2011, alternative sources were used. Primarily, *JRC (Joint Research Centre)* population data in resolution 100x100 m were used (JRC, 2009). The JRC 100x100 m population density data is spatially aggregated into the reference 1x1 km EEA grid. For regions, which are not included nor in the Geostat 2011 nor in the JRC database, we used population density data from *ORNL LandScan Global Population Dataset* (ORNL, 2008). This dataset is in 30x30 arcsec resolution; its values are based on the annual mid-year national population estimates for 2008 from the Geographic Studies Branch, US Bureau of Census, http://www.census.gov. The ORNL data is reprojected and converted from its original WGS1984 30x30 arcsec grids into EEA's reference projection ETRS89-LAEA5210 at 1x1 km resolution by EEA (eea_r_3035_1_km_landscan-eurmed_2008, EEA, 2008).

JRC data were used for Gibraltar. ORNL data were used for Faroe Islands, British crown dependencies (Jersey, Guernsey and Man) and northern Cyprus. In these areas with the lack of Geostat 2011 data, the

Geostat 2011 dataset was supplemented with JRC and ORNL data. Thus, the supplemented Geostat 2011 1x1 km data covers the entire mapping area.

In order to verify the correctness of the merger of Geostat 2011 with JRC and ORNL, we compared the Geostat 2011 data and the JRC supplemented with ORNL data using the national population totals of the individual countries. (For verification of the correctness of the merger of JRC and ORNL data, see Horálek et al., 2015.) Next to this, we compared the national population totals for the Geostat 2011 gridded data and the Eurostat national population data for 2013 (Eurostat, 2015). Figure 3.1 presents both these comparisons.

From the comparisons, one can see the high correlation of the compared national population totals. Slight underestimation of the supplemented JRC data in comparison with the Geostat 2011 data can be seen, which is caused by the fact that the Geostat 2011data is more up-to-date than both JRC and ORNL data. The similar founding is true, if compared the Geostat 2011 and the Eurostat 2013 data. Based on this, the population totals in the report are presented using the actual Eurostat data for 2013, see below.

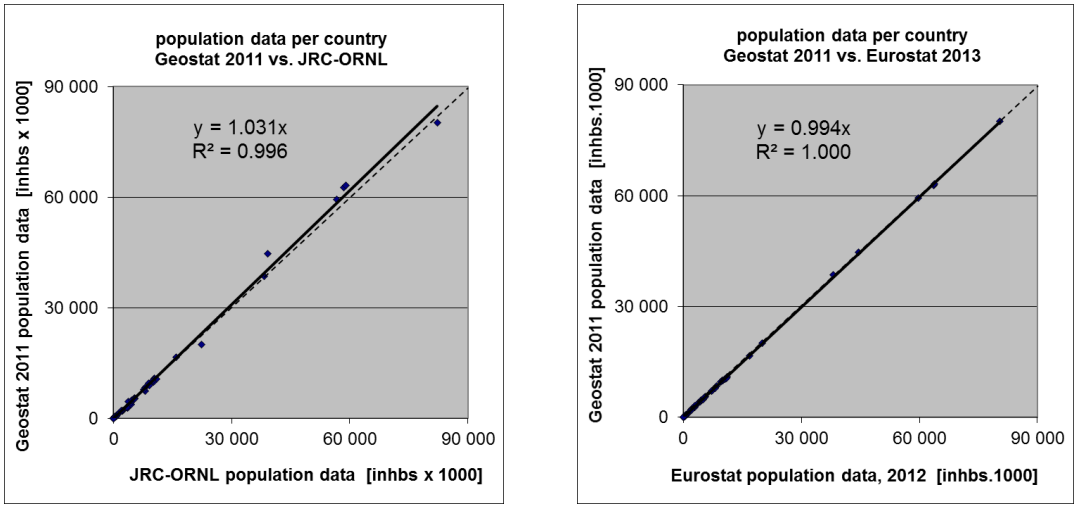

Figure 3.1 Correlation between Geostat 2011 (y-axis) and JRC supplemented with ORNL (x-axis, left) and Eurostat 2013 revision (x-axis, right) for national population totals.

Population density data can be used to classify the spatial distribution of each type of area (rural, urban or mixed population density) in Europe. We use this information to select and weight the air quality value, grid cell by grid cell. Furthermore, we use it to estimate population health exposure and exceedance numbers per country and for Europe as a whole, including involved uncertainties. These activities take place on the 1x1 km resolution grid in accordance with the recommendations of Horálek et al. (2010). The supplemented Geostat data (as described above) are used in all the calculations.

Population totals for individual countries presented in exposure tables in Sections 4.1.2, 4.2.2, 5.1.2, 6.1.2, 6.2.2 and in Annexes are based on Eurostat national population data for 2013 (Eurostat, 2015). For France, Portugal and Spain, the population totals of areas outside the mapping area (i.e. Azores, Canarias, Madeira, French oversea departments) are subtracted. For Monaco, which is not included in the Eurostat database, the population total is based on UN population data (UN, 2015) for 2013.

3.6 Land cover

CORINE Land Cover 2006 – grid 100 x 100 m, Version 17 (12/2013) is used (CLC2006 – 100m, g100_06.zip; EEA, 2013b). The countries missing in this database are Andorra and Greece. Greece is missing in the CLC2006 but present in the CLC2000 version that we used in previous mapping years. Therefore, we inserted for Greece the CLC2000 data (grid 100 x 100 m, Version 17, 12/2013 EEA, 2013a). Due to lacking land cover data for Andorra, we excluded this country from the process of exposure estimates related to the vegetation based AOT40 ozone indicators.

4 PM_{10} maps

This chapter presents the 2013 updates (for the interpolated maps and exposure tables) of the two PM_{10} health related indicators: annual average and 36th highest daily average. The separate rural and urban background concentration maps were calculated on the 10x10 km resolution grid and the subsequent combined concentration map was based on the 1x1 km gridded population density map. The population exposure tables were calculated at 1x1 km grid resolution. All maps here are presented using the 10x10 km grid resolution. The standard EEA ETRS89-LAEA5210 coordinate reference system was applied.

4.1 Annual average

4.1.1 Concentration map

Figure 4.1 presents the combined final map for the 2013 PM_{10} annual average as the result of interpolation and merging of the separate maps as described in detail in De Smet et al. (2011) and Horálek et al. (2007). Red and purple areas and stations exceed the limit value (LV) of 40 $\mu g.m^{-3}$. Supplementary data in the regression used for rural areas consisted of EMEP model output, altitude, wind speed and surface solar radiation and for urban background areas it was EMEP model output only. The relevant linear regression submodels have been identified earlier in Horálek et al. (2008) and De Smet et al. (2009, 2010, 2011).

Table 4.1 presents the estimated parameters of the linear regression models (*c, a_1, a_2,...*) and of the residual kriging (*nugget, sill, range*) and includes the statistical indicators of both the regression and the kriging. The adjusted R^2 and standard error are indicators for the fit of the regression relationship, where the adjusted R^2 should be as close to 1 as possible and the standard error should be as small as possible. The adjusted R^2 was 0.53 for the rural areas and 0.25 for urban areas. The R^2 values show both for rural and urban areas in 2013 the second best fit, compared to its all previous years, see Horálek et al. (2014a) and references cited therein. The continued better regression fit for urban areas as of 2010 is most likely attributable to improvements of the EMEP model since 2010. RMSE and bias are the cross-validation indicators, showing the quality of the resulting map; the bias indicates to what extent the estimation is un-biased. Sections 4.1.2 and 4.1.3 deal with a more detailed analysis and compares with results of the years 2005 – 2013.

Table 4.1 Parameters of the linear regression models (Eq. 2.2) and of the ordinary kriging (OK) variograms (nugget, sill, range) – and their statistics – of PM_{10} indicator annual average for 2013 in rural (left) and urban (right) areas as used for the combined final map.

linear regr. model + OK of its residuals	rural areas parameter values	urban areas parameter values
c (constant)	2.12	1.91
a1 (log. EMEP model 2012)	0.522	0.52
a2 (altitude GTOPO)	-0.00054	
a3 (wind speed 2012)	-0.102	
a4 (s. solar radiation 2012)	*non signif.*	
adjusted R^2	**0.53**	**0.25**
standard error [$\mu g.m^{-3}$]	**0.27**	**0.27**
nugget	0.037	0.014
sill	0.060	0.063
range [km]	480	740
RMSE [$\mu g.m^{-3}$]	**3.38**	**4.27**
Relative RMSE [%]	**19.6**	**17.3**
bias (MPE) [$\mu g.m^{-3}$]	**0.02**	**-0.03**

As indicated in Table 4.1, surface solar radiation was not, in contrast to 2012 (and like in 2010 – 2011), found to be statistically significant and thus used in 2013 mapping. Its further use is to be considered.

In the case of PM_{10}, the linear regression is applied for the logarithmically transformed data of both measured and modelled PM_{10} values. Thus, in Table 4.1 the standard error and variogram parameters refer to these transformed data, whereas RMSE and bias refer to the interpolation after the back-transformation.

The concentration map presented in Figure 4.1 is spatially aggregated from 1x1 km to a 10x10 km grid resolution, see Section 2.1.3. As a result, the urban areas are not properly resolved in this map, due to the smoothing effect of the aggregation. In particular, this is seen in Bulgaria and Poland, i.e. the high observed urban background concentrations do not seem to influence the interpolation results. The main reason is that the map is an aggregation of 1x1 km grid values to a 10x10 km resolution and this aggregation smooths out the elevated values one would likely be able to distinguish in the higher resolution map. Therefore, the exposure estimates of Table 4.2 are derived just from the 1x1 km grid map. Section 4.1.3 discusses the level of the representation of the urban areas in this final combined aggregated 10x10 km map. For better visualising the actual urban concentration levels at the actual urbanised areas, i.e. without the influence of the dominating pattern of extended rural areas, a separate 1x1 km urban background map is presented in Annex 1, Figure A1.1. In this map, the non-urban areas are masked and the 'mixed' areas, i.e. areas with population density weighting of rural – urban characteristics, are semi-transparent.

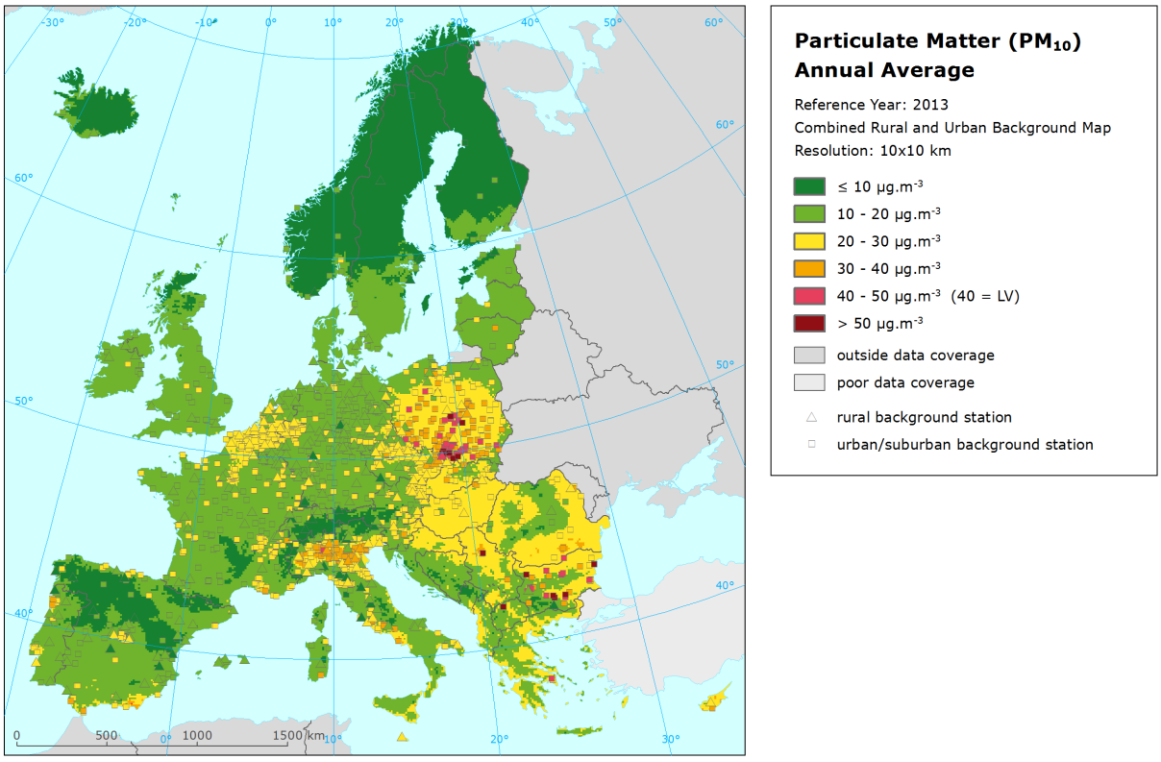

Figure 4.1 Combined rural and urban concentration map of PM_{10} – annual average, year 2013. Spatial interpolated concentration field (10x10 km grid resolution, excluding Turkey due to lack of air quality data) and the measured values in the measurement points. Units: µg.m^{-3}.

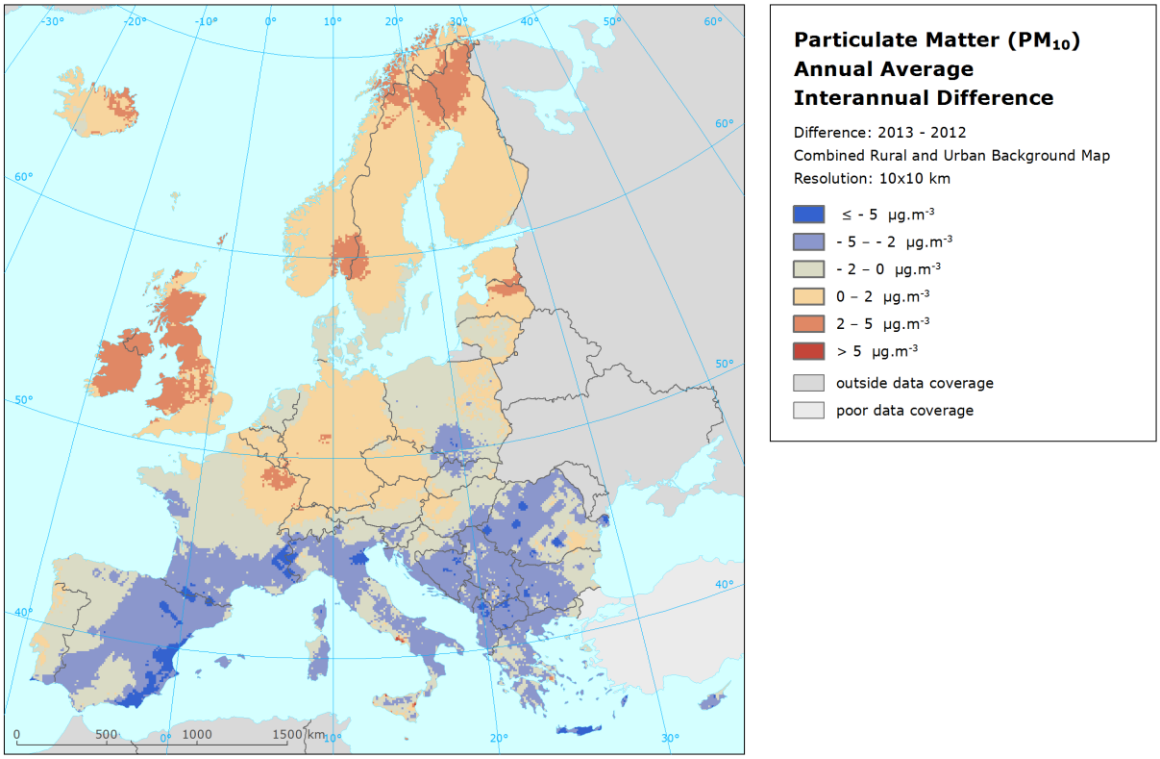

Figure 4.2 Inter-annual difference between mapped concentrations for 2013 and 2012 – PM_{10}, annual average. Units: $\mu g.m^{-3}$.

Figure 4.2 presents the inter-annual difference between 2013 and 2012 for annual average PM_{10}. Red areas show an increase of PM_{10} concentration, while blue areas show a decrease. The highest increases are observed in United Kingdom, Ireland and some parts of Scandinavia. Contrary to that, the decrease can be seen in the most of southern Europe, in large parts of Balkan and in the southern Poland near the Katowice region.

In past year's paper (Horálek et al (2015) the comparison of the difference between 2012 and 2011 showed an increase at the same area of Spain in which the decrease is visible now, indicating the impact of meteorological fluctuations. Similarly, some areas with smaller increases (orange) in 2013, namely Germany and the Benelux, showed decreases in 2012 compared to 2011.

4.1.2 Population exposure

Table 4.2 gives the population frequency distribution for a limited number of exposure classes calculated at the 1x1 km grid resolution, as well as the population n-weighted concentration for individual countries and for Europe as a whole according to Equation 2.3.

About 54 % of the European population (and also of the EU-28 population) has been exposed to annual average concentrations above 20 $\mu g.m^{-3}$, the WHO (World Health Organization) air quality guideline (WHO, 2005). EEA (2015b) estimates that about 61-83 % of the urban population in the EU-28 is exposed to levels above the WHO guideline. The latter estimate accounts for the urban population mainly in the larger cities of the EU-28 It therefore represents areas where, in general, considerably higher PM_{10} concentrations occur throughout the year. The estimates in Table 4.2 includes the total European (resp. EU-28) population, including the rural population in the villages and the smaller cities that are in general exposed to lower levels of PM_{10} throughout the year. It is important to note that this difference in exposure estimates is explained by the use of different area representation in the calculations.

Table 4.2 Population exposure and population-weighted concentration – PM_{10}, annual average, year 2013. Resolution: 1x1 km.

Country		Population	PM_{10} annual average, exposed population [%]						Population weighted conc.
			< LV				> LV		
			< 10	10 - 20	20 - 30	30 - 40	40 - 45	> 45	
		[inhbs . 1000]	µg.m^{-3}	µg.m^{-3}	µg.m^{-3}	µg.m^{-3}	µg.m^{-3}	µg.m^{-3}	[µg.m^{-3}]
Albania	AL	2 899	0.0	8.0	18.1	72.0	1.9		32.5
Andorra	AD	76	0.8	1.1	98.2				25.0
Austria	AT	8 452	1.6	39.8	58.7				20.2
Belgium	BE	11 162		6.2	93.8				23.6
Bosnia & Herzegovina	BA	3 836	0.3	20.5	79.2				23.1
Bulgaria	BG	7 285	0.1	4.2	15.7	44.1	29.1	6.9	36.7
Croatia	HR	4 262	0.0	11.3	88.7				23.5
Cyprus	CY	866		0.5	13.4	86.1			35.8
Czech Republic	CZ	10 516		8.8	79.5	8.6	3.1		25.6
Denmark	DK	5 603	0.0	99.7	0.3				16.3
Estonia	EE	1 320	4.2	95.8					13.5
Finland	FI	5 427	38.9	61.1					10.5
France (metropolitan)	FR	63 652	0.4	44.1	55.4	0.0			20.7
Germany	DE	80 524	0.0	71.1	28.9				19.0
Greece	GR	11 004	0.0	3.4	12.9	61.3	22.3		34.6
Hungary	HU	9 909		0.1	99.4	0.5			25.3
Iceland	IS	322	11.0	89.0					11.8
Ireland	IE	4 591		99.7	0.3				15.1
Italy	IT	59 685	0.3	11.3	56.1	32.3			27.0
Latvia	LV	2 024	0.0	41.6	58.4				19.5
Liechtenstein	LI	37	1.4	98.6					15.5
Lithuania	LT	2 972		30.4	69.6				20.4
Luxembourg	LU	537		100.0					18.8
Macedonia, FYROM of	MK	2 062	0.0	2.3	3.3	10.0	49.3	35.0	44.5
Malta	MT	421			2.5	97			35.7
Monaco	MC	38			100.0				22.7
Montenegro	ME	621	2.5	15.8	41.7	40.0			27.0
Netherlands	NL	16 780		28.3	71.7				20.7
Norway	NO	5 051	26.8	60.1	13.0				13.8
Poland	PL	38 063		6.2	45.7	34.7	13.5		30.4
Portugal (excl. Az., Mad.)	PT	9 977	0.7	40.3	59.0				20.3
Romania	RO	20 020	0.0	9.8	69.2	21.0			26.0
San Marino	SM	34		12.3	87.7				22.1
Serbia (incl. Kosovo*)	RS	8 997	0.0	4.4	35.3	46.2	14.1		31.8
Slovakia	SK	5 411		1.7	77.0	21.3	0.0		26.8
Slovenia	SI	2 059	0.0	20.6	79.4				22.7
Spain (excl. Canarias)	ES	44 623	1.6	60.0	37.1	1.3	0.1		19.1
Sweden	SE	9 556	14.1	85.9					13.2
Switzerland	CH	8 039	2.1	78.0	19.9				18.3
United Kingdom (& dep.)	UK	63 905	0.1	96.9	3.0				17.0
Total		**532 614**	**1.2**	**44.4**	**41.0**	**10.8**	**2.3**	**0.2**	**22.2**
			45.6				**2.6**		
EU-28		**500 603**	**1.0**	**45.0**	**41.7**	**10.1**	**2.0**	**0.1**	**22.1**
			46.0				**2.1**		
Kosovo*	KS	1 816	0.0	5.0	14.1	15.7	65.2	0.0	39.0
Serbia (excl. Kosovo*)	RS	7 182	0.0	4.2	40.5	53.6	1.7	0.0	30.0
*) under the UN Security Council Resolution 1244/99									

Note1: Turkey is not included in the calculation due to lacking air quality data.
Note2: The percentage value "0.0" indicates an exposed population exists, but is small and estimated less than 0.05 %. Empty cells mean: no population in exposure.

Table 4.3 Evolution of population-weighted concentration in the years 2005-2013 (left) and of percentage population living in above limit value in the years 2009-2013 (right) – PM_{10}, annual average. Resolution: 1x1 km.

Country		Population-weighted conc. [µg.m^{-3}]										Popul. above LV 40 µg.m^{-3} [%]					
		2005	2006	2007	2008	2009	2010	2011	2012	2013	diff. '13 - '12	2009	2010	2011	2012	2013	diff. '13 - '12
Albania	AL	36.3	31.8	31.6	33.3	35.3	45.5	26.5	32.0	32.5	0.4	52.1	62.6	0.9	3.2	1.9	-1.3
Andorra	AD	19.5	22.5	20.5	18.7	17.7	17.9	18.0	33.2	25.0	-8.2	0	0	0	0	0	0
Austria	AT	25.4	26.0	22.1	21.3	21.6	22.7	20.8	20.0	20.2	0.2	0	0	0	0	0	0
Belgium	BE	29.2	31.3	24.8	23.9	26.5	25.7	24.8	23.2	23.6	0.4	0	0	0	0	0	0
Bosnia-Herzegovina	BA	34.3	33.1	32.4	29.3	37.2	30.8	22.3	27.2	23.1	-4.0	51.6	17.2	0.7	0	0	0
Bulgaria	BG	42.6	41.6	40.2	44.2	39.8	38.0	27.3	36.6	36.7	0.1	53.8	49.0	7.4	45.6	36.0	-9.6
Croatia	HR	33.6	31.5	30.0	28.1	29.0	27.3	25.0	24.7	23.5	-1.2	3.0	0	0	0	0	0
Cyprus	CY	38.9	35.4	33.9	76.1	41.0	50.2	31.1	42.9	35.8	-7.2	73.0	82.7	12.8	75.0	0	-75.0
Czech Republic	CZ	32.9	33.5	25.6	24.2	25.3	28.3	23.7	25.4	25.6	0.2	3.3	9.4	0.9	4.3	3.1	-1.2
Denmark	DK	21.3	23.5	20.8	18.8	16.3	15.7	18.4	16.3	16.3	0.0	0	0	0	0	0	0
Estonia	EE	17.7	19.7	15.7	12.9	13.4	14.1	9.8	12.1	13.5	1.4	0	0	0	0	0	0
Finland	FI	14.2	17.0	13.7	12.5	11.7	12.2	9.5	10.2	10.5	0.3	0	0	0	0	0	0
France	FR	19.3	20.4	24.6	22.6	24.0	23.0	21.8	21.4	20.7	-0.7	0	0	0	0.0	0	0.0
Germany	DE	23.0	24.2	20.7	19.6	20.7	21.2	19.6	18.4	19.0	0.6	0	0	0	0	0	0
Greece	GR	38.0	33.6	33.5	39.7	35.3	37.3	24.6	30.3	34.6	4.4	23.4	20.9	5.7	5.0	22.3	17.4
Hungary	HU	34.8	32.9	28.7	26.8	27.6	28.1	29.1	26.1	25.3	-0.8	0	0	0	0	0	0
Iceland	IS	13.8	17.4	12.2	15.2	9.0	10.7	9.3	9.6	11.8	2.1	0	0.1	0	0	0	0
Ireland	IE	12.7	14.9	14.7	15.4	12.8	13.7	12.8	12.4	15.1	2.7	0	0	0	0	0	0
Italy	IT	34.9	33.9	33.2	30.1	28.7	26.4	27.7	27.0	27.0	0.0	8.8	0	13.7	0.1	0	-0.1
Latvia	LV	19.8	21.9	17.8	19.1	18.8	21.5	14.6	18.0	19.5	1.5	0	0	0	0	0	0
Liechtenstein	LI	23.4	24.9	20.7	20.6	18.3	17.3	11.3	14.3	15.5	1.2	0	0	0	0	0	0
Lithuania	LT	20.7	22.5	18.5	17.3	19.0	22.0	14.8	18.1	20.4	2.3	0	0	0	0	0	0
Luxembourg	LU	18.7	20.8	19.5	18.2	21.0	19.4	16.4	17.2	18.8	1.6	0	0	0	0	0	0
Macedonia, FYR of	MK	46.2	39.3	38.5	41.6	45.4	43.9	23.0	42.3	44.5	2.2	74.5	70.0	2.3	63.2	84.3	21.2
Malta	MT	37.1	29.4	27.0	27.5	27.2	32.5	27.8	25.4	35.7	10.3	0	0	0	0	0	0
Monaco	MC		36.7	34.5	29.5	26.8	24.0	22.8	28.0	22.7	-5.3	0	0	0	0	0	0
Montenegro	ME	35.1	33.1	33.1	33.6	35.0	32.8	21.5	28.3	27.0	-1.2	61.1	42.1	0	0.9	0	-0.9
Netherlands	NL	29.2	29.1	25.8	24.0	24.3	24.3	25.1	21.1	20.7	-0.4	0	0	0	0	0	0
Norway	NO	18.1	19.6	15.6	15.7	14.1	14.7	9.3	12.2	13.8	1.6	0	0	0	0	0	0
Poland	PL	32.7	37.0	28.8	28.3	30.8	35.2	27.2	32.4	30.4	-2.0	14.7	30.0	5.2	19.7	13.5	-6.3
Portugal	PT	30.9	28.4	27.0	21.8	22.9	21.7	20.8	19.9	20.3	0.3	0	0	0	0	0	0
Romania	RO	42.7	39.1	35.0	30.8	28.9	25.2	27.2	28.9	26.0	-2.9	4.0	2.0	0.9	4.2	0	-4.2
San Marino	SM	31.7	33.9	31.2	29.6	26.0	25.0	20.9	25.8	22.1	-3.7	0	0	0	0	0	0
Serbia (incl. Kosovo)	RS	44.2	41.8	39.4	40.1	39.5	33.1	30.1	34.9	31.8	-3.2	55.5	20.7	13.4	23.0	14.1	-8.9
Slovakia	SK	34.3	33.8	29.1	26.7	26.9	30.2	27.4	27.9	26.8	-1.1	1.2	3.0	0.1	0.0	0.0	0.0
Slovenia	SI	30.8	29.0	27.2	25.0	25.2	26.0	25.4	24.3	22.7	-1.7	0	0	0	0	0	0
Spain	ES	29.6	31.4	29.6	25.2	23.7	21.4	18.8	20.9	19.1	-1.8	0	0	0	0.8	0.1	-0.7
Sweden	SE	16.9	19.0	15.7	16.3	13.8	12.8	12.3	12.4	13.2	0.8	0	0	0	0	0	0
Switzerland	CH	21.3	23.2	21.4	20.5	21.0	19.8	17.7	17.6	18.3	0.6	0	0	0	0	0	0
United Kingdom	UK	21.4	23.2	21.6	19.5	18.4	18.2	17.5	16.5	17.0	0.5	0	0	0	0	0	0
Total		**28.0**	**28.5**	**26.2**	**24.8**	**24.6**	**24.3**	**22.1**	**22.7**	**22.2**	**-0.4**	**6.0**	**5.2**	**2.5**	**3.4**	**2.6**	**-0.9**
EU-28		**27.6**	**28.3**	**26.0**	**24.4**	**24.2**	**24.0**	**22.1**	**22.4**	**22.1**	**-0.3**	**4.1**	**4.1**	**2.4**	**2.9**	**2.1**	**-0.8**

Slightly more than half (52 %) of the European population in 2013 lived in areas where the PM_{10} annual mean concentration was estimated to be between 20 and 40 µg.m^{-3}. About 2.6 % of the population lived in areas where the PM_{10} annual limit value was exceeded. In Bulgaria, Greece, FYR of Macedonia, Poland and Serbia more than 5 % of the population is exposed to concentrations above the LV. However, the current mapping methodology tends to underestimate high values (see Section 4.1.3). Therefore, the exceedance percentage would most likely be underestimated; additional exceedances might be expected in countries like Albania, Czech Republic and Cyprus.

The inter-annual variation in population exposure during the past nine years is presented in Table 4.3. It is based on results presented in previous reports (Horálek et al., 2015, and references cited therein)

for the years 2008 – 2012, based on the recalculated results for 2005 and 2007 and based on the paper with the tests of a new methodology (Horálek et al., 2010) for 2006. We present the evolution in the whole nine-year period for the population-weighted concentration, while for the population living in the areas above LV it is only the years 2009 – 2013. (For previous years, see Horálek et al., 2015, Table 4.3.) The overall picture of the population-weighted concentration of the European totals in Table 4.3 demonstrates a slightly continuous downward trend for the years 2005 – 2013.

The percentage population living in above limit value is not statistically a very robust parameter. Small changes in concentration might result in large changes in exposed population. From Table 4.3, one can conclude that the probability of an exceedance is rather persistent in certain areas.

The frequency distribution shows large variability over Europe, with several countries showing in 2013 exposures above the limit value, like in 2012 but most of them with an increased percentage population in exceedance (e.g. Albania, Bulgaria, Czech Republic, Poland and Serbia). Greece and FYR of Macedonia shows increase. Cyprus shows a decrease from 75 % in 2012 to no exceedance in 2013. In the period 2005 – 2012, the year 2012 appears to show a slight increase in the number of population, whereas the year 2013 shows the similar number like 2011. Compared to 2011, an overall decrease of 1.0 % occurred in 2013.

In a number of countries in northern and north-western Europe, the LV of 40 $\mu g.m^{-3}$ seems to continue not to be exceeded. When comparing between years the total population exposed to the low levels, i.e. below 20 $\mu g.m^{-3}$, it is found that the percentage for 2013 of 46 % is higher than the five previous years 2008 – 2012 (with 29 – 45 %), which on its turn is higher than in 2006 – 2007 (with 29 – 24 %). The tendency of reduced exposure of population living in areas with concentrations above the limit value, established in previous years (from 10 – 13 % in 2005 – 2006 to 5 – 6 % in 2007 – 2010), seems to continue with values of between 2 – 3 % in the years 2011 – 2013. The tendency comes with a degree of uncertainty however and should not be qualified as a clear downward trend without more detailed analysis.

Considering the average for the whole of Europe in Table 4.3, the overall population-weighted annual mean PM_{10} concentration in 2013 was 22.2 $\mu g.m^{-3}$. This is almost the same as in previous year. One may observe a steady reduction of the population-weighted concentration over the period of time 2005 – 2011, with perhaps some consolidation effect in 2012 – 2013.

4.1.3 Uncertainties

Uncertainty estimated by cross-validation

Using RMSE as the most common indicator, the *absolute mean uncertainty* of the combined final map at areas 'in between' the station measurements can be expressed in $\mu g.m^{-3}$. Table 4.1 shows that the absolute mean uncertainty of the combined final map of PM_{10} annual average expressed by RMSE is 3.4 $\mu g.m^{-3}$ for the rural areas and 4.3 $\mu g.m^{-3}$ for the urban areas. The RMSEs for both rural and urban areas are the lowest ones obtained so far.

Alternatively, one could express this uncertainty in relative terms by relating the absolute RMSE uncertainty to the mean air pollution indicator value for all stations. This *relative mean uncertainty* (RRMSE) of the combined final map of PM_{10} annual average is 19.6 % for rural areas and 17.3 % for urban areas. This is both for rural and urban areas the lowest result in the whole period 2005 – 2013. The low uncertainty levels for urban areas in the year 2013 are influenced specifically by the lack of Turkish urban background stations in this year. These stations were reported since 2008 to 2012, but not in 2013. (Turkish urban stations show high concentrations, uncertainty statistics are sensitive to such values.) These relative uncertainty values fulfil the data quality objectives for models as set in Annex I of the air quality Directive 2008/50/EC (EC, 2008). See section 7 for a further discussion on uncertainties over these past nine modelling years.

Figure 4.3 shows the cross-validation scatter plots, obtained according Section 2.3, for both rural and urban areas. The R^2 indicates that for the rural areas about 70 % and for the urban areas about 74 % of the variability is attributable to the interpolation. The 2013 interpolation performance at the rural

locations is the highest so far, while at the urban locations it is slightly below the average of the earlier six years (see Table 7.5).

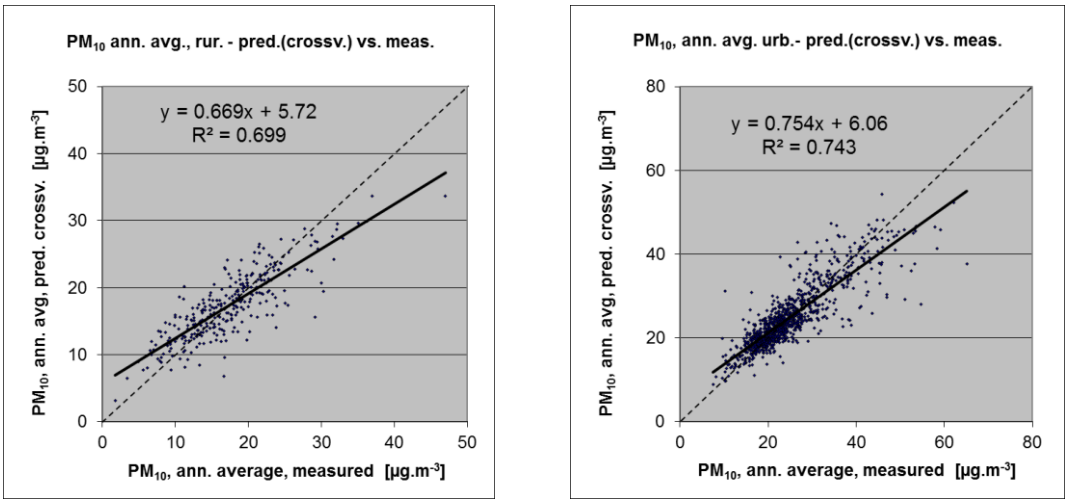

Figure 4.3 Correlation between cross-validation predicted values (y-axis) and measurements (x-axis) for the PM_{10} annual average for 2013 for rural (left) and urban (right) areas. R^2 and the slope a (from the linear regression equation $y = a \cdot x + c$) should be as close 1 as possible, the intercept c should be as close 0 as possible

The scatter plots indicate that in areas with high concentrations the interpolation methods tend to underestimate the levels. For example, in rural areas an observed value of 40 µg.m^{-3} is estimated in the interpolations to be about 32 µg.m^{-3}, about 19 % too low. This underestimation at high values is natural to all spatial interpolations. It can be reduced by either using a higher number of stations with an improved spatial distribution, or by introducing an improved regression by using other supplementary data.

Comparison of point measurement values with the predicted grid value

In addition to the above point observation – point prediction cross-validation discussed in the previous subsection, a simple comparison has been made between the point observation values and interpolated prediction values spatially averaged at grid cells. This *point-grid* comparison indicates to what extent the predicted value of a grid cell represents the corresponding measured values at stations located in that cell. The comparison has been made primarily for the separate rural and separate urban background map at 10x10 km resolution. (One can directly relate this comparison result to the cross-validation results of Figure 4.3.)

Next to this, the comparison has been done also for the final combined maps at 1x1 km resolution and for the spatial aggregated final maps at 10x10 km resolution. Figure 4.4 shows the scatterplots for these comparisons.

The results of the point observation – point prediction cross-validation of Figure 4.3 and those of the point-grid validation for separate rural and separate urban background maps, and for the final combined maps at both resolutions are summarised in Table 4.4.

By the comparing the scatterplots and the statistical indicators for the separate rural and separate urban background map with the final combined maps in both resolutions, one can evaluate the level of representation of the rural resp. urban background areas in the final combined maps. The rural air quality is fairly well represented in both the 1x1 km and the aggregated 10x10 km final combined map. The urban air quality is quite well represented in the final combined 1x1 km map, but not in the aggregated final combined 10x10 km map as one can deduce from its higher RMSE, its bias being further from zero and its lower R^2. Therefore, we present in Figure A1.1 of Annex 1 the 1x1 km urban background map in addition to the 10x10 km final combined map of Figure 4.1.

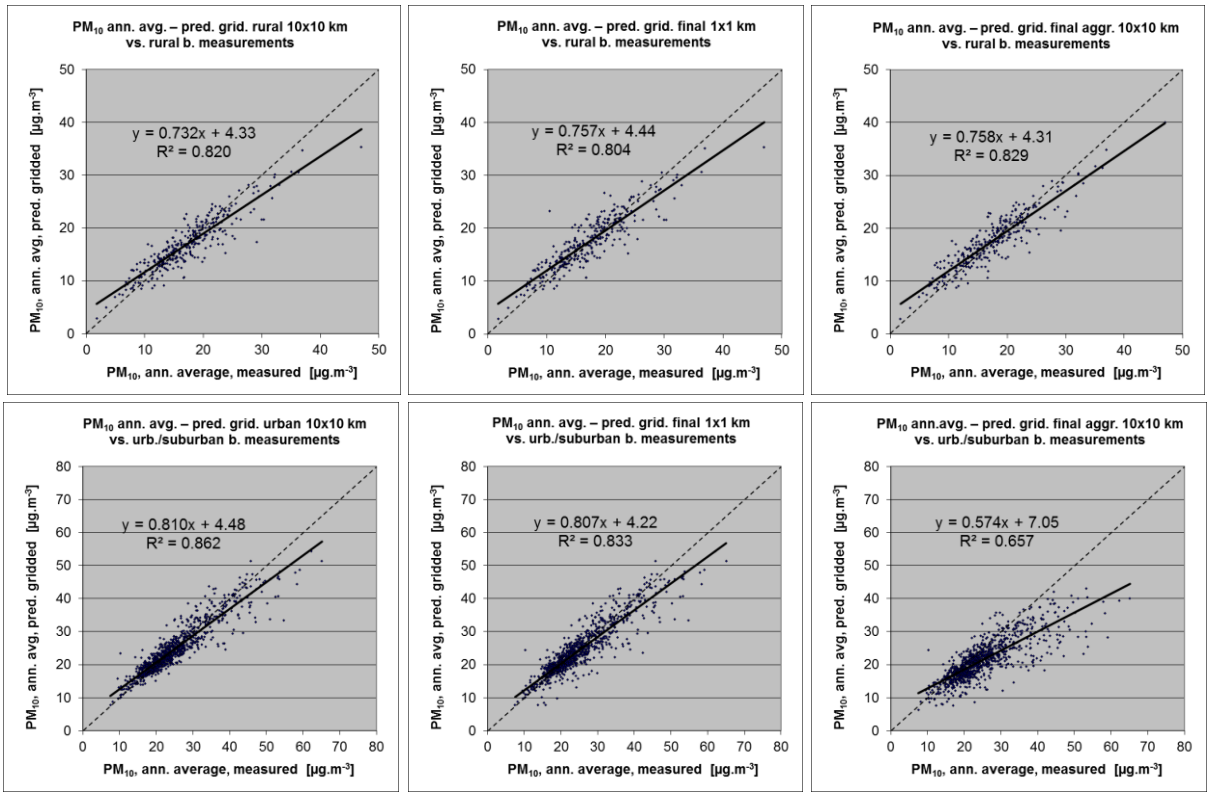

Figure 4.4 Correlation between predicted grid values from rural 10x10 km (upper left), urban 10x10 km (bottom left), final combined 1x1 km (upper and bottom middle) and final combined spatially aggregated 10x10 km (upper and bottom right) map (y-axis) versus measurements from rural (top), resp. urban/suburban (bottom) background stations (x-axis) for PM_{10} annual average 2013.

Table 4.4 Statistical indicators RMSE, bias, coefficient of determination R^2 and linear regression equation from the scatter plots for the predicted point values based on cross-validation and the predicted grid values from separate (rural resp. urban) 10x10 km, final combined 1x1 km and final combined spatially aggregated 10x10 km map versus the measured point values for rural (left) and urban (right) background stations for PM_{10} annual average of 2013.

	rural backgr. stations				urb./suburban backgr. stations			
	RMSE	bias	R^2	equation	RMSE	bias	R^2	equation
cross-valid. prediction, separate (r or ub) map	3.4	0.0	0.699	y = 0.669x + 5.72	4.3	0.0	0.743	y = 0.754x + 6.06
grid prediction, 10x10 km separate (r or ub) map	2.7	-0.3	0.820	y = 0.732x + 4.33	3.2	-0.2	0.862	y = 0.810x + 4.48
grid prediction, 1x1 km final merged map	2.8	0.3	0.804	y = 0.757x + 4.44	3.5	-0.6	0.833	y = 0.807x + 4.22
grid prediction, aggr. 10x10 km final merged map	2.6	0.1	0.829	y = 0.758x + 4.31	6.1	-3.5	0.657	y = 0.574x + 7.05

The Table 4.4 shows a better relation (i.e. lower RMSE, higher R^2, smaller intercept and slope closer to 1) between station measurements and the interpolated values of the corresponding grid cells at both rural and urban background map areas than it does at the point cross-validation predictions. That is because the simple comparison between point measurements and the gridded interpolated values shows the uncertainty at the actual station locations (points), while the point cross-validation prediction simulates the behaviour of the interpolation at point positions assuming no actual measurement would exist at that point. The uncertainty at measurement locations is caused partly by the smoothing effect of the interpolation and partly by the spatial averaging of the values in the 10x10 km grid cells. The level of the smoothing effect leading to underestimation at areas with high values is there smaller than it is in situations where no measurement is represented in such areas. For example, in urban areas the predicted interpolation gridded value in the separate urban background map will be about 53 $\mu g.m^{-3}$ at the corresponding station point with the measured value of 60 $\mu g.m^{-3}$. This means an underestimation of about 12 %. It is less than the prediction underestimation of 15 % at the same point location, when

leaving out this one actual measurement point and one does the interpolation without this station (see the previous subsection).

Probability of Limit Value exceedance

Next to the point cross-validation analysis, we constructed the map of probability of limit value exceedance. For this purpose, we used the final combined concentration map in the 10x10 km grid resolution. Based on this map, we derived, with support of the 10x10 km uncertainty map and the limit value (40 $\mu g.m^{-3}$), the probability of exceedance (PoE) map at that same resolution (Figure 4.5). It is important to emphasize that the exceedance of the spatial average of a 10x10 km grid cell can show low probability even though some smaller (e.g. urban) areas inside such a grid cell show high probability of exceedance (using finer grid cell resolution). Next to this – keeping in mind that the interpolated maps refer to the rural or (sub)urban *background* situations only, it cannot be excluded that exceedances of limit values may occur at *hotspot* and traffic locations.

The map demonstrates areas with a probability of limit value exceedance above 75 % marked in red (*high* probability) and areas below 25 % in green (*low* probability). Red indicates areas for which exceedance is *very likely* to occur due to either high concentrations close to or already above the LV accompanied with such uncertainty that exceedance is very likely, or areas with lower concentrations accompanied with high uncertainty levels reaching above the LV that excess is very likely. Vice versa, in the green areas it is *not likely* to have predicted concentrations and accompanying uncertainties at levels that do reach above the LV.

In the probability maps, the areas with 25-50 % and 50-75 % probability of LV exceedance are marked in yellow and orange respectively. The yellow colour indicates the areas with the estimated concentrations below limit value, but for which there exists a *modest* probability of exceeding the limit. On the contrary, the orange areas have estimated concentrations above the limit value, but with a chance of non-exceedance caused by its accompanying uncertainty. Table 4.5 summarises the classes and terminology for probability (i.e. likelihood) that are distinguished in this paper.

Table 4.5 Probability mapping classes and terminology use in this paper.

Map class colour	Percentage probability of threshold exceedance	Degree of probability (or likelihood) of exceedance	Likelihood of exceedance
Green	0 – 25	Low/ Little	Not likely
Yellow	25 – 50	Modest	Somewhat likely
Orange	50 – 75	Moderate	Rather Likely
Red	75 – 100	High / Large	Very likely

The patterns in the spatial distribution of the different PoE classes over Europe differ in 2013 somewhat from those of 2012. The region of southern Poland – north-eastern Czech Republic with the industrial zones of Krakow, Katowice (PL) and Ostrava (CZ) shows in 2013, a smaller area with the highest probability of exceedance (75-100 %) compared to 2012. The Po Valley in Italy shows a reduced probability of exceedance compared to 2012. In both these areas, the reduction was present already between the years 2011 and 2012. In south-eastern Europe, where relatively few measurement stations are located, especially at some larger cities with mostly high traffic density and heavy industry, only somewhat elevated PoE do show up at a few cities. In comparison with 2012, their number has reduced considerably. In other parts of Europe there exists just little likelihood of exceedance. In general, one can conclude that the likelihood of exceedance in 2013 has reduced compared to the levels of 2012. This is caused mainly by the lower concentration levels in the highly polluted areas and partly because of a reduced mapping uncertainty.

It should be noted that the PoE is related to the aggregated 10x10 km grid. In case we would produce such map on a 1x1 km grid resolution the map pattern would demonstrate elevated PoE levels clearly distinguishing smaller cities and towns as well, which are not resolved at the 10x10 km grid resolution. Furthermore, one should bear in mind that the map is based on rural and (sub)urban *background* station data only. As such the map reflects rural and urban background situations only. Therefore, this type of

map will not resolve the exceedances of limit values that may occur at the many *hotspot* and traffic locations throughout Europe.

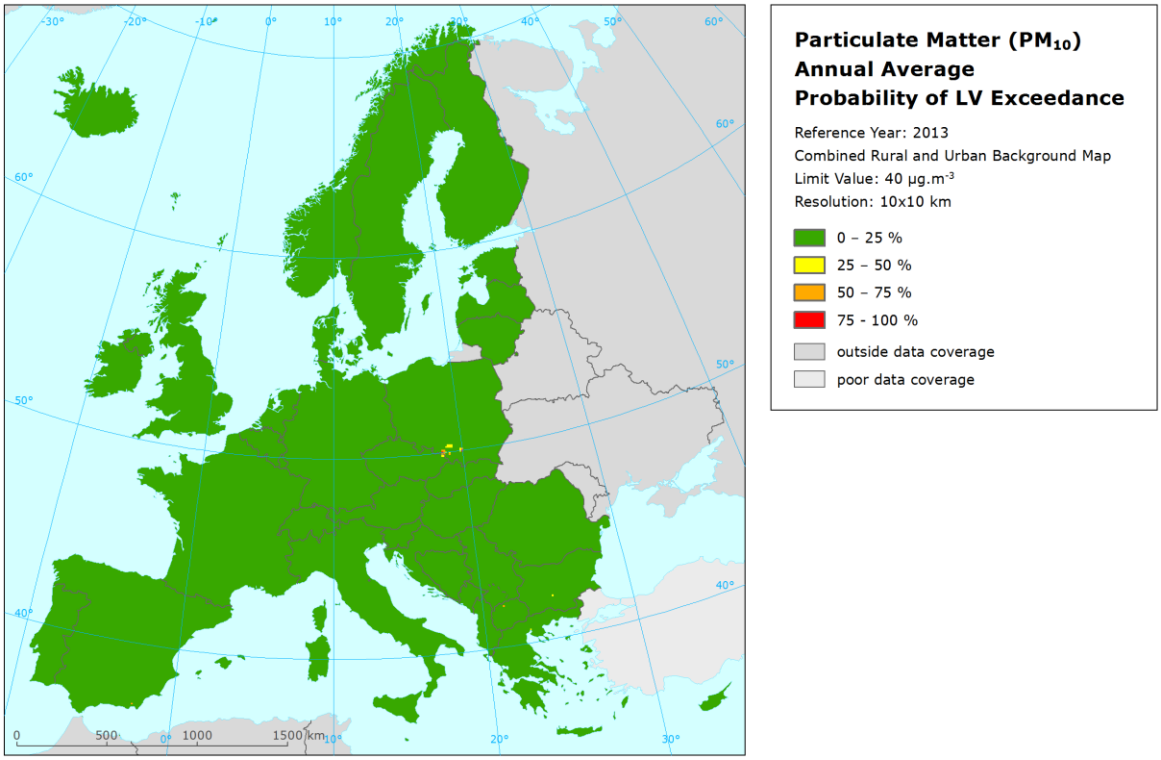

Figure 4.5 Map with the probability of the limit value exceedance for PM_{10} annual average (µg.m^{-3}) for 2013 on European scale calculated on the 10 x 10 km grid resolution. Interpolation uncertainty is considered only, no other sources of uncertainty.

4.2 36th highest daily average

4.2.1 Concentration map

Similar to the PM_{10} annual average map, the combined final map of 36th highest daily value has been derived from the separate rural, urban and joint rural/urban maps, using the same set of supplementary data parameters (Section 4.1.1) in the regression models and interpolation of residuals. Table 4.6 presents the estimated parameters of the linear regression models and of the residual kriging, including their statistical indicators.

Surface solar radiation was, like in 2010 – 2012 (and in contrast to 2006 – 2009), found to be statistically non-significant and thus it was not used in 2013 mapping.

Like in the case of annual average, the linear regression is applied for the logarithmically transformed data of both measured and modelled PM_{10} values. Thus, in Table 4.6 the standard error and variogram parameters refer to these transformed data, whereas RMSE and bias refer to the interpolation after the back-transformation.

The regressions on the 2013 data have an adjusted R^2 of 0.50 for rural areas and 0.23 for urban areas. Such a fit for rural areas is at the similar level as in 2011 – 2012 and better than all other previous years. In urban areas, the fit was the second best in the whole nine-year period, see Horálek et al. (2015) and references cited therein. RMSE and bias are the cross-validation indicators for the quality of the resulting map. Section 4.2.3 discusses in more detail the RMSE analysis and the comparison with 2005 – 2012.

Table 4.6 Parameters of the linear regression models (Eq.2.1) and of their residual ordinary kriging (OK) variograms (nugget, sill, range) - and their statistics - of PM_{10} indicator 36th highest daily mean for 2013 in the rural (left) and urban (right) areas as used for final mapping.

linear regr. model + OK on its residuals	rural areas parameter values	urban areas parameter values
c (constant)	2.27	2.05
a1 (lnEMEP model 2013)	0.555	0.555
a2 (altitude GTOPO)	-0.00049	
a3 (wind speed 2013)	-0.109	
a4 (s. solar radiation 2013)	*non signif.*	
adjusted R^2	**0.50**	**0.23**
standard error [µg.m^{-3}]	**0.27**	**0.30**
nugget	0.033	0.013
sill	0.061	0.069
range [km]	480	520
RMSE [µg.m^{-3}]	**6.37**	**8.37**
relative RMSE [%]	**21.0**	**19.2**
bias (MPE) [µg.m^{-3}]	**0.00**	**-0.06**

Figure 4.6 presents the combined final map, where areas and stations exceeding the limit value (LV) of 50 µg.m^{-3} on more than 35 days are coloured red and purple.

The concentration map is spatially aggregated from a 1x1 km to a 10x10 km grid resolution. The urban areas are not properly resolved in this map, due to the smoothing effect of the aggregation. In particular, this is seen in Bulgaria. Section 4.2.3 discusses the level of the representation of the urban areas in this final combined aggregated 10x10 km map. For better visualising the actual urban concentration levels, without the influence of the dominating pattern of extended rural areas, a separate urban background map is presented in Annex 1, Figure A1.2.

Figure 4.7 presents the inter-annual difference between 2013 and 2012 for 36th highest daily mean.

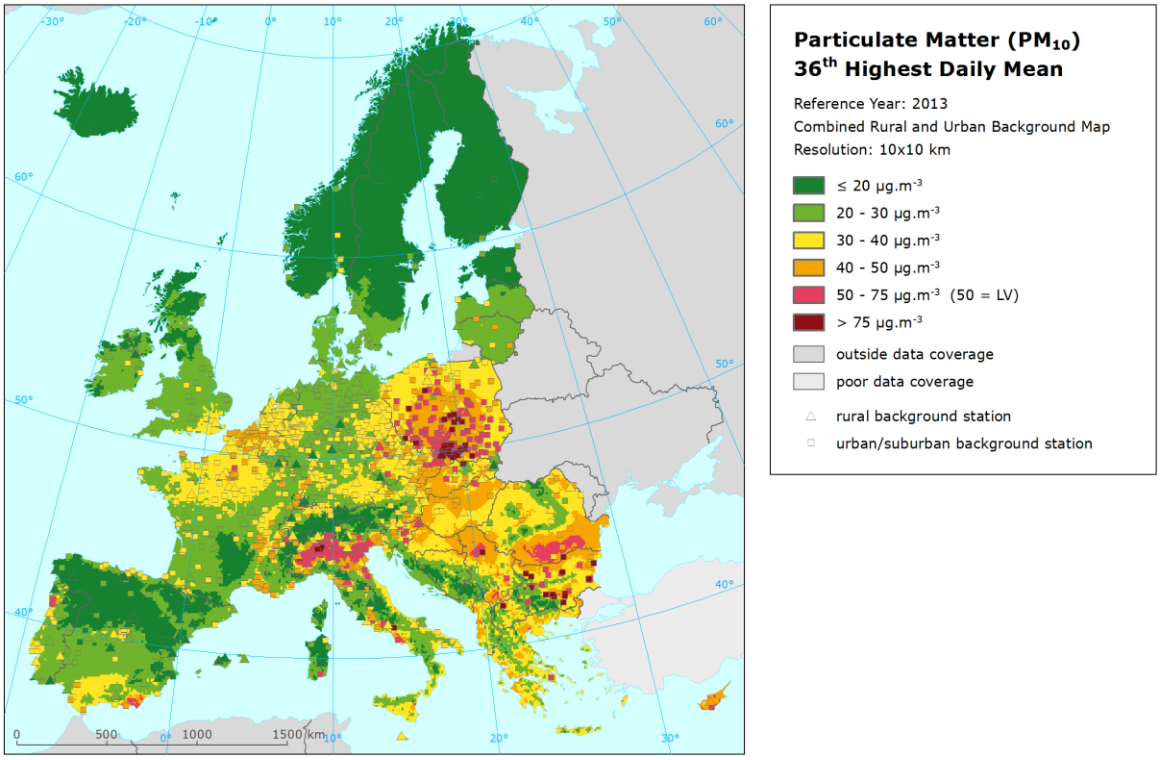

Figure 4.6 Combined rural and urban concentration map of PM_{10} – 36th highest daily average value, year 2013. Spatial interpolated concentration field (10x10 km grid resolution, excluding Turkey due to lack of air quality data) and the measured values in the measuring points. Units: µg.m^{-3}.

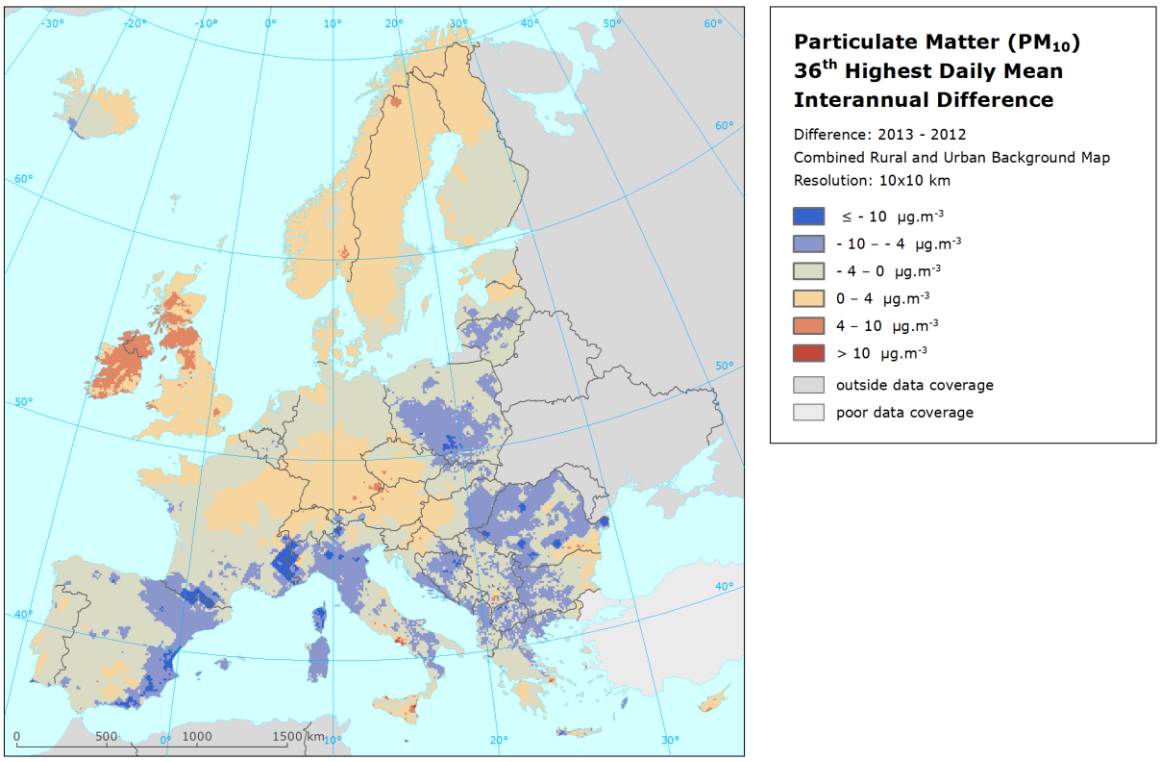

Figure 4.7 Inter-annual difference between mapped concentrations for 2013 and 2012 – PM_{10}, 36th highest daily average value. Units: µg.m^{-3}. Resolution: 10x10 km.

Red areas in the inter-annual difference map show an increase of PM_{10} concentration, while blue areas show a decrease. The highest increase s are observed in Ireland and Scotland. The largest decrease is observed in the Iberian Peninsula, the Pyrenees and the western part of the Alps similar to that of the increases observed in the '2012-2011' difference map (Horálek et al, 2015). Next to this, the decreased indicator values in 2012, compared to those of 2011, can be seen in the large part of Italy, Romania and some other Balkan countries and Poland.

4.2.2 Population exposure

Table 4.7 gives the population frequency distribution for a limited number of exposure classes calculated at 1x1 km grid resolution, as well as the population-weighted concentration for individual countries and for Europe as a whole. Table 4.8 shows the evolution of the population exposure in the last nine years.

It has been estimated that in 2013 about 16 % of the European population lived in areas where the 36th highest daily mean of PM_{10} exceeded the limit value of 50 $\mu g.m^{-3}$. This is the same as in 2012 and 2009, slightly more than in 2011, and less than in the years 2010 and 2005 – 2008. In Albania, Bulgaria, Cyprus, Greece, FYR of Macedonia, Malta. Montenegro, Poland and Serbia both the population-weighted indicator concentration and the median were above the LV, implying that in these countries the average concentration exceeded the LV and more than half of the population was exposed to concentrations exceeding the LV. In comparison with 2012, a decrease of both population living above the LV and an increased population-weighted concentration occurs in some countries of central and south-eastern Europe (in Poland, Slovakia, the Czech Republic, Slovenia, Hungary, Romania, Bosnia-Herzegovina, Serbia). An increase of both exposure indicators is detected in Greece, FYR of Macedonia and Bulgaria.

In the EU-28, about 15 % of the population lived in areas above the limit value. According to EEA (2015), in 2013 about 17 % of the urban population in the EU-28 was exposed to PM_{10} above the limit value. The difference between the two estimates is caused by the fact that the EEA estimated only for the urban population of the larger cities, while in Table 4.8 the total population of the EU-28, including inhabitants in rural areas, smaller cities and villages has been considered.

The European-wide population-weighted concentration of the 36th highest daily mean is estimated for the year 2013 at 38.6 $\mu g.m^{-3}$, being the lowest in the period of 2005 – 2013.

Like at previous years, for 2013 the comparison between the examined PM_{10} exceedances, i.e. the annual average of section 4.1.2 with the 36th highest daily average in this section, leads to the conclusion that the daily average limit value is more stringent of the two.

Table 4.7 Population exposure and population-weighted concentration – PM_{10}, 36th highest daily average value, year 2013. Resolution: 1x1 km.

Country		Population	PM_{10}, 36th highest d. a., exposed population [%]						Pop. weighted conc.
			< LV				> LV		
			< 20	20 - 30	30 - 40	40 - 50	50 - 75	> 75	
		[inhbs . 1000]	µg.m^{-3}	µg.m^{-3}	µg.m^{-3}	µg.m^{-3}	µg.m^{-3}	µg.m^{-3}	[µg.m^{-3}]
Albania	AL	2 899	0.1	3.5	9.6	9.6	74.2	2.9	59.4
Andorra	AD	76	0.6	0.6	1.0	97.7			47.5
Austria	AT	8 452	2.0	10.2	51.7	36.1			36.7
Belgium	BE	11 162		1.8	28.3	69.9			40.7
Bosnia & Herzegovina	BA	3 836	1.1	8.5	18.1	55.1	17.2		43.3
Bulgaria	BG	7 285	0.2	1.7	5.3	10.6	59.5	22.7	66.8
Croatia	HR	4 262	0.2	5.9	18.0	52.6	23.3		44.0
Cyprus	CY	866			0.9	11.2	87.9		55.9
Czech Republic	CZ	10 516		1.3	18.7	63.5	13.2	3.2	45.8
Denmark	DK	5 603	0.5	98.6	0.7	0.2			26.2
Estonia	EE	1 320	23.9	76.1					22.4
Finland	FI	5 427	92.4	7.6					17.6
France (metropolitan)	FR	63 652	1.0	16.8	51.9	30.2	0.0	0.0	36.2
Germany	DE	80 524	0.0	23.4	75.9	0.6			32.7
Greece	GR	11 004	0.0	1.3	6.8	7.2	64.2	20.4	59.7
Hungary	HU	9 909			20.9	72.9	6.2		43.8
Iceland	IS	322	61.3	37.5	1.1				19.4
Ireland	IE	4 591	3.5	82.8	13.8				25.6
Italy	IT	59 685	0.6	5.9	19.1	29.3	45.1	0.0	48.9
Latvia	LV	2 024	1.5	28.3	70.3				32.5
Liechtenstein	LI	37	1.4	8.5	90.0				32.3
Lithuania	LT	2 972		24.1	72.0	3.9			33.5
Luxembourg	LU	537		18.8	81.2				31.3
Macedonia, FYROM of	MK	2 062	0.0	1.0	2.2	1.4	9.9	85.4	88.8
Malta	MT	421			1.3	1	97.6		61.5
Monaco	MC	38			100.0				38.4
Montenegro	ME	621	4.0	9.6	8.0	10.0	68.1	0.3	51.9
Netherlands	NL	16 780		12.2	86.5	1			33.8
Norway	NO	5 051	36.4	38.5	25.0	0.0			23.4
Poland	PL	38 063	0.0	0.4	19.1	23.7	44.0	12.7	54.1
Portugal (excl. Az., Mad.)	PT	9 977	2.6	25.2	53.1	19.0	0.0		34.0
Romania	RO	20 020	0.1	3.0	34.1	38.6	24.2	0.0	43.5
San Marino	SM	34		4.7	14.9	80			39.8
Serbia (incl. Kosovo*)	RS	8 997	0.0	1.8	6.5	20.3	54.3	17.0	59.4
Slovakia	SK	5 411	0.0	0.4	7.8	65.5	26.3	0.0	46.6
Slovenia	SI	2 059	0.0	5.8	27.5	61.1	5.6		41.8
Spain (excl. Canarias)	ES	44 623	2.9	43.6	41.9	10.4	1.1	0.0	30.4
Sweden	SE	9 556	22.7	77.2	0.1				21.8
Switzerland	CH	8 039	2.1	10.5	64.3	23.1			36.4
United Kingdom (& dep.)	UK	63 905	0.9	66.5	32.5	0.1			28.1
Total		**532 614**	**2.5**	**23.5**	**38.7**	**18.9**	**14.0**	**2.3**	**38.6**
			83.6				**16.4**		
EU-28		**500 603**	**2.2**	**24.3**	**39.5**	**18.9**	**13.3**	**1.8**	**38.1**
			84.9				**15.1**		
Kosovo*	KS	1 816	0.0	1.4	7.5	5.7	18.0	67.3	77.4
Serbia (excl. Kosovo*	RS	7 182	0.0	1.9	6.3	23.8	63.2	4.8	55.0

*) under the UN Security Council Resolution 1244/99

Note1: Turkey is not included in the calculation due to lacking air quality data.
Note2: The percentage value "0.0" indicates an exposed population exists, but is small and estimated less than 0.05 %. Empty cells mean: no population in exposure.

Table 4.8 Evolution of population-weighted concentration in the years 2005-2013 (left) and of percentage population living in above limit value in the years 2009-2013 (right) – PM_{10}, 36th highest daily average value. Resolution: 1x1 km.

Country		Population-weighted conc. [µg.m^{-3}]										Popul. above LV 50 µg.m^{-3} [%]					
		2005	2006	2007	2008	2009	2010	2011	2012	2013	diff. '13 - '12	2009	2010	2011	2012	2013	diff. '13 - '12
Albania	AL	59.8	54.0	53.3	55.7	51.3	69.5	42.8	56.1	59.4	3.3	62.4	78.4	21.2	66.6	77.2	10.6
Andorra	AD	31.1	35.7	32.1	29.3	29.4	28.5	29.2	75.2	47.5	-27.7	0	0	0	88.4	0	-88.4
Austria	AT	45.7	47.1	39.9	36.9	36.7	42.8	38.7	35.8	36.7	0.9	0	23.8	22.8	0	0	0
Belgium	BE	46.9	51.3	43.5	38.4	45.8	42.7	45.1	43.5	40.7	-2.7	3.3	0	7.0	0	0	0
Bosnia-Herzegovina	BA	57.3	57.4	52.7	50.6	57.8	53.7	40.8	50.8	43.3	-7.5	65.7	64.9	19.1	59.3	17.2	-42.1
Bulgaria	BG	73.3	74.2	67.5	78.2	70.3	69.2	46.6	65.8	66.8	1.0	73.4	80.2	20.8	74.2	82.3	8.0
Croatia	HR	57.6	53.7	49.6	48.6	46.9	50.5	46.6	44.8	44.0	-0.8	27.7	58.6	37.6	17.8	23.3	5.5
Cyprus	CY	63.7	58.2	54.4	130.7	68.6	74.5	46.2	60.2	55.9	-4.3	80.6	99.0	12.9	81.3	87.9	6.6
Czech Republic	CZ	60.2	57.5	46.2	42.5	43.6	53.7	46.2	46.7	45.8	-0.9	14.7	47.2	31.0	22.4	16.4	-6.0
Denmark	DK	34.5	37.0	32.5	29.0	26.0	25.5	31.6	25.9	26.2	0.3	0	0	0	0	0	0
Estonia	EE	31.7	34.1	28.0	22.4	22.4	25.8	17.6	21.4	22.4	1.0	0	0	0	0	0	0
Finland	FI	24.2	29.5	23.9	21.9	19.4	22.7	16.9	18.1	17.6	-0.5	0	0	0	0	0	0
France	FR	29.8	32.9	41.0	36.3	39.2	37.1	36.6	37.6	36.2	-1.4	3.0	0	3.2	1.4	0.1	-1.3
Germany	DE	38.6	41.3	35.7	31.7	34.4	37.2	35.7	32.6	32.7	0.1	0	0.5	0.5	0	0	0
Greece	GR	59.9	54.3	53.0	64.9	54.7	64.8	37.6	47.1	59.7	12.6	38.2	95.7	7.5	24.8	84.7	59.9
Hungary	HU	61.6	58.5	48.5	47.5	46.4	52.3	55.4	46.0	43.8	-2.2	24.4	69.4	92.1	18.2	6.2	-12.0
Iceland	IS	19.0	27.2	21.4	25.4	15.8	16.8	15.8	17.1	19.4	2.4	0	0.0	0	0	0	0
Ireland	IE	17.8	24.1	24.8	25.8	21.7	23.2	23.2	21.2	25.6	4.4	0	0	0	0	0	0
Italy	IT	60.2	58.6	57.4	51.7	48.6	45.2	48.6	47.2	48.9	1.7	31.9	31.2	39.5	34.6	45.1	10.5
Latvia	LV	35.9	40.0	31.9	32.7	33.4	37.8	26.7	33.0	32.5	-0.5	0	0	0	0	0	0
Liechtenstein	LI	40.2	47.5	39.3	38.5	31.5	33.6	21.3	27.6	32.3	4.7	0	0	0	0	0	0
Lithuania	LT	37.7	39.7	33.2	29.5	32.7	39.5	26.6	33.1	33.5	0.4	0	0	0	0	0	0
Luxembourg	LU	31.2	35.9	32.5	29.1	34.3	31.9	29.4	30.0	31.3	1.3	0	0	0	0	0	0
Macedonia, FYR of	MK	77.5	69.9	57.8	71.5	75.6	80.1	37.9	78.3	88.8	10.5	80.3	87.7	3.5	80.7	95.3	14.7
Malta	MT	62.7	44.8	42.6	40.3	38.7	49.4	39.7	37.2	61.5	24.3	0	3.3	0	0	97.6	97.6
Monaco	MC		59.7	46.2	46.0	41.5	36.1	37.0	45.5	38.4	-7.1	0	0	0	0	0	0
Montenegro	ME	58.7	57.9	53.6	56.7	51.8	54.0	36.2	53.5	51.9	-1.5	65.7	66.9	12.3	67.2	68.3	1.1
Netherlands	NL	47.5	46.1	41.9	37.7	39.0	40.2	44.0	35.1	33.8	-1.3	0	0	0	0	0	0
Norway	NO	29.3	31.9	26.3	26.1	24.0	25.7	16.3	21.6	23.4	1.8	0	0	0	0	0	0
Poland	PL	58.6	64.0	50.8	48.6	55.4	65.7	51.4	60.6	54.1	-6.5	60.5	71.3	41.3	65.3	56.7	-8.6
Portugal	PT	52.0	48.3	45.0	35.5	38.5	35.6	35.4	35.1	34.0	-1.2	0	0.2	4.9	1.6	0.0	-1.5
Romania	RO	73.4	65.4	57.7	53.1	49.0	45.2	48.1	48.8	43.5	-5.3	39.8	28.2	43.3	35.7	24.2	-11.5
San Marino	SM	51.7	57.4	54.1	48.9	40.6	44.0	35.9	43.8	39.8	-4.0	0	0	0	0	0	0
Serbia (incl. Kosovo)	RS	73.1	73.1	61.8	68.6	67.6	60.1	54.6	62.1	59.4	-2.7	77.8	80.5	52.9	74.3	71.4	-2.9
Slovakia	SK	60.9	58.5	50.5	47.5	46.2	56.0	51.5	50.4	46.6	-3.8	33.5	82.3	62.4	41.1	26.4	-14.7
Slovenia	SI	53.7	49.2	46.1	42.7	41.9	47.2	48.1	43.5	41.8	-1.8	0	38.6	39.1	19.6	5.6	-14.0
Spain	ES	46.7	49.3	46.9	40.1	38.0	33.4	30.5	33.5	30.4	-3.1	1.0	0.1	1.1	1.1	1.1	0.0
Sweden	SE	28	32.0	25.8	26.4	23.3	22.1	21.1	20.5	21.8	1.3	0	0	0	0	0	0
Switzerland	CH	36.0	43.9	39.9	36.5	37.1	36.3	33.0	32.6	36.4	3.8	0.9	0	1.3	0.9	0	-0.9
United Kingdom	UK	33	35.5	34.7	32.1	30.1	28.8	30.3	28.8	28.1	-0.7	0	0	0	0	0	0
Total		**46.8**	**47.8**	**44.1**	**41.3**	**41.2**	**41.9**	**39.0**	**39.7**	**38.6**	**-1.1**	**16.5**	**20.6**	**15.8**	**16.5**	**16.4**	**-0.1**
EU-28		**46.1**	**47.2**	**43.8**	**40.5**	**40.5**	**41.3**	**39.0**	**39.2**	**38.1**	**-1.1**	**14.6**	**18.8**	**15.4**	**14.7**	**15.1**	**0.4**

4.2.3 Uncertainties

Uncertainty estimated by cross-validation

Cross-validation analysis determines the uncertainty. For the combined map of PM_{10} indicator 36th highest daily mean in 2013, Table 4.6 shows an absolute mean uncertainty (expressed as the RMSE) of 6.4 µg.m^{-3} for rural areas and 8.4 µg.m^{-3} for urban areas. This indicates the best fit for both rural and urban areas compared to all its previous. The relative mean uncertainty (absolute RMSE relative to the

mean indicator value) of the 2013 map of PM_{10} indicator 36th highest daily mean is 21.0 % for rural and 19.2 % for urban areas, i.e. in both the cases the lowest result for the whole nine-year period. In urban areas, the low uncertainty level is influenced by the lack of Turkish urban background stations in 2013. These stations were reported since 2008 to 2012, but not in 2013. (Turkish urban stations show high concentrations, uncertainty statistics are sensitive to such values.) Table 7.5 summarises both the absolute and relative uncertainties over the past nine years.

Figure 4.8 shows the cross-validation scatter plots for both rural and urban areas. The R^2 indicates that for rural areas about 69 % and for urban areas about 75 % of the variability is attributable to the interpolation. Corresponding values with those of the years 2015 – 2012 (see Table 7.5) do show that the fit of 2013 is the best for rural areas and comparable to the last five years for urban areas.

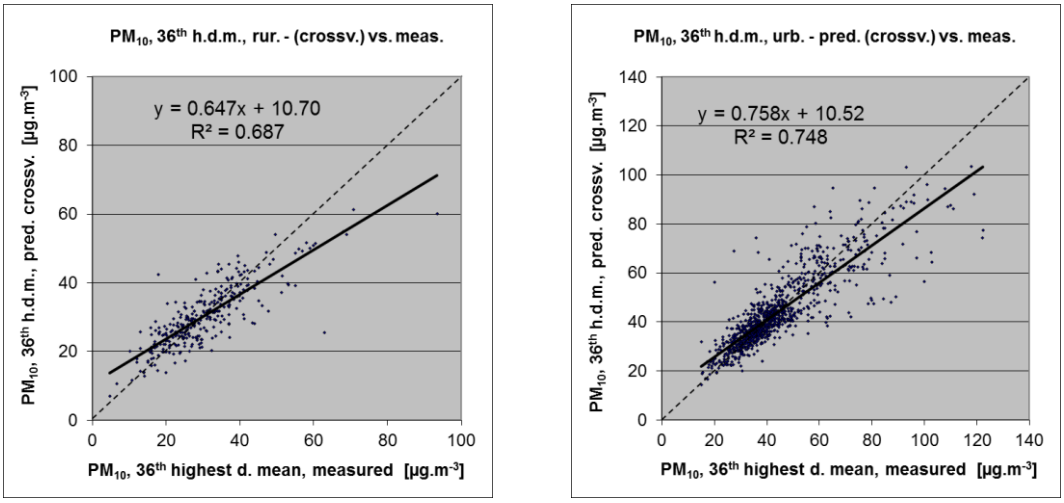

Figure 4.8 Correlation between cross-validation predicted values (y-axis) and measurements (x-axis) for the PM_{10} indicator 36th highest daily mean for 2013 for rural (left) and urban (right) areas.

The scatter plots indicate that in areas with high concentrations the interpolation methods tend to underestimate the levels. For example, in urban areas (Figure 4.8, right panel) an observed value of 100 $\mu g.m^{-3}$ would be estimated in the interpolation as about 86 $\mu g.m^{-3}$, i.e. about 14 % too low. For rural areas, the underestimation is slightly stronger.

Comparison of point measurement values with the predicted grid value

In addition to the point observation – point prediction cross-validation, a simple comparison was made between the point observation values and interpolation predicted grid values. The comparison has been made primarily for the separate rural and separate urban background maps at 10x10 km resolution. (This comparison result one can directly relate to the cross-validation results of Figure 4.8.)

Next to this, the comparison has been done also for the final combined maps at 1x1 km resolution and for the spatial aggregated final maps at 10x10 km resolution. Figure 4.9 shows the scatterplots for these comparisons.

The results of the point observation – point prediction cross-validation of Figure 4.8 and those of the point-grid validation for separate rural and separate urban background maps, and for the final combined maps at both resolutions are summarised in Table 4.9.

By the comparing the scatterplots and the statistical indicators for the separate rural and separate urban background map with the final combined maps in both resolutions, one can evaluate the level of representation of the rural resp. urban background areas in the final combined maps. The rural air quality is fairly well represented in both the 1x1 km and the aggregated 10x10 km final combined map. The urban air quality is quite well represented in the final combined 1x1 km map, but not in the aggregated final combined 10x10 km map as one can deduct from its higher RMSE, its bias being further from zero

and its lower R^2. Therefore, we present in Figure A1.2 of Annex 1 the 1x1 km urban background map in addition to the 10x10 km final combined map of Figure 4.6.

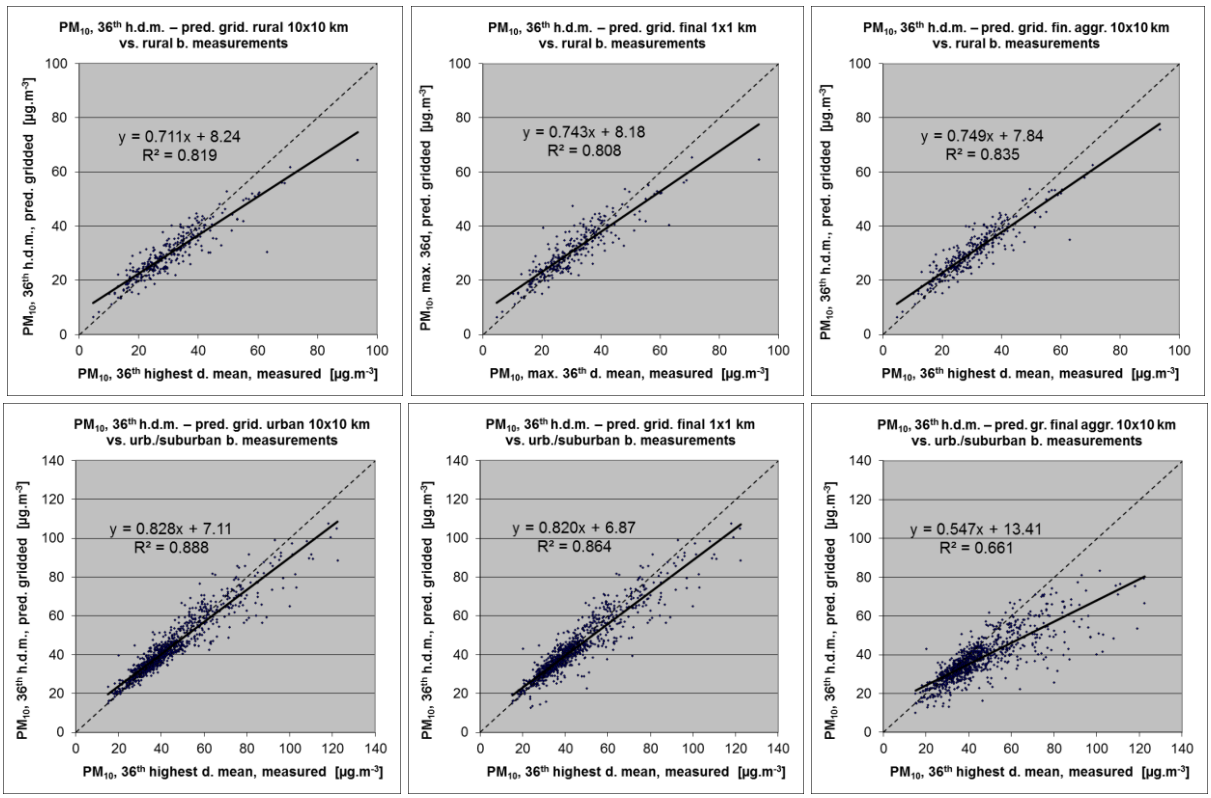

Figure 4.9 Correlation between predicted grid values from rural 10x10 km (upper left), urban 10x10 km (bottom left), final combined 1x1 km (upper and bottom middle) and final combined spatially aggregated 10x10 km (upper and bottom right) map (y-axis) versus measurements from rural (top), resp. urban/suburban (bottom) background stations (x-axis) for PM_{10} indicator 36th highest daily mean 2013.

The comparison of the cross-validation with the gridded validation shows higher correlation of the gridded validation for both the rural and the urban background maps. That is because the simple grid validation shows the uncertainty at the actual measurement locations, while the point cross-validation prediction simulates the behaviour of the interpolation at points assuming no actual measurements would exist at these points. The uncertainty at measurement locations is caused partly by the smoothing effect of the interpolation and partly by the spatial averaging of the values in the 10x10 km grid cells. The level of smoothing, which leads to underestimation in areas with high values, is weaker in areas where measurements exist than in areas where a measurement point is not available. For example, in urban areas the predicted interpolation gridded value in the separate urban background map would be about 90 µg.m^{-3} at a corresponding station point with a measurement value of 100 µg.m^{-3}. This is an underestimation of 10 %. It is less than the prediction underestimation of 14 % at the point locations without measuring stations (see the previous subsection).

Table 4.9 Statistical indicators RMSE, bias, coefficient of determination R^2 and linear regression equation from the scatter plots for the predicted point values based on cross-validation and the predicted grid values from separate (rural resp. urban) 10x10 km, final combined 1x1 km and final combined spatially aggregated 10x10 km map versus the measured point values for rural (left) and urban (right) background stations for PM_{10} indicator 36th highest daily mean for 2013.

	rural backgr. stations				urb./suburban backgr. stations			
	RMSE	bias	R^2	equation	RMSE	bias	R^2	equation
cross-valid. prediction, separate (r or ub) map	6.4	0.0	0.687	y = 0.647x + 10.1	8.4	-0.1	0.748	y = 0.758x + 10.5
grid prediction, 10x10 km separate (r or ub) map	5.0	-0.5	0.819	y = 0.711x + 8.2	5.7	-0.4	0.888	y = 0.828x + 7.1
grid prediction, 1x1 km final merged map	5.1	0.4	0.808	y = 0.743x + 8.2	6.3	-1.0	0.864	y = 0.820x + 6.8
grid prediction, aggr. 10x10 km final merged map	4.7	0.2	0.835	y = 0.749x + 7.8	11.8	-6.4	0.661	y = 0.547x + 13.4

Probability of Limit Value exceedance

Again, we constructed the map with the probability of the limit value exceedance (PoE), using an aggregated 10x10 km gridded concentration map, the 10x10 km gridded uncertainty map and the limit value (LV, 50 $\mu g.m^{-3}$). Figure 4.10 presents the probability of exceedance 10x10 km gridded map classifying the areas with probability of LV exceedance below 25 % (little PoE) in green, between 25-50 % (modest PoE) in yellow, between 50-75 % (moderate PoE) in orange and above 75 % in red (large PoE). Section 4.1.3 explains in more detail the significance of the colour classes in the map.

Comparing the probabilities of exceedance (PoE) of 2012 (see Horálek et al, 2015) and 2011 (Horálek et al., 2014a) with those of 2013, one can conclude that a decrease in the spatial extents and PoE levels in south-eastern Europe continues to occur in 2013.

The Po Valley in northern Italy has slightly reduced PoE pattern compared to 2012. Throughout the years 2009 – 2013, areas with continued increased PoE levels do occur in southern Poland and north-eastern Czech Republic. However, their extent towards northern and southern direction (central Poland, Slovakia, and Hungary) reduced considerably compared to 2011 and 2012. Northern Serbia, southern Romania, and the centre of Bulgaria show throughout the years 2010 – 2013 areas with continued high PoE levels, however the extent of these areas was reduced.

The increased levels of PoE area around Almería, southern Spain, has slightly reduced in 2013 compared to the year 2012.

It should be noted that the PoE is related to the aggregated 10x10 km grid. In case we would produce such map on a 1x1 km grid resolution the map pattern would demonstrate elevated PoE levels clearly distinguishing smaller cities and towns as well, which are not resolved at the 10x10 km grid resolution. Next to this – bearing in mind that the interpolated maps refer to the rural or (sub)urban background situations only, it cannot be excluded that exceedances of limit values may occur at the many *hotspot* and traffic locations throughout Europe, which are not resolved by this type of map.

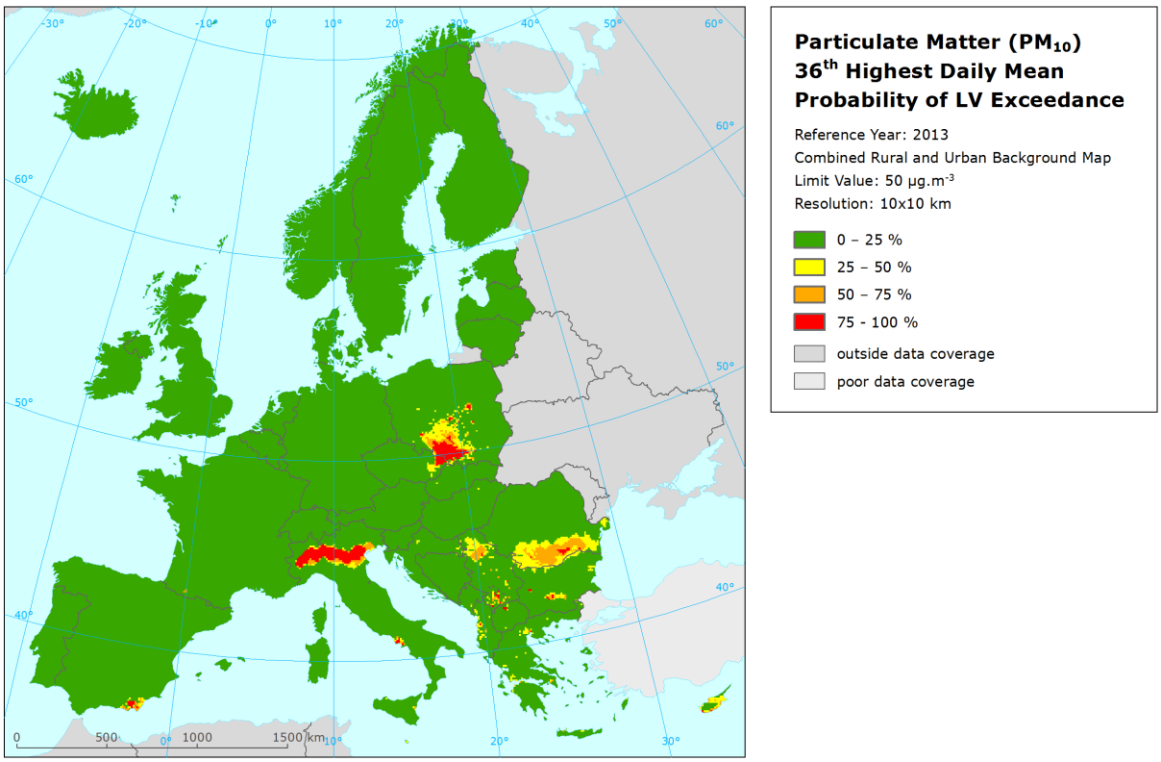

Figure 4.10 Map with the probability of the limit value exceedance for PM_{10} indicators 36th highest daily mean ($\mu g.m^{-3}$) for 2013 on the European scale calculated on the 10 x 10 km grid resolution. Interpolation uncertainty is considered only, no other sources of uncertainty.

5 $PM_{2.5}$ maps

This chapter presents the health indicator $PM_{2.5}$ annual average, based on the mapping methodology developed in Denby et al. (2011b, 2011c). To increase the spatial coverage of measurements, pseudo $PM_{2.5}$ stations data were used in addition to quite limited number of stations with measured $PM_{2.5}$ data. The separate urban and rural concentration maps were calculated on a grid of 10x10 km resolution and the subsequent combined concentration map was based on the 1x1 km gridded population density map. Population exposure tables are calculated on a grid of 1x1 km resolution. All maps are presented in at 10x10 km resolution. The standard EEA ETRS89-LAEA5210 coordinate reference system was applied.

5.1 Annual average

5.1.1 Concentration map

Figure 5.1 presents the combined final map for the 2013 $PM_{2.5}$ annual average as the result of the interpolation and merging of the separate maps as described in detail in De Smet et al. (2011), using both measured $PM_{2.5}$ and pseudo $PM_{2.5}$ station data, as described in Denby (2011c). The purple areas and stations exceed the target value (TV) of 25 $\mu g.m^{-3}$. This TV will become a limit value in year 2015. In the AQ directive there is also an indicative LV of 20 $\mu g.m^{-3}$ which could come into force in 2020. Red areas and stations show exceedances of this indicative LV. Pseudo $PM_{2.5}$ stations data are estimated using PM_{10} measured data, surface solar radiation, latitude and longitude.

Supplementary data in the regression used for rural areas consist of EMEP model output, altitude, wind speed, surface solar radiation and population density. Based on advice of Horálek et al. (2015), we used EMEP model output as a supplementary data source for the urban areas. The relevant supplementary data for the estimation of both pseudo $PM_{2.5}$ station data and the linear regression submodel and its residual kriging in the rural areas were identified earlier in Denby et al. (2011b, 2011c).

As one can observe in a few areas of the map, the high urban background measurement values do not seem to influence the interpolation results despite their clustering. The main reason is that the map presented here is an aggregation of 1x1 km grid values to a 10x10 km resolution and this aggregation smooths out the elevated values one would more likely be able to distinguish in a higher resolution map, especially in the case of urban stations representing the urban background areas. Another less prominent reason is the smoothing effect kriging has in general. However in the case of clustering, kriging would not mask these elevations in the separate 1x1 km urban and rural maps.

Table 5.1 presents the regression coefficients determined for pseudo $PM_{2.5}$ stations data estimation, based on the stations with both $PM_{2.5}$ and PM_{10} measurements (see Section 2.1.1). The number of such type of stations is 487. The same supplementary data as in Denby (2011c) are used. However, the including of the population density in the regression model was found not be significant (like in 2010 – 2012). Its further use is to be considered.

Table 5.1 Parameters of the linear regression model (Eq. 2.1) and its statistics for generation of pseudo $PM_{2.5}$ stations data, without regard to the rural or urban/suburban type of the stations, for $PM_{2.5}$ 2013 annual average.

linear regr. model	both rural and urban areas parameter values
c (constant)	36.70
b (PM_{10} measured data, 2013 annual average)	0.666
a1 (population)	*non signif.*
a2 (surface solar radiation 2012)	-1.440
a3 (latitude)	-0.446
a4 (longitude)	0.071
adjusted R^2	**0.89**
standard error [$\mu g.m^{-3}$]	**2.22**

The R^2 values show a weaker fit of the regression than observed in 2010 (0.95), but stronger than observed in the year 2008 (0.84) and similar as observed in the years 2012, 2011 and 2007 (0.89). No $PM_{2.5}$ map was produced for 2009, as we only started producing such map on a regular basis for the year 2010 and onward.

Table 5.2 presents the estimated parameters of the linear regression models (c, a_1, a_2,...) and of the residual kriging (*nugget, sill, range*) and includes the statistical indicators of both the regression and the kriging. The adjusted R^2 and standard error are indicators for the quality of the fit of the regression relation, where the adjusted R^2 should at the best be as close to 1 as possible and the standard error should be as small as possible. The adjusted R^2 is 0.55 for the rural areas. Such a fit is worse than for 2012 (0.57) and 2011 (0.60), while better than for other previous years, see Horálek et al. (2015) and references cited therein. The adjusted R^2 is 0.40 for urban areas, i.e. more than in 2012 (0.35). No supplementary data were used in the previous years; see Denby et al. (2011c).

RMSE and bias are the cross-validation indicators, showing the quality of the resulting map; the bias indicates to what extent the estimation is un-biased. Only stations with measured (i.e. non-pseudo) $PM_{2.5}$ data are used for calculating RMSE and bias. Section 5.1.3 deals with a more detailed cross-validation analysis.

Like in the case of PM_{10}, the linear regression is applied on the logarithmically transformed data of both measured and modelled $PM_{2.5}$ values. Thus, in Table 5.2 the standard error and variogram parameters refer to these transformed data, whereas RMSE and bias refer to the interpolation after the back-transformation.

Table 5.2 Parameters of the linear regression models (Eq. 2.2) and of their residual ordinary kriging (OK) variograms (nugget, sill, range) – and their statistics – of $PM_{2.5}$ indicator annual average for 2013 in the rural (left) and urban (right) areas as used for the combined final map.

linear regr. model + OK on its residuals	rural areas parameter values	urban areas parameter values
c (constant)	1.17	1.44
a1 (log. EMEP model 2013)	0.689	0.63
a2 (altitude GTOPO)	-0.00023	
a3 (wind speed 2013)	-0.071	
a4 (s. solar radiation 2013)	*non signif.*	
a4 (log. population density)	0.022	
adjusted R^2	**0.55**	**0.40**
standard error [µg.m^{-3}]	**0.31**	**0.28**
nugget	0.037	0.015
sill	0.059	0.055
range [km]	300	540
RMSE [µg.m^{-3}]	**2.73**	**2.90**
relative RMSE [%]	**22.1**	**17.5**
bias (MPE) [µg.m^{-3}]	**-0.05**	**0.26**

The merging of the separate rural and urban background maps takes place on the 1x1 km resolution map of population density.

According to Figure 5.1, the most polluted areas seem to be the Katowice (PL) and Ostrava (CZ) industrial region, together with the Po Valley in Northern Italy. Furthermore, the southern part of

Romania with Bucharest as in it suffers from elevated $PM_{2.5}$ annual average concentrations and to a somewhat less extent the area around cities Belgrade and Novi Sad in Serbia.

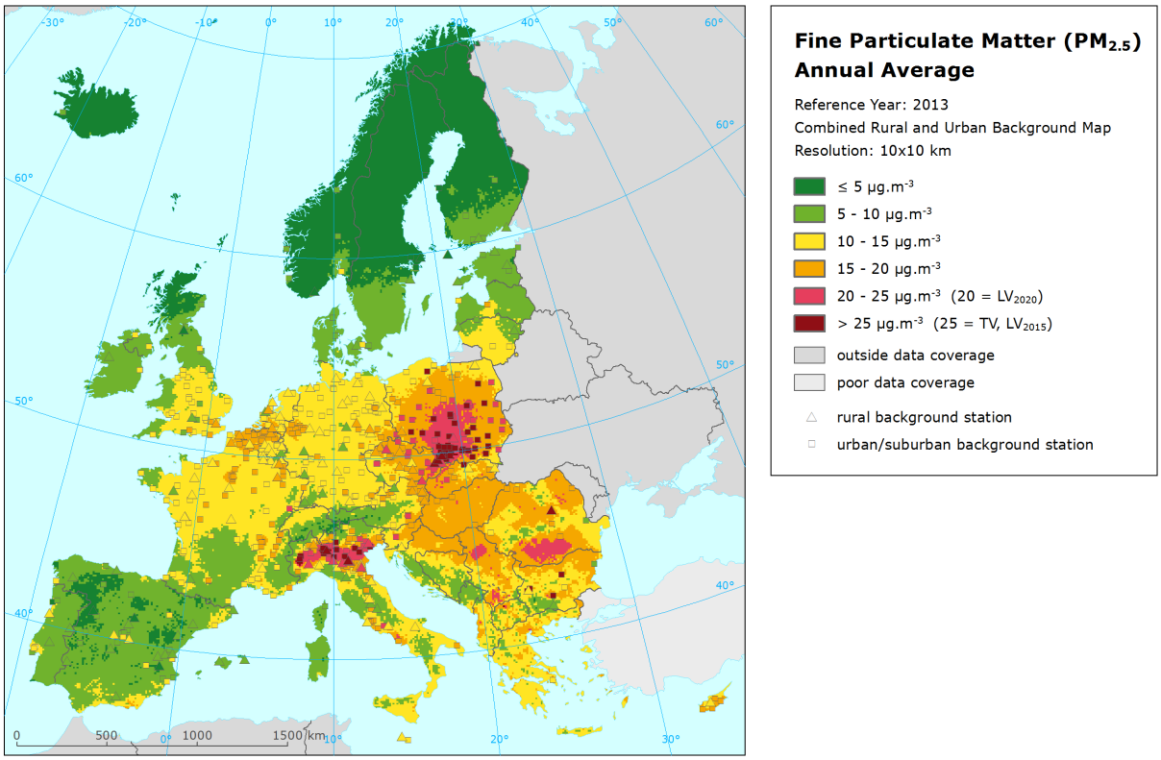

Figure 5.1 Combined rural and urban concentration map of $PM_{2.5}$ – annual average, year 2013. Spatial interpolated concentration field and the measured values in the measuring points. Units: µg.m^{-3}.

The concentration map presented in Figure 5.1 is spatially aggregated from 1x1 km to a 10x10 km grid resolution. As a result, the urban areas are not properly resolved in this map, due to the smoothing effect of this aggregation. Section 5.1.3 discusses the level of the representation of the urban areas in this final combined aggregated 10x10 km map. For better visualising the actual urban concentration levels at the actual urbanised areas, i.e. without the influence of the dominating pattern of extended rural areas, a separate 1x1 km urban background map is presented in Annex 1, Figure A1.3.

Figure 5.2 presents the inter-annual difference between 2013 and 2012 for annual average $PM_{2.5}$. Red areas show an increase of $PM_{2.5}$ concentration, while blue areas show a decrease. The highest increases we see in the British Isles, in the western France, in the large areas of the central Europe like Germany, Switzerland, the Czech Republic, Austria and Poland, and in the central and north-western parts of Romania. The steepest decrease one can see in the south-eastern part of Spain, southern France, Po Valley and the eastern and western parts of Romania. The area around Almería, southern Spain, and the French Alps demonstrate decreased concentrations in 2013 compared to 2012 (blue) versus an increase in 2012 compared to 2011, indicating a temporal elevation in 2012 of indicator concentrations.

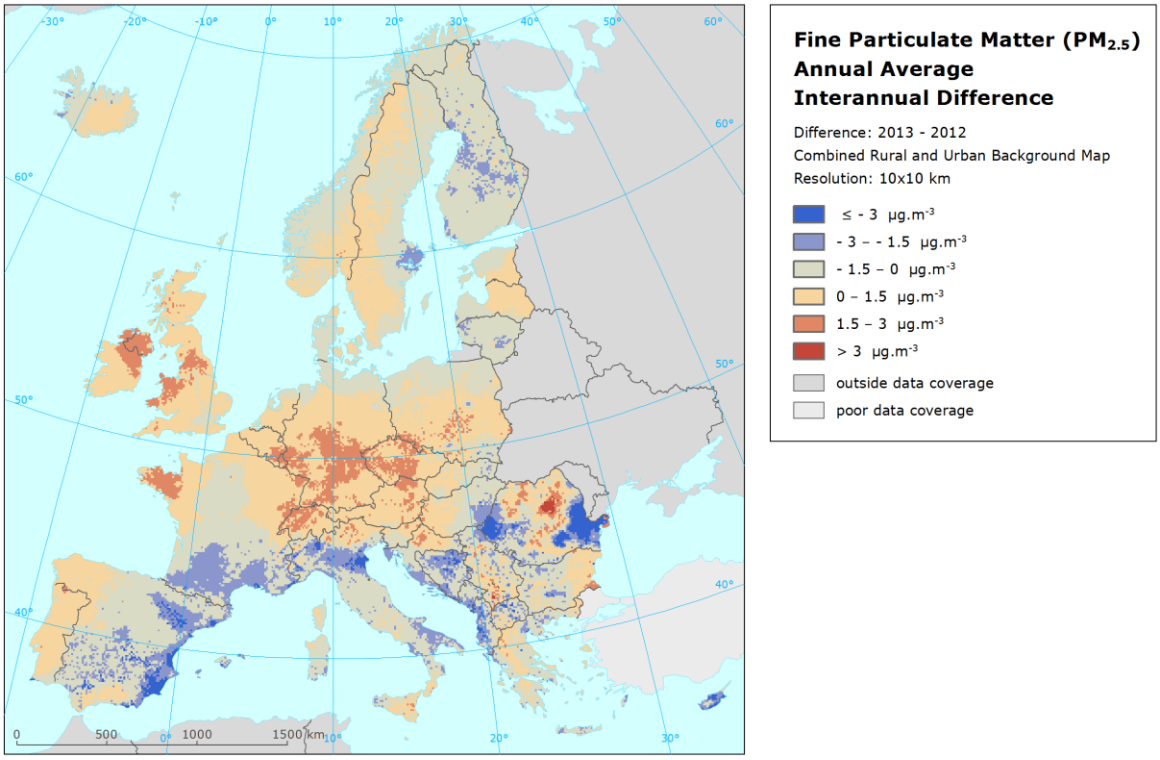

Figure 5.2 Inter-annual difference between mapped concentrations for 2013 and 2012 – $PM_{2.5}$, annual average. Units: µg.m^{-3}. Resolution: 10x10 km.

5.1.2 Population exposure

Table 5.3 gives the population frequency distribution for a limited number of exposure classes calculated on a grid of 1x1 km resolution, as well as the population-weighted concentration for individual countries and for Europe as a whole according to Equation 2.3.

In 2013, only 12 % of the European population has been exposed to $PM_{2.5}$ annual mean concentrations below 10 µg.m^{-3}, the WHO (World Health Organization) air quality guideline (WHO, 2005). Almost half of the population (45 %) lived in areas where the $PM_{2.5}$ annual mean concentration is estimated to be between 10 and 15 µg.m^{-3}, while more than a quarter of the population (29 %) lived in areas with $PM_{2.5}$ values between 15 and 20 µg.m^{-3}. About 6 % of the population lived in areas where the $PM_{2.5}$ annual mean exceeds the target value (TV). In FYR of Macedonia more than half of the population was exposed to levels above the target value, while in Poland and Bulgaria more than 30 %. The populated weighted concentration above the target value occurred at FYR of Macedonia, while Albania, Bulgaria, Poland, Serbia and Slovakia show this concentration level below the target value, but above 20 µg.m^{-3}. However, as the next section discusses, the current mapping methodology tends to underestimate high values. Therefore, the exceedance percentages and the number of countries with population exposed to concentrations above the target value will most likely be higher.

According to EEA (2015b), about 9 % of the urban population in the EU-28 was exposed to $PM_{2.5}$ above the target value threshold in 2013. The difference with the estimated 6 % in Table 5.3 is caused by the different set of population taken into consideration. In the EEA estimate only the urban population in the larger cities is taken into account, while in Tables 5.3 and 5.4 it concerns the total population, including that of smaller cities, towns, villages and the rural areas.

Table 5.3 Population exposure and population-weighted concentration – $PM_{2.5}$, annual average, year 2013. Resolution: 1x1 km.

Country		Population	$PM_{2.5}$ annual average, exposed population [%]						Population weighted conc. [µg.m^{-3}]
			< LV_{2020}				> LV_{2020}		
			< TV					> TV	
		[inhbs . 1000]	< 5 µg.m^{-3}	5 - 10 µg.m^{-3}	10 - 15 µg.m^{-3}	15 - 20 µg.m^{-3}	20 - 25 µg.m^{-3}	> 25 µg.m^{-3}	
Albania	AL	2 899		0.4	14.8	19.1	63.8	2.0	20.3
Andorra	AD	76		1.8	98.2				11.9
Austria	AT	8 452	0.0	4.7	36.6	58.5	0.1		15.7
Belgium	BE	11 162		0.0	17.7	82.3			16.6
Bosnia & Herzegovina	BA	3 836		2.8	23.7	73.4	0.1		16.0
Bulgaria	BG	7 285		0.5	5.8	18.9	30.2	44.6	24.1
Croatia	HR	4 262		2.4	16.7	80.9			16.8
Cyprus	CY	866			1.4	98.6			17.0
Czech Republic	CZ	10 516		0.0	5.0	66.3	20.0	8.7	19.6
Denmark	DK	5 603	0.4	67.3	32.3				9.6
Estonia	EE	1 320	0.1	99.9					7.8
Finland	FI	5 427	20.9	79.1					5.9
France (metropolitan)	FR	63 652	0.0	5.5	53.5	40.8	0.1		14.5
Germany	DE	80 524		0.5	69.4	30.1	0.1		14.2
Greece	GR	11 004		0.1	9.9	55.8	16.5	17.7	19.7
Hungary	HU	9 909			0.6	81.7	17.8		18.2
Iceland	IS	322	10.6	89.4					6.5
Ireland	IE	4 591	0.0	71.3	28.7				9.2
Italy	IT	59 685	0.0	2.4	30.0	35.9	18.7	13.0	18.2
Latvia	LV	2 024		20.1	51.1	28.8			12.8
Liechtenstein	LI	37		7.1	92.9				11.4
Lithuania	LT	2 972		5.2	48.3	46.5			13.9
Luxembourg	LU	537			69.4	30.6			14.3
Macedonia, FYROM of	MK	2 062		0.1	2.3	2.9	9.2	85.5	30.4
Malta	MT	421			100.0				12.5
Monaco	MC	38			100.0				13.8
Montenegro	ME	621		10.6	13.6	43.2	32.7		17.1
Netherlands	NL	16 780		0.0	65.1	34.8			14.3
Norway	NO	5 051	29.0	51.7	19.3				7.1
Poland	PL	38 063		0.0	9.0	24.7	34.8	31.5	22.8
Portugal (excl. Az., Mad.)	PT	9 977	0.7	45.6	53.7				10.0
Romania	RO	20 020		0.0	19.4	47.6	29.1	4.0	18.5
San Marino	SM	34			18.1	82			15.1
Serbia (incl. Kosovo*)	RS	8 997		0.2	3.5	31.4	42.6	22.4	22.5
Slovakia	SK	5 411			1.5	48.2	46.8	3.4	20.1
Slovenia	SI	2 059		0.1	14.9	77.2	7.9		17.4
Spain (excl. Canarias)	ES	44 623	0.4	35.4	62.4	1.8	0.0		11.0
Sweden	SE	9 556	29.3	70.7					6.0
Switzerland	CH	8 039	0.1	6.3	67.2	26.5			13.9
United Kingdom (& dep.)	UK	63 905	0.2	14.2	85.5	0.0			11.8
Total		**532 614**	**1.1**	**11.1**	**44.4**	**28.7**	**8.9**	**5.8**	**15.3**
			12.2		**73.2**		**14.7**		
EU-28		**500 603**	**0.9**	**11.0**	**45.6**	**28.9**	**8.2**	**5.4**	**15.1**
			11.9		**74.5**		**13.6**		
Kosovo*	KS	1 816	0.0	0.0	2.4	11.1	13.6	72.8	28.0
Serbia (excl. Kosovo*)	RS	7 182	0.0	0.2	3.7	36.3	49.7	10.1	21.1

*) under the UN Security Council Resolution 1244/99

Note1: Turkey is not included in the calculation due to lacking air quality data.
Note2: The percentage value "0.0" indicates an exposed population exists, but is small and estimated less than 0.05 %. Empty cells mean: no population in exposure.

The comparison of the $PM_{2.5}$ exposures of Table 5.3 with that of the PM_{10} exposure of Table 4.2 shows the $PM_{2.5}/PM_{10}$ ratio of population-weighted concentrations to be between 0.6 and 0.8, for most countries. The exceptions are Portugal, Spain, Andorra, Malta, Cyprus, Greece, Iceland, Norway, Sweden, Finland and Estonia (between 0.35 and 0.6); a plausible cause for southern countries might be the influence of Saharan dust containing there a relative large fraction of coarse particles.

Table 5.4 Evolution of population-weighted concentration and percentage population living in above limit value (right) in the years 2007-2013 – $PM_{2.5}$, annual average. Resolution: 1x1 km.

Country		Population-weighted conc. [µg.m^{-3}]								Population above TV 25 µg.m^{-3} [%]							
		2007	2008	2009	2010	2011	2012	2013	diff. '13 - '12	2007	2008	2009	2010	2011	2012	2013	diff. '13 - '12
Albania	AL	20.8	19.6		25.1	17.2	21.1	20.3	-0.8	1.6	1.6		53.4	1.6	28.5	2.0	-26.5
Andorra	AD	11.5	11.3		12.4	13.7	15.9	11.9	-4.0	0	0		0	0	0	0	0
Austria	AT	16.3	16.4		17.7	16.3	14.8	15.7	0.9	0	0		0	0	0	0	0
Belgium	BE	16.6	17.1		18.8	17.3	15.8	16.6	0.8	0	0		0	0	0	0	0
Bosnia-Herzegovina	BA	21.7	20.3		22.2	17.2	18.5	16.0	-2.5	12.8	10.9		47.2	8.2	4.2	0	-4.2
Bulgaria	BG	28.8	28.4		24.5	18.3	24.9	24.1	-0.8	68.8	68.4		60.9	8.4	51.0	44.6	-6.3
Croatia	HR	19.5	18.5		20.0	19.6	16.8	16.8	0.0	0.2	0		1.0	2.2	0	0	0.0
Cyprus	CY	25.0	25.3		21.8	21.0	25.0	17.0	-8.0	77.6	79.6		0	0.8	72.8	0	-72.8
Czech Republic	CZ	17.5	17.7		21.5	18.8	18.8	19.6	0.8	8.0	8.3		15.7	10.2	9.4	8.7	-0.7
Denmark	DK	11.5	11.1		11.4	12.5	10.0	9.6	-0.3	0	0		0	0	0	0	0
Estonia	EE	8.8	8.9		8.9	8.0	7.9	7.8	-0.1	0	0		0	0	0	0	0
Finland	FI	7.7	7.4		7.8	7.4	7.1	5.9	-1.2	0	0		0	0	0	0	0
France	FR	14.9	14.7		16.2	15.3	14.7	14.5	-0.2	0	0		0	0	0	0	0
Germany	DE	14.0	14.1		16.3	14.8	13.3	14.2	0.9	0	0		0	0	0	0	0
Greece	GR	22.0	21.7		20.0	16.8	19.2	19.7	0.5	18.5	18.4		6.3	7.0	12.3	17.7	5.4
Hungary	HU	19.3	19.4		20.3	23.1	18.9	18.2	-0.7	0	0		6.7	22.2	0.0	0	0.0
Iceland	IS	7.1	7.1		6.9	4.6	4.7	6.5	1.8	0	0		0	0	0	0	0
Ireland	IE	8.5	9.6		10.3	7.9	8.1	9.2	1.1	0	0		0	0	0	0	0
Italy	IT	19.0	19.1	not	17.5	19.8	18.9	18.2	-0.8	12.4	12.3	not	6.0	21.8	19.5	13.0	-6.5
Latvia	LV	15.3	16.4	mapped	14.7	11.1	12.4	12.8	0.5	0	0	mapped	0	0	0	0	0
Liechtenstein	LI	15.5	15.5		15.3	8.5	10.2	11.4	1.1	0	0		0	0	0	0	0
Lithuania	LT	13.8	15.5		15.6	12.7	12.9	13.9	1.0	0	0		0	0	0	0	0
Luxembourg	LU	13.9	14.5		15.8	13.3	12.6	14.3	1.7	0	0		0	0	0	0	0
Macedonia, FYR of	MK	24.4	23.6		27.5	15.8	29.2	30.4	1.2	61.5	61.0		73.8	2.8	69.5	85.5	15.9
Malta	MT	14.9	14.9		13.8	15.6	12.4	12.5	0.1	0	0		0	0	0	0	0
Monaco	MC	16.5	16.5		14.9	16.4	18.2	13.8	-4.4	0	0		0	0	0	0	0
Montenegro	ME	21.4	19.9		24.6	15.1	18.7	17.1	-1.6	12.6	12.6		64.6	4.9	1.5	0	-1.5
Netherlands	NL	16.9	17.0		17.6	17.1	13.7	14.3	0.6	0	0		0	0	0	0	0
Norway	NO	8.6	8.2		8.8	6.3	7.2	7.1	0.0	0	0		0	0	0	0	0
Poland	PL	20.8	21.1		26.4	21.8	23.9	22.8	-1.1	20.6	21.0		53.1	24.4	42.6	31.5	-11.1
Portugal	PT	11.5	10.9		10.5	10.5	9.9	10.0	0.1	0	0		0	0	0	0	0
Romania	RO	22.4	21.8		17.0	20.5	20.8	18.5	-2.3	28.5	27.7		7.8	14.0	18.9	4.0	-14.9
San Marino	SM	18.2	18.2		16.3	14.7	16.7	15.1	-1.6	0	0		0	0	0	0	0
Serbia (incl. Kosovo)	RS	26.6	25.4		22.7	21.2	24.3	22.5	-1.8	69.4	64.7		30.6	18.3	48.3	22.4	-25.9
Slovakia	SK	20.2	20.6		21.3	21.8	20.5	20.1	-0.4	12.4	11.5		14.3	5.4	11.6	3.4	-8.2
Slovenia	SI	18.5	18.0		19.0	19.4	17.7	17.4	-0.3	0	0		0	0	0	0	0
Spain	ES	14.1	13.6		11.8	11.1	11.9	11.0	-0.9	0	0		0	0	0	0	0
Sweden	SE	9.2	8.8		8.1	8.1	7.2	6.0	-1.2	0	0		0	0	0	0	0
Switzerland	CH	14.9	14.8		15.5	12.6	12.6	13.9	1.3	0	0		0	0	0	0	0
United Kingdom	UK	12.2	12.5		13.0	12.4	11.9	11.8	-0.1	0	0		0	0	0	0	0
Total		**16.3**	**16.3**		**16.8**	**15.9**	**15.6**	**15.3**	**-0.4**	**7.8**	**7.6**		**8.3**	**6.2**	**9.0**	**5.8**	**-3.2**
EU-28		**16.1**	**16.1**		**16.7**	**15.9**	**15.5**	**15.1**	**-0.3**	**6.4**	**6.3**		**7.1**	**6.2**	**6.2**	**5.4**	**-0.8**

Considering the average for the whole of Europe, the overall population-weighted annual mean $PM_{2.5}$ concentration in 2013 was 15.3 µg.m^{-3}. This is slightly less than in the previous years as can be seen in Table 5.4. This table shows the evolution of the population exposure for the years 2007 – 2013. For all the years, the same mapping method has been used.

Compared to the year 2012, an increase of both the population exposed to levels above the TV and the population-weighted concentration in 2013 can be observed in Greece and FYR of Macedonia, while decreases for both are observed at Albania, Bosnia-Herzegovina, Bulgaria, Cyprus, Montenegro, Slovakia, Poland and Italy.

However, the results for the south-eastern Europe, and specifically for the West-Balkan countries are strongly influenced by the limited number of measurement stations.

5.1.3 Uncertainties

Uncertainty estimated by cross-validation

Using RMSE as the most common indicator, the *absolute mean uncertainty* of the combined final map at areas 'in between' the station measurements can be expressed in µg.m^{-3}. Table 5.2 shows that the absolute mean uncertainty of the combined final map of $PM_{2.5}$ annual average expressed as RMSE is 2.7 µg.m^{-3} for the rural areas and 2.9 µg.m^{-3} for the urban areas. Alternatively, one can express this uncertainty in relative terms by relating the absolute RMSE uncertainty to the mean air pollution indicator value for all stations. This *relative mean uncertainty* of the combined final map of PM_{10} annual average is 22.1 % for rural areas and 17.5 % for urban areas. These relative uncertainty values fulfil the data quality objectives for models as set in Annex I of the air quality Directive 2008/50/EC (EC, 2008). Table 7.6 summarises both the absolute and relative uncertainties of different years.

Figure 5.3 shows the cross-validation scatter plots, obtained according to Section 2.3, for both the rural and urban areas. The R^2 indicates that both for the rural and for the urban areas about 78 % of the variability is attributable to the interpolation.

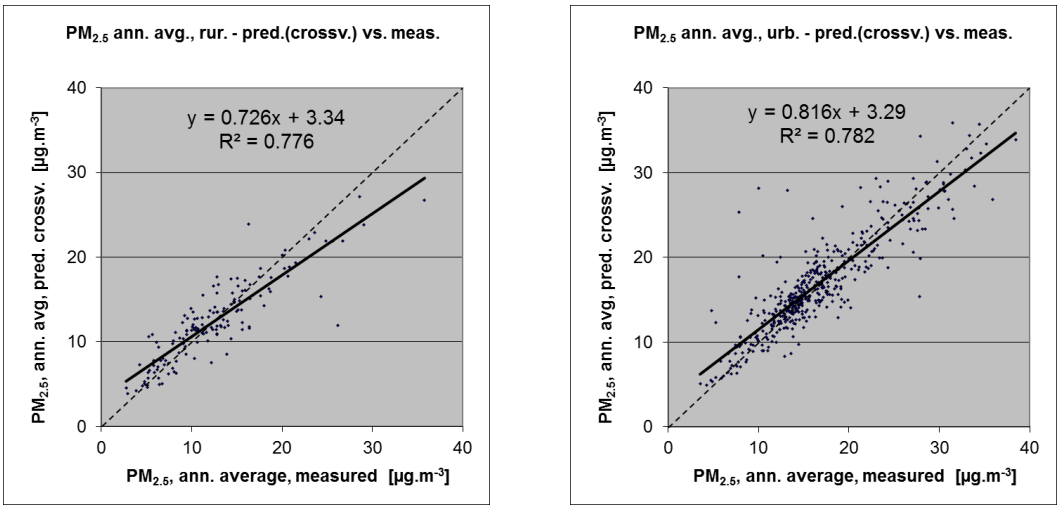

Figure 5.3 Correlation between cross-validation predicted values (y-axis) and measurements (x-axis) for the $PM_{2.5}$ annual average for 2013 for rural (left) and urban (right) areas. R^2 and the slope a (from the linear regression equation $y = a \cdot x + c$) should be as close 1 as possible, the intercept c should be as close 0 as possible

The scatter plots indicate that in areas with high concentrations the interpolation methods tend to underestimate the levels. For example, in urban areas an observed value of 30 µg.m^{-3} is estimated in the interpolations to be about 28 µg.m^{-3}, about 7 % too low. This underestimation at high values is an inherent feature of all spatial interpolations. It can be reduced by either using a higher number of the stations at improved spatial distribution, or introducing a closer regression by using other supplementary data.

Comparison of point measurement values with the predicted grid value

In addition to the above point observation – point prediction cross-validation, a simple comparison has been made between the point observation values and interpolated prediction values spatially averaged in grid cells. This point-grid comparison indicates to what extent the predicted value of a grid cell represents the corresponding measured values at stations located in that cell.

The comparison has been made primarily for the separate rural and separate urban background map at 10x10 km resolution. (One can directly relate this comparison result to the cross-validation results of Figure 5.3.)
Next to this, the comparison has been done also for the final combined maps at 1x1 km resolution and for the spatial aggregated final maps at 10x10 km resolution. Figure 5.4 shows the scatterplots for these comparisons.

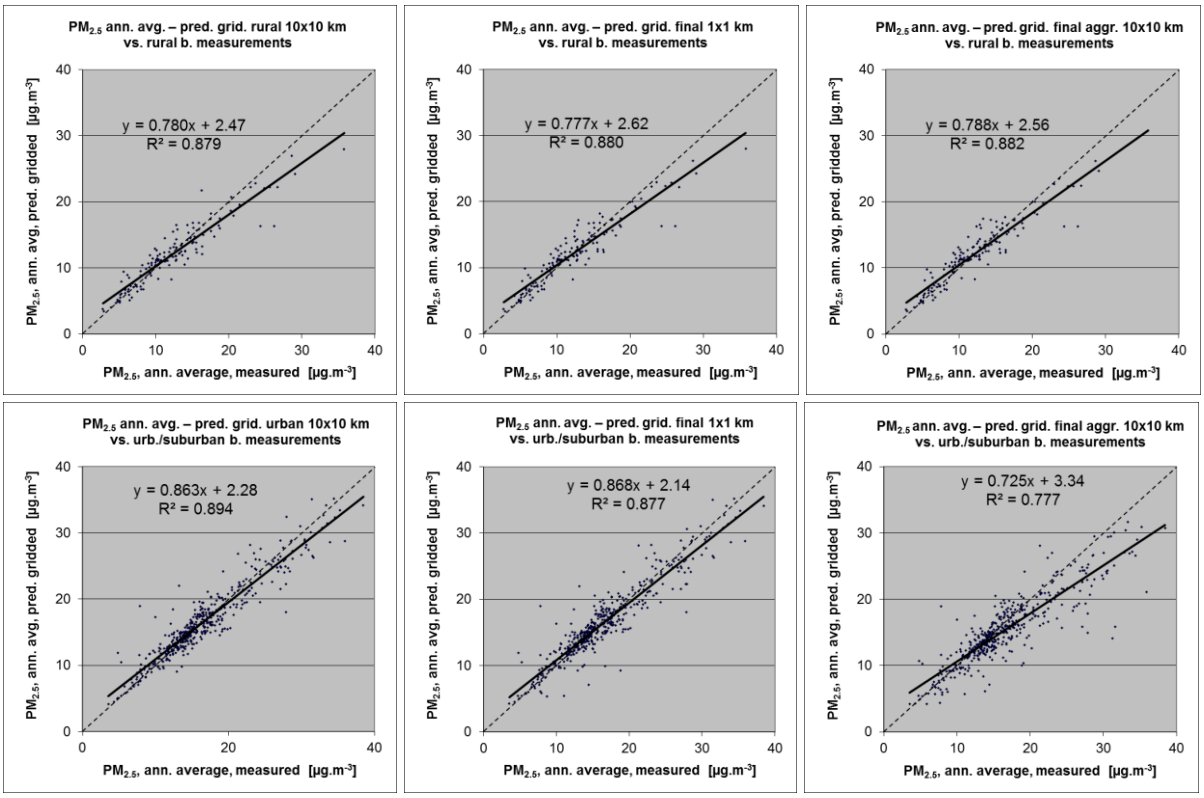

Figure 5.4 Correlation between predicted grid values from rural 10x10 km (upper left), urban 10x10 km (bottom left), final combined 1x1 km (upper and bottom middle) and final combined spatially aggregated 10x10 km (upper and bottom right) map (y-axis) versus measurements from rural (top), resp. urban/suburban (bottom) background stations (x-axis) for $PM_{2.5}$ annual average 2013.

The results of the point observation – point prediction cross-validation of Figure 5.3 and those of the point-grid validation for separate rural and separate urban background maps, and for the final combined maps at both resolutions are summarised in Table 5.4.

By the comparing the scatterplots and the statistical indicators for the separate rural and separate urban background map with the final combined maps in both resolutions, one can evaluate the level of representation of the rural resp. urban background areas in the final combined maps. The rural air quality is fairly well represented in both the 1x1 km and the aggregated 10x10 km final combined map. The urban air quality is quite well represented in the final combined 1x1 km map, but not in the aggregated final combined 10x10 km map as can be deduced from the higher RMSE, the bias being further from

zero and the lower R^2. Therefore, we present in Figure A1.3 of Annex 1 the 1x1 km urban background map in addition to the 10x10 km final combined map of Figure 5.1.

Table 5.4 shows a better correlated relation between station measurements and the interpolated values of the corresponding grid cells (i.e. lower RMSE, higher R^2, smaller intercept and slope closer to 1) at both rural and urban background map areas than it does at the point cross-validation predictions. That is because the simple comparison between point measurements and the gridded interpolated values shows the uncertainty at the actual station locations (points), while the point cross-validation prediction simulates the behaviour of the interpolation at point positions assuming no actual measurements would exist at these points within the area covered by measurements. The uncertainty at measurement locations is caused partly by the smoothing effect of the interpolation and partly by the spatial averaging of the values in the 10x10 km grid cells. The level of smoothing, which leads to underestimation in areas with high values, is weaker in areas where measurements exist than in areas where a measurement point is not available. For example, in urban areas the predicted interpolation gridded value in the separate urban background map will be about 28 $\mu g.m^{-3}$ at the corresponding station point with the measured value of 30 $\mu g.m^{-3}$, about 6 % too low. It is slightly less than the prediction underestimation of 7 % at the same point location, when leaving out this one actual measurement point and one does the interpolation without the station (see the previous subsection).

Table 5.4 Statistical indicators RMSE, bias, coefficient of determination R^2 and linear regression equation from the scatter plots for the predicted point values based on cross-validation and the predicted grid values from separate (rural resp. urban) 10x10 km, final combined 1x1 km and final combined spatially aggregated 10x10 km map versus the measured point values for rural (left) and urban (right) background stations for $PM_{2.5}$ annual average of 2013.

	RMSE	bias	R^2	equation	RMSE	bias	R^2	equation
cross-valid. prediction, separate (r or ub) map	2.7	-0.1	0.78	y = 0.726x + 3.34	2.9	0.3	0.782	y = 0.816x + 3.29
grid prediction, 10x10 km separate (r or ub) map	2.1	-0.3	0.88	y = 0.780x + 2.47	2.0	0.0	0.894	y = 0.863x + 2.28
grid prediction, 1x1 km final merged map	2.1	-0.1	0.88	y = 0.777x + 2.62	2.2	-0.1	0.88	y = 0.868x + 2.14
grid prediction, aggr. 10x10 km final merged map	2.1	-0.3	0.88	y = 0.788x + 2.56	3.2	-1.2	0.777	y = 0.725x + 3.34

Probability of Target Value exceedance

The probability of target value exceedance map was created for the $PM_{2.5}$ indicator in similar fashion as the PoE maps for PM_{10} indicators. This map at 10x10 km resolution is presented in Figure 5.4, with the Target Value (TV) of 25 $\mu g.m^{-3}$.

The areas with the highest probability of TV exceedance include the Po Valley in northern Italy with Turin and Milan, the region of southern Poland – north-eastern Czech Republic with the industrial zones of Krakow, Katowice and Ostrava, and the cities in the central part of Poland. Next to this, increased PoE do occur in south-eastern Europe at the larger cities of FYR of Macedonia, Serbia and in Romania, where only a rather limited set of measurement stations is located. They occur mostly in some urban areas or larger agglomerations such as Bucharest and Craiova with their rather high traffic density and heavy industry. In the other parts of Europe, there exists little to no likelihood of exceedance.

In comparison with 2012, a reduced area in the Po Valley with increased levels of PoE does occur. Furthermore, a reduction in areas with more elevated PoE is visible in some agglomerations of Serbia, Bulgaria and Romania (i.e. shifts from orange/yellow to green). In Bulgaria only limited reduction do occur.

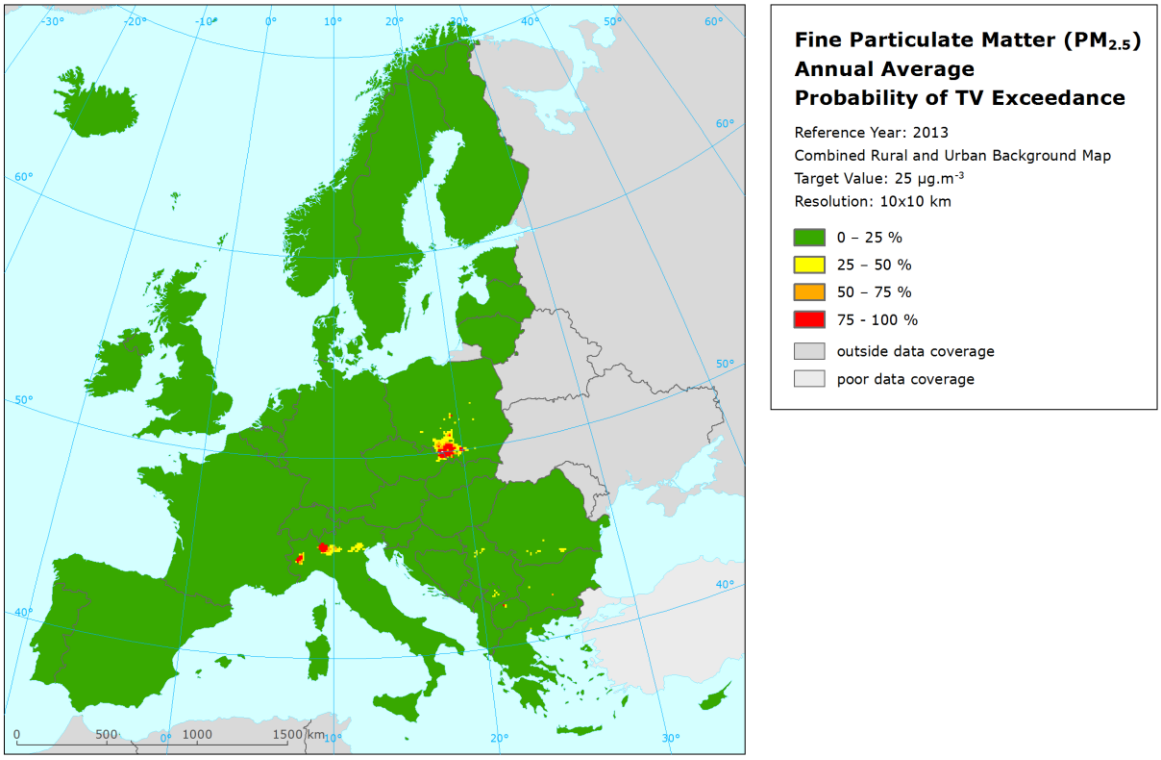

Figure 5.5 Map with the probability of the limit value exceedance for $PM_{2.5}$ annual average (µg.m^{-3}) for 2013 on European scale calculated on the 10 x 10 km grid resolution. Interpolation uncertainty is considered only.

It should be noted that the PoE is related to the aggregated 10x10 km grid. In case we would produce such map on a 1x1 km grid resolution the map pattern would demonstrate elevated PoE levels clearly distinguishing smaller cities and towns as well, which are not resolved at the 10x10 km grid resolution. Furthermore, one should bear in mind that the map is based on rural and (sub)urban *background* station data only. As such the map reflects rural and urban background situations only. Therefore, this type of map will not resolve the exceedances of limit values that may occur at the many *hotspot* and traffic locations throughout Europe.

6 Ozone maps

For ozone, the two health-related indicators (26th highest daily maximum 8-hour running mean and SOMO35) and the two vegetation-related indicators (AOT40 for crops and AOT40 for forests) are considered.

The separate urban and rural health-related indicator fields are calculated at a resolution of 10x10 km. The final health-related indicator maps are then created by combining rural and urban areas based on the 1x1 km resolution gridded population density map, as described in Chapter 2. We present the maps on a 10x10 km grid resolution.

The vegetation-related indicator maps are calculated and presented for rural areas only (assuming urban areas do not cover vegetation) and on a grid of 2x2 km resolution, covering the same mapping domain as at the human health indicators. This resolution serves the needs of the EEA Core Set Indicator 005 on ecosystem exposure to ozone. Map projection is the standard EEA ETRS89-LAEA5210.

6.1 26th highest daily maximum 8-hour average

6.1.1 Concentration map

Figure 6.1 presents the combined final map for 26th highest daily maximum 8-hour average as a result of combining the separate rural and urban interpolated map following the procedures as described in more detail in De Smet et al. (2011) and Horálek et al. (2007). Both separate maps were created by combining the measured ozone concentrations with supplementary data in a linear regression model, followed by kriging of its residuals. The supplementary data used in the regression model are EMEP model output, altitude and surface solar radiation for rural areas and EMEP model output, wind speed and surface solar radiation for urban areas, respectively.

Table 6.1 presents the estimated parameters of the linear regression models and of the residual kriging, including the statistical indicators of both the regression and the kriging.

Table 6.1 Parameters of the linear regression models (Eq. 2.2) and of the ordinary kriging (OK) variograms (nugget, sill, range) – and their statistics – of ozone indicator 26th highest daily maximum 8-hour mean for 2013 in the rural (left) and urban (right) areas as used for the combined final map.

linear regr. model + OK on its residuals	rural areas parameter values	urban areas parameter values
c (constant)	2.4	35.0
a1 (EMEP model 2012)	0.97	0.76
a2 (altitude GTOPO)	0.0038	
a3 (wind speed 2012)		-2.73
a4 (s. solar radiation 2012)	0.49	0.10
adjusted R^2	**0.58**	**0.48**
standard error [µg.m^{-3}]	**9.37**	**11.49**
nugget	50	54
sill	81	93
range [km]	320	310
RMSE [µg.m^{-3}]	**8.34**	**9.01**
realtive RMSE [%]	**7.2**	**8.0**
bias (MPE) [µg.m^{-3}]	**0.15**	**-0.03**

The fit of the 2013 regression relationship, expressed as the adjusted R^2, is 0.58 for rural areas and 0.48 for urban areas. These values are worse compared to 2012, similar as in 2009 – 2011 and better compared to 2005 – 2008 for the rural areas, while comparable all the previous years for the urban areas, see

Horálek et el. (2015) and references cited therein. RMSE and bias are the cross-validation indicators, showing the quality of the resulting map. Section 5.1.3 discusses in more detail the RMSE analysis and comparison with results of 2005 – 2012.

In the combined final map of Figure 6.1, the red and purple areas and stations do exceed the target value (TV) of 120 µg.m^{-3}. Note that in Directive 2008/50/EC the target value is defined as 120 µg.m^{-3} not to be exceeded on more than 25 days per calendar year *averaged over three years*.

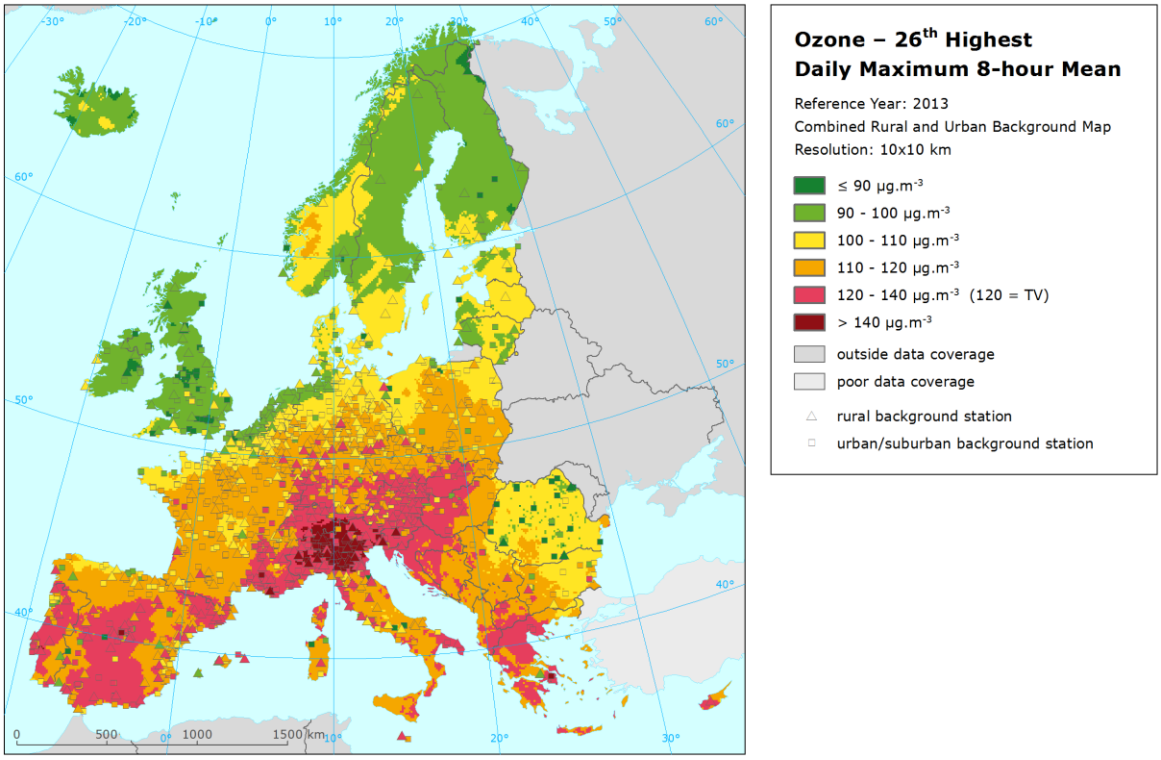

Figure 6.1 Combined rural and urban concentration map of ozone health indicator 26th highest daily maximum 8-hour value in µg.m^{-3} for the year 2013. Its target value is 120 µg.m^{-3}. Resolution: 10x10 km.

As one can observe in a few areas of the map, the high measurement values do not seem to influence the interpolation results despite their clustering. The main reasons are (i) that the map presented here is an aggregation of 1x1 km values into a 10x10 km resolution and this aggregation smooths out the elevated values, and (ii) the smoothing effect kriging has in general.

The concentration map presented in Figure 6.1 is spatially aggregated from 1x1 km to a 10x10 km grid resolution. As a result the urban areas are not properly resolved in this map, due to the smoothing effect of this aggregation. Section 6.1.3 discusses the level of the representation of the urban areas in this final combined aggregated 10x10 km map. For better visualising the actual urban concentration levels at the actual urbanised areas, i.e. without the influence of the dominating pattern of extended rural areas, a separate 1x1 km urban background map is presented in Annex 1, Figure A1.4.

Figure 6.2 presents the inter-annual difference between 2013 and 2012 for 26th highest daily maximum 8-hour value. Red areas show an increase of ozone concentration, while blue areas show a decrease. The highest decreases can be seen in central Italy, and in south-eastern Europe, especially in Romania, Bulgaria, the Balkan countries and Greece. Somewhat less extended decreases do occur at southern Italy, Hungary, Slovakia, southern part of Poland, and Lithuania. Considerable decreases are visible in most of France, and less prominent in Southeast United Kingdom, Portugal, the Benelux, Germany,

northern part of Poland, Iceland, central and eastern Sweden and parts of Finland. In the most of these areas the '2012 - 2011' difference map showed the opposite effect.

In general, we can observe an increase of concentrations in the North-West of Europe and a decrease the South-East. The reason lies probably in the meteorological conditions as we discovered a similar behaviour of inter-annual difference for the temperature.

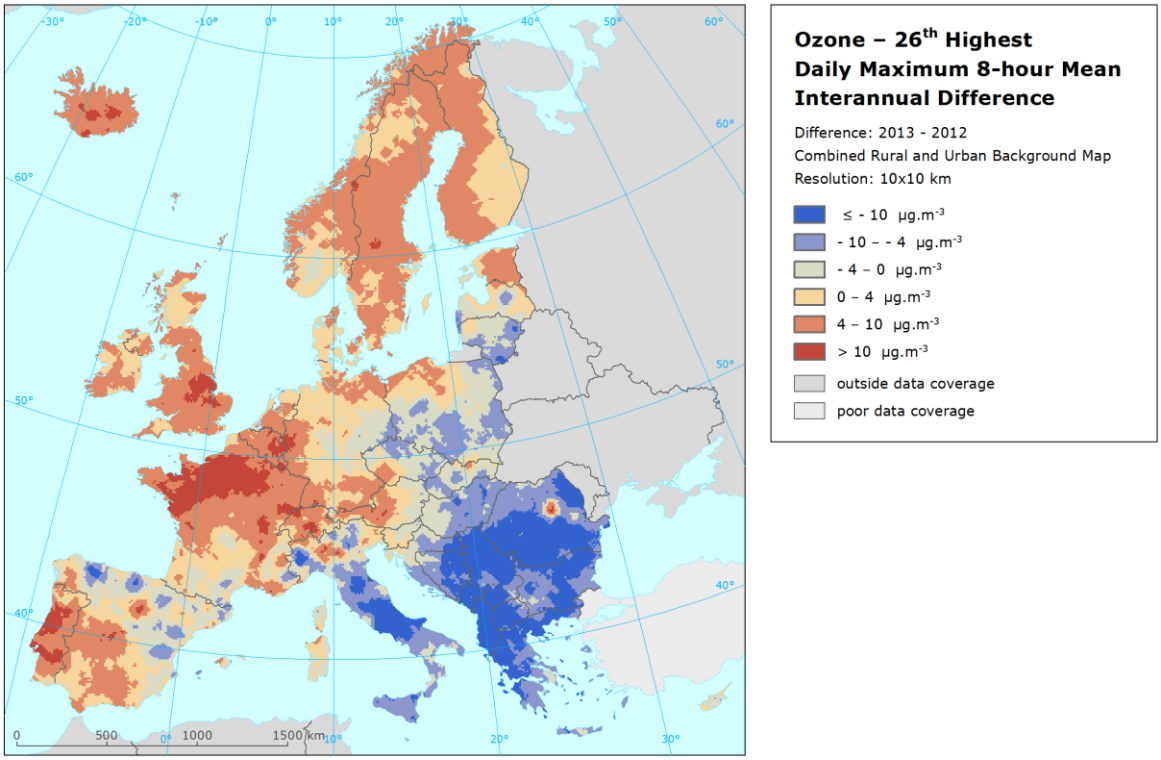

Figure 6.2 Inter-annual difference between mapped concentrations for 2013 and 2012 – ozone, 26th highest daily maximum 8-hour value. Units: µg.m-3.

6.1.2 Population exposure

Table 6.2 gives, for 26th highest daily maximum 8-hour running mean, the population frequency distribution for a limited number of exposure classes, as well as the population-weighted concentration for individual countries and for Europe as a whole. In Table 6.3, the evolution of population exposure of the last eight years is presented.

It has been estimated that in 2013 some 15 % of the European population lived in areas where the ozone concentration exceeded the health related target value threshold (TV of 120 µg.m-3). This is about 6 percent point lower than in 2012 and quite similar as in 2008 – 2011 (Tables 6.3 and 7.3). Similar to previous years there are no exceedances in 2013 in Belgium, the Netherlands, Scandinavia and the Baltic countries, the UK, Ireland and Iceland.

In Andorra, Austria, Greece, Italy, Slovenia, Switzerland and Liechtenstein both the population-weighted indicator concentration and the median were above the target value (TV), implying that in these countries the average concentration exceeded the TV and more than half of the population was exposed to concentrations exceeding the TV.

Table 6.2 Population exposure and population weighted concentration – ozone, 26th highest daily maximum 8-hour mean for the year 2013.

Country		Population	Ozone, 26th highest dmax. 8-h, exposed population [%]						Population-weighted conc.
			< TV				> TV		
		[inhbs . 1000]	< 90 µg.m-3	90 - 100 µg.m-3	100 - 110 µg.m-3	110 - 120 µg.m-3	120 - 140 µg.m-3	> 140 µg.m-3	[µg.m-3]
Albania	AL	2 899				79.7	20.3		117.4
Andorra	AD	76					100		122.0
Austria	AT	8 452				31.2	68.8	0.0	121.0
Belgium	BE	11 162	0.1	27.9	69.6	2.3			101.5
Bosnia & Herzegovina	BA	3 836			10.0	81.5	8.5		115.5
Bulgaria	BG	7 285	6.3	20.1	60.5	13.1	0.1		103.2
Croatia	HR	4 262			5.1	61.2	33.7	0.0	118.8
Cyprus	CY	866			50.4	44.3	5.3		110.4
Czech Republic	CZ	10 516			23.8	73.5	2.7		113.4
Denmark	DK	5 603	1.0	81.8	16.9	0.2			96.4
Estonia	EE	1 320	2.0	79.0	19.0				97.4
Finland	FI	5 427	27.6	67.0	5.4				92.3
France (metropolitan)	FR	63 652		5.5	18.6	64.3	11.5	0.1	112.8
Germany	DE	80 524		5.7	50.6	39.6	4.1		109.9
Greece	GR	11 004			4.9	27.7	67.4		123.0
Hungary	HU	9 909	0.0	4.3	19.3	62.2	14.1		113.1
Iceland	IS	322	86.17	13.8	0.0				87.2
Ireland	IE	4 591	41.5	58.0	0.5				91.2
Italy	IT	59 685		1.4	16.5	33.2	26.4	22.4	125.3
Latvia	LV	2 024	6.5	69.9	23.6				97.4
Liechtenstein	LI	37					100.0		124.7
Lithuania	LT	2 972		81.8	18.2				98.1
Luxembourg	LU	537			80.8	19.2			108.8
Macedonia, FYROM of	MK	2 062			0.1	79.5	20.4		117.8
Malta	MT	421			2.6	95.8	1.5		111.3
Monaco	MC	38					100.0		121.9
Montenegro	ME	621			11.2	88.0	0.7		112.7
Netherlands	NL	16 780		60.6	39.3	0.1			98.8
Norway	NO	5 051	12.8	81.2	5.9	0.1			94.1
Poland	PL	38 063		6.6	54.6	38.8	0.1		108.6
Portugal (excl. Az., Mad.)	PT	9 977		10.4	29.5	40.8	19.1	0.2	112.5
Romania	RO	20 020	67.0	18.9	12.5	1.6			85.6
San Marino	SM	34			80.5	15.5	4.0		110.5
Serbia (incl. Kosovo*)	RS	8 997		3.6	47.3	47.9	1.2		109.7
Slovakia	SK	5 411			5.7	75.1	19.2		116.7
Slovenia	SI	2 059				22.2	77.7	0.1	124.8
Spain (excl. Canarias)	ES	44 623		0.9	27.9	46.0	25.1		114.4
Sweden	SE	9 556	9.8	80.3	9.8	0.1			94.5
Switzerland	CH	8 039				17.0	79.0	4.0	124.0
United Kingdom (& dep.)	UK	63 905	60.4	39.2	0.4	0.0			89.4
Total		**532 614**	**10.9**	**15.9**	**25.4**	**32.8**	**12.4**	**2.6**	**108.3**
			26.8		**58.2**		**15.0**		
EU-28		**500 603**	**11.4**	**16.0**	**26.0**	**32.2**	**11.7**	**2.7**	**108.1**
			27.4		**58.2**		**14.4**		
Kosovo*	KS	1 816			20.4	77.1	2.5		113.1
Serbia (excl. Kosovo*)	RS	7 182		4.4	53.9	40.8	0.9		108.9

*) under the UN Security Council Resolution 1244/99

Note1: Turkey is not included in the calculation due to lack of air quality data.
Note2: The percentage value "0.0" indicates an exposed population exists, but is small and estimated less than 0.05 %. Empty cells mean: no population in exposure.

Table 6.3 Evolution of population-weighted concentration in the years 2005-2013 (left) and of percentage population living in above limit value in the years 2009-2013 (right) – O_3, 26th highest daily maximum 8-hour mean. Resolution: 1x1 km.

Country		Population-weighted conc. [µg.m^{-3}]										Population above TV 120 µg.m^{-3} [%]					
		2005	2006	2007	2008	2009	2010	2011	2012	2013	diff. '12	2009	2010	2011	2012	2013	diff. '13 - '12
Albania	AL	122.7	117.9	126.9	115.3	114.7	109.5	121.1	133.4	117.4	-16.0	13.2	0.0	52.6	100	20.3	-79.7
Andorra	AD	127.2	119.1	118.6	122.0	115.6	122.4	120.6	122.2	122.0	-0.2	13.5	100	100	100	100	0
Austria	AT	120.6	124.9	122.8	114.8	116.4	118.4	118.6	118.5	121.0	2.4	14.5	26.8	45.2	45.1	68.8	23.7
Belgium	BE	104.0	126.0	98.9	103.6	101.5	97.7	104.4	94.1	101.5	7.4	0	0	0	0	0	0
Bosnia-	BA	119.9	118.1	122.5	113.7	114.5	107.4	109.9	125.1	115.5	-9.6	25.7	16.5	24.1	76.8	8.5	-68.3
Bulgaria	BG	109.9	105.0	115.7	114.4	112.0	103.8	105.1	115.6	103.2	-12.5	16.3	0.3	2.2	25.9	0.1	-25.9
Croatia	HR	122.8	124.8	124.7	115.5	115.6	114.3	118.3	125.0	118.8	-6.2	19.2	20.3	40.4	83.2	33.7	-49.5
Cyprus	CY	114.5	102.1	116.9	115.2	120.8	109.8	112.0	115.5	110.4	-5.1	50.9	0.0	4.3	16.3	5.3	-11.0
Czech Republic	CZ	121.6	126.5	121.0	114.6	113.5	114.1	114.8	116.5	113.4	-3.1	6.6	0.9	11.1	21.5	2.7	-18.8
Denmark	DK	95.0	104.9	95.2	102.6	95.5	91.4	96.9	95.1	96.4	1.3	0	0	0	0	0	0
Estonia	EE	94.2	105.1	94.1	96.3	90.8	97.2	94.8	92.9	97.4	4.5	0	0	0	0	0	0
Finland	FI	92.9	100.7	89.0	94.3	90.6	92.2	93.0	88.4	92.3	3.9	0	0	0	0	0	0
France	FR	113.8	122.0	109.0	107.3	107.3	111.6	112.8	104.4	112.8	8.4	9.6	22.0	14.0	5.9	11.6	5.7
Germany	DE	113.8	125.8	113.3	113.5	108.8	112.8	111.5	106.7	109.9	3.2	2.0	13.0	3.8	0.4	4.1	3.7
Greece	GR	125.4	115.8	126.5	131.1	122.8	119.4	126.5	131.1	123.0	-8.1	59.4	43.2	84.2	95.2	67.4	-27.8
Hungary	HU	119.7	121.7	125.0	117.5	124.2	110.9	117.1	121.4	113.1	-8.3	85.6	3.5	24.3	69.2	14.1	-55.0
Iceland	IS	85.2	93.3	81.1	90.8	81.4	78.3	83.6	80.7	87.2	6.5	0	0	0	0	0	0
Ireland	IE	86.5	90.2	84.2	92.1	84.9	85.6	84.4	86.6	91.2	4.6	0	0	0	0	0	0
Italy	IT	131.1	135.1	129.5	123.2	125.8	124.3	127.7	129.9	125.3	-4.6	57.3	48.8	69.0	77.0	48.9	-28.1
Latvia	LV	91.3	104.5	95.8	94.9	91.9	93.2	96.3	97.9	97.4	-0.5	0	0	0	0	0	0
Liechtenstein	LI	106.9	127.3	119.9	119.4	118.9	123.3	116.4	117.9	124.7	6.8	17.8	100	9.5	14.7	100	85.3
Lithuania	LT	103.0	110.1	98.1	102.0	95.8	96.9	101.4	100.4	98.1	-2.3	0	0	0	0	0	0
Luxembourg	LU	119.9	130.0	111.7	112.1	108.6	111.4	110.4	98.2	108.8	10.6	0	2.9	1.8	0	0	0.0
Macedonia, FYR of	MK	117.5	110.3	121.1	121.0	111.3	109.0	117.4	134.6	117.8	-16.8	16.6	0.0	17.7	98.7	20.4	-78.3
Malta	MT	105.9	115.6	109.1	108.4	107.7	109.4	112.6	115.2	111.3	-3.9	0	0.7	4.0	6.5	1.5	-4.9
Monaco	MC		142.4	127.3	123.1	127.2	124.0	126.6	118.6	121.9	3.3	100	100	100	0.7	100	99.3
Montenegro	ME	120.8	114.3	122.3	118.1	111.7	108.6	115.1	126.1	112.7	-13.5	14.5	5.3	31.0	87.7	0.7	-86.9
Netherlands	NL	93.7	116.1	94.1	98.4	94.7	90.7	98.6	93.3	98.8	5.5	0	0	0	0	0	0
Norway	NO	98.1	101.7	91.3	99.0	94.0	88.8	93.7	90.6	94.1	3.5	0	0	0	0	0	0
Poland	PL	113.6	120.4	112.9	109.7	107.8	106.6	109.5	111.4	108.6	-2.8	0.4	0.0	2.4	9.0	0.1	-8.9
Portugal	PT	119.0	119.4	111.0	102.7	112.4	112.0	108.4	105.4	112.5	7.1	18.5	23.3	5.7	0.9	19.3	18.4
Romania	RO	112.1	105.7	116.9	110.1	108.8	94.0	91.1	102.4	85.6	-16.7	8.0	0.0	0.7	8.1	0.0	-8.1
San Marino	SM	130.8	120.8	130.4	119.0	118.1	116.1	117.9	120.9	110.5	-10.4	13.8	11.6	13.8	15.3	4.0	-11.3
Serbia (incl.	RS	115.6	108.5	122.5	117.3	115.8	102.5	112.0	122.5	109.7	-12.8	38.2	4.1	16.5	67.2	1.2	-66.0
Slovakia	SK	121.3	122.2	122.2	116.4	122.7	112.8	118.5	120.7	116.7	-4.0	88.3	1.1	28.7	61.9	19.2	-42.8
Slovenia	SI	122.6	132.6	126.6	116.9	119.7	122.1	125.5	125.4	124.8	-0.5	38.2	56.5	99.5	96.3	77.8	-18.5
Spain	ES	117.7	116.2	115.4	110.7	113.1	115.4	112.1	112.2	114.4	2.2	18.1	30.7	7.5	7.3	25.1	17.9
Sweden	SE	97.6	104.5	93.5	97.6	94.2	91.2	96.1	93.6	94.5	0.9	0	0	0	0	0	0
Switzerland	CH	122.6	132.6	120.1	116.8	117.3	124.7	120.8	117.0	124.0	7.1	15.4	99.5	40.6	12.8	83.0	70.2
United Kingdom	UK	87.2	98.0	83.3	93.1	86.8	81.6	87.8	83.6	89.4	5.8	0	0	0	0	0	0
Total		**112.1**	**118.2**	**110.7**	**109.8**	**108.1**	**106.8**	**108.9**	**107.9**	**108.3**	**0.4**	**16.0**	**16.3**	**16.5**	**20.7**	**15.0**	**-5.7**
EU-28		**111.8**	**118.3**	**110.2**	**109.5**	**107.8**	**106.8**	**108.7**	**107.2**	**108.1**	**0.9**	**15.7**	**15.5**	**16.8**	**18.6**	**14.4**	**-4.3**

Compared with 2012, an increase of both the number of population living above the TV and the population-weighted concentration occurred in some countries in Central and Western Europe, with Austria, Switzerland, Liechtenstein, Germany, France, Spain and Portugal. A decrease of both exposure indicators is detected in the Czech Republic, Slovakia, Hungary, Poland, Italy, and especially in south-

eastern Europe, such as most of the Balkan countries, Romania, Bulgaria, Malta, Cyprus and Greece in France, Germany, Luxembourg, Portugal, Slovenia and Switzerland.

Part of the population in France, Portugal and Slovenia (all lower than 1 %), Switzerland (4 %), and more substantially in Italy (about 22 %) was estimated to be exposed to ozone levels of more than 140 µg.m^{-3} (Table 6.2). As the current mapping methodology tends to underestimate high values due to interpolation smoothing, these actual numbers will most likely be even higher.

Most of the western and northern European countries showed in 2013 an increase in their population-weighted concentrations compared to 2012. The most prominent decreases are observed for the Balkan countries, including Bulgaria and Romania. The development was in the opposite side than between the years 2011 and 2012.

The overall European population-weighted ozone concentration in terms of the 26th highest daily maximum 8-hour mean was estimated for 2013 as being 108 µg.m^{-3}, which is at the similar level like in 2012.

6.1.3 Uncertainties

Uncertainty estimated by cross-validation

The basic uncertainty analysis is provided by cross-validation. Table 6.1 shows RMSE values of 8.3 µg.m^{-3} for the rural areas and 9.0 µg.m^{-3} for the urban areas of the combined final map. That is in the same order of magnitude as of the years 2007 – 2012, and lower than 2005 – 2006, (Horálek et al. 2015 and references cited therein). The relative mean uncertainty of the 2013 ozone map is 7.2 % for rural areas and 8.0 % for urban areas. Table 7.7 summarises both the absolute and relative uncertainties over the past nine years.

Figure 6.3 shows the cross-validation scatter plots for both the rural and urban areas of the 2013 map. The R^2, an indicator for the interpolation correlation with the observations, shows that for the rural areas about 67 % and for the urban areas about 68 % of the variability is attributable to the interpolation. A similar fit is found in the previous six years (see Table 7.7).

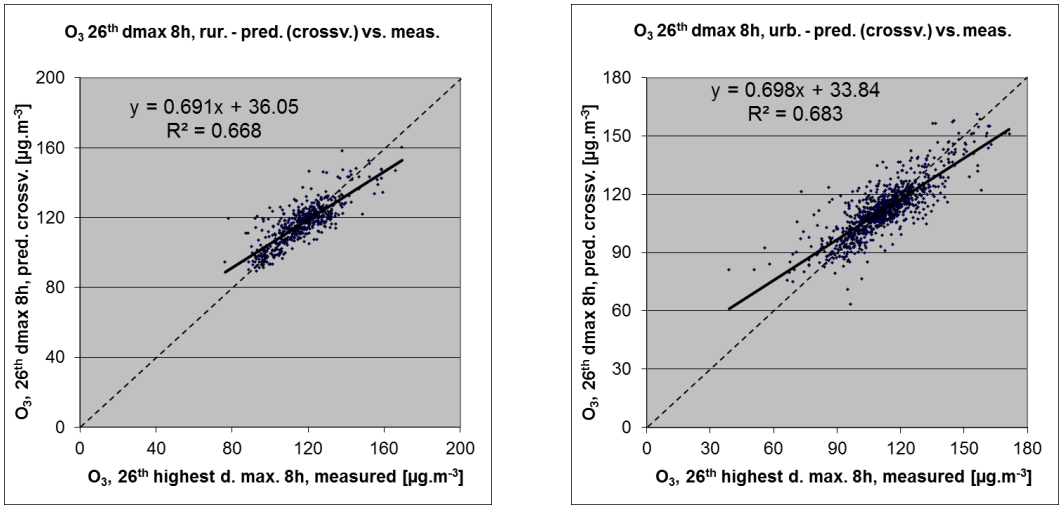

Figure 6.3 Correlation between cross-validation predicted values (y-axis) and measurements (x-axis) for the ozone indicator 26th highest daily maximum 8-hour mean for rural (left) and urban (right) areas in 2013.

The scatter plots indicate that the higher values are underestimated and the lower values somewhat overestimated by the interpolation method; a typical smoothing effect inherent to the interpolation method with the linear regression and its residuals kriging. For example, in rural areas (Figure 6.3, left panel) an observed value of 150 µg.m^{-3} is estimated in the interpolation as 139 µg.m^{-3}, which is 7 % too low.

Comparison of point measurement values with the predicted grid value

In addition to the above point observation – point prediction cross-validation, a simple comparison was made between the point observation values and interpolated predicted grid values.

The comparison has been made primarily for the separate rural and separate urban background maps at 10x10 km resolution. (One can directly relate this comparison result to the cross-validation of Figure 6.3.) Next to this, the comparison has been done also for the final combined maps at 1x1 km resolution and for the spatial aggregated final maps at 10x10 km resolution. Figure 6.4 shows the scatterplots for these comparisons.

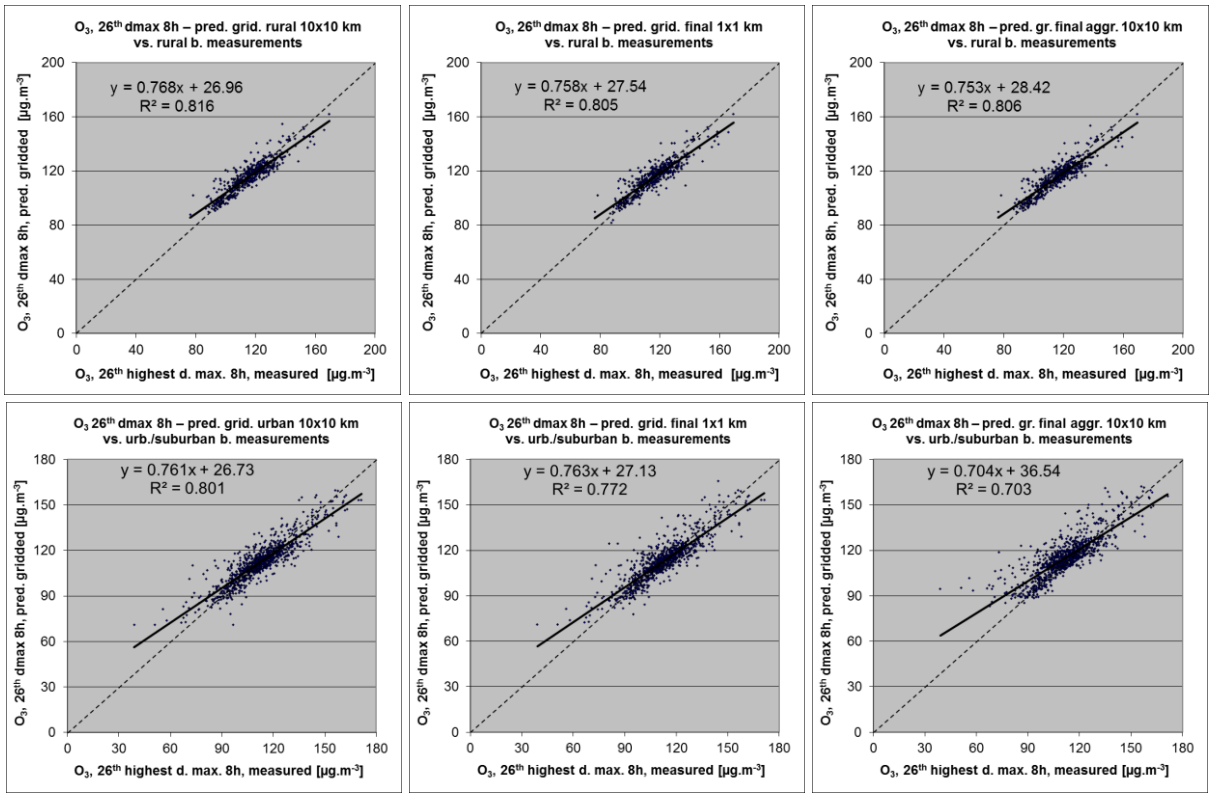

Figure 6.4 Correlation between predicted grid values from rural 10x10 km (upper left), urban 10x10 km (bottom left), final combined 1x1 km (upper and bottom middle) and final combined spatially aggregated 10x10 km (upper and bottom right) map (y-axis) versus measurements from rural (top), resp. urban/suburban (bottom) background stations (x-axis) for the ozone indicator 26th highest daily maximum 8-hour mean for 2013.

The results of the point observation – point prediction cross-validation of Figure 6.3 and those of the point-grid validation for the separate rural and the separate urban background map, and for the final combined maps at both resolutions (Figure 6.4), are summarised in Table 6.4.

By the comparing the scatterplots and the statistical indicators for the separate rural and separate urban background map with the final combined maps in both resolutions, one can evaluate the level of representation of the rural resp. urban background areas in the final combined maps. The rural air quality is fairly well represented in both the 1x1 km and the aggregated 10x10 km final combined map. The urban air quality is quite well represented in the final combined 1x1 km map, but not in the aggregated final combined 10x10 km map, as one can deduct from the higher RMSE, the bias being further from zero and the lower R^2. Therefore, we present in Figure A1.4 of Annex 1 the 1x1 km urban background map in addition to the 10x10 km final combined map of Figure 6.1.

The uncertainty of the rural and urban background maps at measurement locations is caused partly by the smoothing effect of interpolation and partly by the spatial averaging of the values in the 10x10 km grid cells. The level of smoothing, which leads to underestimation in areas with high values, is weaker in areas where measurements exist than in areas where a measurement point is not available. For example, in rural areas the predicted interpolation grid value in the separate rural map will be about 142 $\mu g.m^{-3}$ at the corresponding station point with the observed value of 150 $\mu g.m^{-3}$. This is an underestimation of about 5 %. It is less than the prediction underestimation of 7 % at the same point location, when leaving out this one actual measurement point and one does the interpolation without this station (see the previous subsection).

Table 6.4 Statistical indicators RMSE, bias, coefficient of determination R^2 and linear regression equation from the scatter plots for the predicted point values based on cross-validation and the predicted grid values from separate (rural resp. urban) 10x10 km, final combined 1x1 km and final combined spatially aggregated 10x10 km map versus the measured point values for rural (left) and urban (right) background stations for the ozone indicator 26th highest daily maximum 8-hour mean of 2013.

	rural backgr. stations				urb./suburban backgr. stations			
	RMSE	bias	R^2	equation	RMSE	bias	R^2	equation
cross-valid. prediction, separate (r or ub) map	8.3	0.1	0.668	y = 0.691x + 36.1	9.0	0.0	0.683	y = 0.698x + 33.8
grid prediction, 10x10 km separate (r or ub) map	6.3	0.1	0.816	y = 0.768x + 27.0	7.2	0.0	0.80	y = 0.761x + 26.3
grid prediction, 1x1 km final merged map	6.5	-0.6	0.81	y = 0.758x + 27.5	7.7	0.6	0.77	y = 0.763x + 27.1
grid prediction, aggr. 10x10 km final merged map	6.4	-0.3	0.81	y = 0.753x + 28.4	9.3	3.4	0.70	y = 0.704x + 36.5

Probability of Target Value exceedance

Figure 6.5 presents a gridded map of 10x10 km resolution showing the probability of target value exceedance. It was constructed on the basis of the 10x10 km gridded concentration map (Figure 6.1, derived from the 1x1 km resolution results), the 10x10 km gridded uncertainty map and the target value (TV) of 120 $\mu g.m^{-3}$. Section 4.1.3 explains the significance of the colour classes in the map.

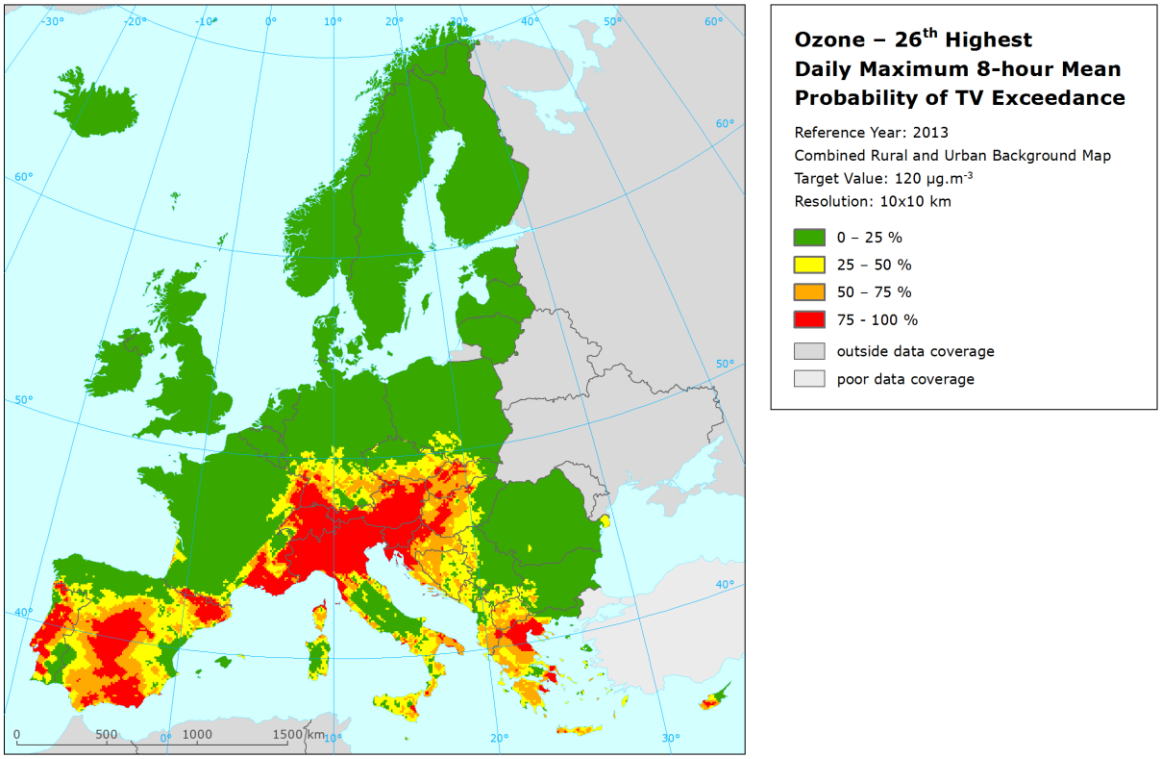

Figure 6.5 Map with the probability of the target value exceedance for ozone indicator 26th highest daily maximum 8-hour average (µg.m-3) for 2013 on European scale calculated on the 10 x 10 km grid resolution. Interpolation uncertainty is considered only, no other sources of uncertainty.

The PoE map for 2013 compared to 2012, demonstrates that most of the red areas (high PoE) in the Alpine region, northern Italy, southern France, central Spain, Austria and Slovenia did not change compared to 2012. Especially in the Balkan countries, Hungary, Slovakia, Romania, Bulgaria and the central Italy the PoE decreased considerably in its level (from 75 – 100 % in 2012 to less than 75 % in 2013) and in general in its extent. In some areas north of the Alps, the levels of PoE increased somewhat, as well as in the Iberian Peninsula, changing from green and yellow to large PoE (orange and red).

In south-eastern Europe and in central Italy there with its clear decreases of the areas with elevated PoE one has to be aware that the small number of rural background stations in this area result in a high sensitivity of the map to the few measurement stations represented in this region.

The meteorologically induced variations from year to year, combined with methodological uncertainties, limited number of years considered here and the limited number of measurement stations at some regions do not allow for conclusions on whether, or not, there is any significant tendency on a European-wide range in this ozone indicator. For that purpose, one would need a longer time series, a higher and more evenly distributed number of station data and further reduced uncertainties.

6.2 SOMO35

6.2.1 Concentration map

Figure 6.6 presents the combined final map for SOMO35 as result of combining the separate rural and urban interpolated map following the procedure as described in De Smet et al. (2011) and Horálek et al. (2007). SOMO35 is not subject to any of the EU air quality directives and there are no limit or target values defined.

As one can observe in a few areas of the map, the high or low measurement values do not seem to influence the interpolation results despite their clustering. The main reason is that the map presented here is an aggregation of 1x1 km values to 10x10 km resolution and this aggregation smooths out the values one would more likely be able to distinguish in the higher resolution map, especially in the case of urban stations representing the urban areas. Another less prominent reason is the smoothing effect kriging has in general.

The supplementary data used in the regression models are the same as for 26th highest daily maximum 8-hour mean, i.e. EMEP model output, altitude and surface solar radiation for rural areas and EMEP model output, wind speed and surface solar radiation for urban areas.

Table 6.5 presents the estimated parameters of the linear regression models and of the residual kriging, including the statistical indicators of both the regression and the kriging. The fit of the regression is expressed by the adjusted R^2 and standard error. The adjusted R^2 in 2013 for the rural areas is 0.59 and for the urban areas 0.53. This fit is somewhat worse than in 2012 and quite a similar or better compared to previous years, see Horálek et al. (2014a) and references cited therein. RMSE and bias are the cross-validation indicators showing the quality of the resulting map. Section 6.2.3 discusses in more detail the RMSE analysis and comparison with results of 2005 – 2012.

Table 6.5 Parameters of the linear regression models (Eq. 2.2) and of the ordinary kriging (OK) variograms (nugget, sill, range) – and their statistics – of ozone indicator SOMO35 for 2013 in the rural (left) and urban (right) areas as used for final mapping.

linear regr. model + OK on its residuals	**rural areas**	**urban areas**
	parameter values	**parameter values**
c (constant)	-975	-300
a1 (EMEP model 2013)	0.59	0.56
a2 (altitude GTOPO)	1.66	
a3 (wind speed 2013)		-81.46
a4 (s. solar radiation 2013)	228.48	140.37
adjusted R^2	**0.59**	**0.53**
standard error [µg.m^{-3}.d]	**1647**	**1396**
nugget	1.8E+06	9.0E+05
sill	2.3E+06	1.4E+06
range [km]	410	480
RMSE [µg.m^{-3}.d]	**1596**	**1194**
relative RMSE [%]	**29.2**	**28.1**
bias (MPE) [µg.m^{-3}.d]	**13**	**-5**

The concentration map presented in Figure 6.6 is spatially aggregated from 1x1 km to 10x10 km resolution. As a result, the urban areas are not properly resolved in this map, due to the smoothing effect of this aggregation. Section 6.2.3 discusses the level of the representation of the urban areas in this final combined aggregated 10x10 km map. For better visualising the actual urban concentration levels at the actual urbanised areas, i.e. without the influence of the dominating pattern of extended rural areas, a separate 1x1 km urban background map is presented in Annex 1, Figure A1.5.

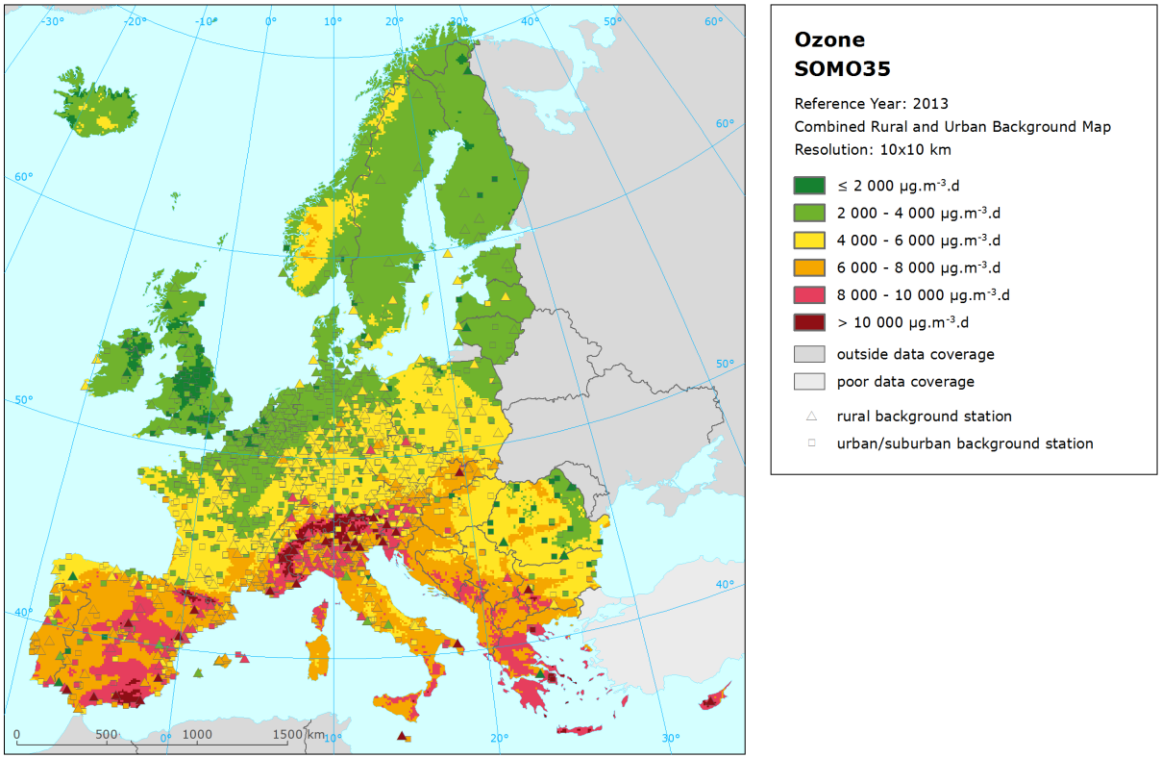

Figure 6.6 Combined rural and urban concentration map of ozone indicator SOMO35 in µg.m^{-3}.days for the year 2013. Resolution: 10x10 km.

Figure 6.7 presents the inter-annual difference between 2013 and 2012 for SOMO35. Red areas show an increase of ozone concentration, while blue areas show a decrease. A considerable increase is observed in Scandinavia, Portugal and the western part of France, while strong decrease is visible in West Balkan, Bulgaria and central and southern Italy. However, it should be noted the lack of the measuring stations in the most of these areas.

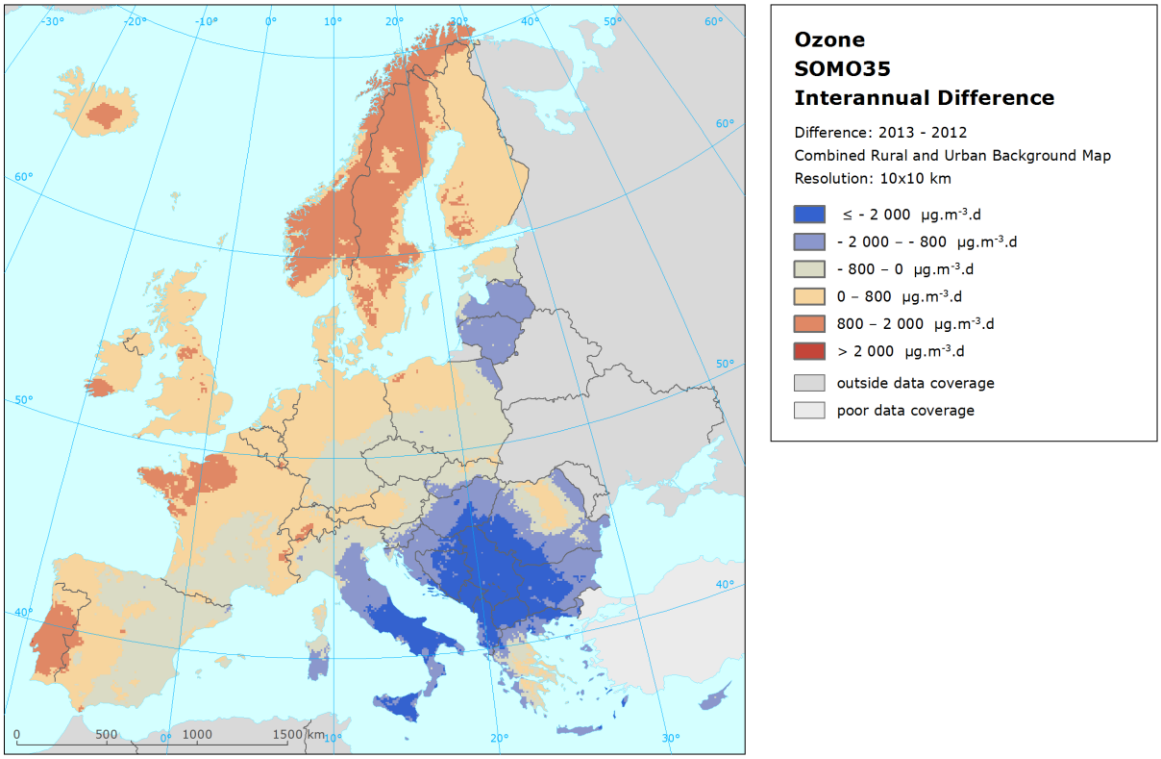

Figure 6.7 Inter-annual difference between mapped concentrations for 2013 and 2012 – ozone, SOMO35. Units: µg.m^{-3}.days.

6.2.2 Population exposure

Table 6.6 gives for SOMO35 the population frequency distribution for a limited number of exposure classes, as well as the population-weighted concentration for individual countries and for Europe as a whole. In the Table 6.7, the evolution of population exposure in the last nine years is presented.

It has been estimated that in 2013 about 19 % of the European population lived in areas with SOMO35 values above 6 000 µg.m^{-3}.d [(*)]. This is is about 6 percent point lower than in 2011 and 2012 and slightly more than in 2010. In 2013, the northern and north-western European countries show no people living in areas above 6 000 µg.m^{-3}.d (Figure 6.6), similarly to that of the years 2009 – 2012. The most of the countries in the southern and south-eastern regions show exposures above or well above 6 000 µg.m^{-3}.d, specifically Italy, Cyprus, Malta and the countries of the Balkan region.

(*) Note that the 6 000 µg.m^{-3}.d does not represent a health-related legally binding 'threshold'. In this and previous papers it concerns a somewhat arbitrarily chosen threshold to facilitate the discussion of the observed distributions of SOMO35 levels in their spatial and temporal context. This choice is motivated by a comparison of the 26th highest daily max. 8-hour means versus the SOMO35 of the ozone concentration measurements at all background stations. There is no simple relation between the two indicators, however it seems that the target value of the 26th highest daily maximum 8-hour mean, being 120 µg.m^{-3}, is related approximately with SOMO35 in the range 6 000 – 8 000 µg.m^{-3}.

Table 6.6 Population exposure and population-weighted concentration – ozone, SOMO35, year 2013.

Country		Population	Ozone, SOMO35, exposed population [%]						Population-weighted conc.
			< 2000	2000 - 4000	4000 - 6000	6000 - 8000	8000 - 10000	> 10000	
		[inhbs.1000]	µg.m^{-3}.d	µg.m^{-3}.d	µg.m^{-3}.d	µg.m^{-3}.d	µg.m^{-3}.d	µg.m^{-3}.d	[µg.m^{-3}.d]
Albania	AL	2 899			1.0	95.7	3.3		7 179
Andorra	AD	76				97.7	1.5	0.8	7 303
Austria	AT	8 452		6.5	75.1	14.8	3.3	0.2	5 389
Belgium	BE	11 162	7.3	92.1	0.7				2 520
Bosnia & Herzegovina	BA	3 836			78.0	21.3	0.7		5 670
Bulgaria	BG	7 285	0.7	52.2	40.2	6.6	0.3	0.0	4 082
Croatia	HR	4 262			59.4	37.9	2.7		5 989
Cyprus	CY	866				55.5	43.2	1.3	7 909
Czech Republic	CZ	10 516		40.4	59.2	0.4			4 266
Denmark	DK	5 603		98.1	1.9				2 749
Estonia	EE	1 320	0.1	99.8	0.2				2 545
Finland	FI	5 427	56.7	43.2	0.0				2 011
France (metropolitan)	FR	63 652		55.4	34.9	9.1	0.6	0.0	4 098
Germany	DE	80 524		83.8	16.1	0.1	0.0	0.0	3 506
Greece	GR	11 004			1.0	21.3	76.6	1.1	8 532
Hungary	HU	9 909		19.4	74.6	6.0			4 604
Iceland	IS	322	87.8	12.2	0.0				1 473
Ireland	IE	4 591	52.7	46.8	0.5				2 043
Italy	IT	59 685		0.2	29.2	63.5	6.9	0.2	6 576
Latvia	LV	2 024	0.8	99.2	0.0				2 614
Liechtenstein	LI	37			92.9	7.0	0.1		5 221
Lithuania	LT	2 972		100.0	0.0				2 703
Luxembourg	LU	537		97.0	3.0				3 167
Macedonia, FYROM of	MK	2 062			17.7	82.0	0.3		6 326
Malta	MT	421				96.0	4.0		7 403
Monaco	MC	38				100.0			7 795
Montenegro	ME	621			16.4	78.2	5.4		6 674
Netherlands	NL	16 780	14.9	85.1					2 410
Norway	NO	5 051	35.0	62.5	2.5	0.0			2 443
Poland	PL	38 063		65.4	34.3	0.4	0.0		3 792
Portugal (excl. Az., Mad.)	PT	9 977		28.7	44.7	26.2	0.4		5 091
Romania	RO	20 020	58.6	29.2	11.6	0.5			2 221
San Marino	SM	34			92.2	7.8			5 067
Serbia (incl. Kosovo*)	RS	8 997		18.7	72.0	9.1	0.3		4 738
Slovakia	SK	5 411		2.2	89.1	8.6	0.0		5 116
Slovenia	SI	2 059			47.9	40.3	11.8	0.0	6 540
Spain (excl. Canarias)	ES	44 623		7.7	40.6	49.5	2.1	0.1	5 895
Sweden	SE	9 556	42.0	56.3	1.7				2 317
Switzerland	CH	8 039			87.7	8.5	3.2	0.6	4 919
United Kingdom (& dep.)	UK	63 905	85.4	14.4	0.1	0.0			1 606
Total		**532 614**	**15.2**	**39.7**	**26.2**	**15.9**	**2.9**	**0.1**	**4 089**
			81.1			**18.9**			
EU-28		**500 603**	**15.8**	**41.2**	**24.5**	**15.5**	**3.0**	**0.1**	**4 040**
			81.5			**18.5**			
Kosovo*	KS	1 816	0.0	0.0	75.9	23.9	0.2	0.0	5 691
Serbia (excl. Kosovo*)	RS	7 182	0.0	23.2	71.0	5.4	0.3	0.0	4 505

*) under the UN Security Council Resolution 1244/99

Note1: Turkey is not included in the calculation due to lacking air quality data.
Note2: The percentage value "0.0" indicates an exposed population exists, but is small and estimated less than 0.05 %. Empty cells mean: no population in exposure.

Table 6.7 Evolution of population-weighted concentration in the years 2005-2013 (left) and of percentage population living in above limit value in the years 2009-2013 (right) – ozone, SOMO35. Resolution: 1x1 km.

Country		Population-weighted conc. [µg.m^{-3}.d]										Population above 6000 µg.m^{-3}.d [%]					
		2005	2006	2007	2008	2009	2010	2011	2012	2013	diff. '13 - '12	2009	2010	2011	2012	2013	diff. '13 - '12
Albania	AL	7911	7193	7817	7668	6754	5617	7769	8760	7179	-1581	97.6	32.1	99.3	100	99.0	-1.0
Andorra	AD	7520	6587	7121	6319	7186	7282	7891	8058	7303	-754	100	100	100	100	100	0
Austria	AT	5946	6237	5874	5099	5050	4969	5452	5419	5389	-30	13.4	12.1	22.0	20.7	18.3	-2.4
Belgium	BE	2775	4017	2235	2520	2599	2401	2714	2050	2520	471	0	0	0	0	0	0
Bosnia-Herzegovina	BA	6714	6571	6938	5972	5536	4879	5702	7322	5670	-1653	33.8	29.0	38.0	86.0	22.0	-64.0
Bulgaria	BG	5311	4896	6064	5797	5686	4377	5215	5960	4082	-1878	32.7	8.4	29.6	38.6	7.0	-31.6
Croatia	HR	6324	6928	6756	5899	5491	5419	6470	7143	5989	-1153	32.5	28.6	48.6	92.4	40.6	-51.7
Cyprus	CY	7155	5759	7739	8027	8788	7374	8773	8369	7909	-461	100	100	90.4	100	100	0
Czech Republic	CZ	5845	6097	5123	4576	4487	4160	4743	4806	4266	-541	0.8	0.2	8.5	4.0	0.4	-3.6
Denmark	DK	2519	3578	2440	3080	2440	2245	2752	2662	2749	87	0	0	0	0	0	0
Estonia	EE	2437	3594	2061	2363	1762	2646	2516	2310	2545	235	0	0	0	0	0	0
Finland	FI	2275	3141	1332	1938	1623	1925	2052	1650	2011	361	0	0	0	0	0	0
France	FR	4591	4972	3686	3563	4025	4139	4439	3635	4098	463	13.2	13.4	14.6	12.3	9.8	-2.5
Germany	DE	3940	4860	3648	3822	3507	3652	3668	3357	3506	149	0.4	0.3	0.4	0.1	0.1	0.0
Greece	GR	8321	6657	8330	8969	8330	7483	9182	9378	8532	-846	98.8	86.4	98.5	99.8	99.0	-0.8
Hungary	HU	5751	5738	6547	5751	6631	4408	5828	6342	4604	-1737	89.9	0.9	33.7	68.6	6.0	-62.7
Iceland	IS	1329	2265	1168	2224	833	775	1094	1242	1473	230	0	0	0	0	0	0
Ireland	IE	1701	2453	1412	2096	1487	1419	1353	1479	2043	564	0	0	0	0	0	0
Italy	IT	7634	8205	7506	6386	6986	6302	7532	7328	6576	-752	75.3	61.7	89.9	83.6	70.6	-13.0
Latvia	LV	2391	3734	2262	2347	1837	2304	2708	3103	2614	-489	0	0	0	0	0	0
Liechtenstein	LI	5233	6258	4826	4930	5271	5244	5128	5132	5221	89	12.2	10.8	12.2	11.5	7.1	-4.4
Lithuania	LT	3671	4535	2744	3059	2291	2608	3131	3358	2703	-655	0	0	0	0	0	0
Luxembourg	LU	4769	5090	3424	3557	3500	3505	3527	2561	3167	607	0	0	0	0	0	0
Macedonia, FYR of	MK	7069	6297	6690	7133	6229	5081	7110	8472	6326	-2146	41.5	13.6	89.9	100	82.3	-17.7
Malta	MT	6971	7797	7209	6582	6634	6722	7127	8022	7403	-619	100	100	97.1	100	100	0
Monaco	MC		8903	8381	7246	8325	8028	8354	6979	7795	816	100	100	100	100	100	0
Montenegro	ME	7608	6554	7379	7120	6237	5653	6970	8584	6674	-1910	37.1	33.1	60.2	100	83.6	-16.4
Netherlands	NL	1901	3245	1816	2104	1922	1916	2283	1949	2410	461	0	0	0	0	0	0
Norway	NO	2580	3496	1705	2514	2000	1803	2395	2128	2443	315	0	0	0	0	0	0
Poland	PL	4784	5416	4179	3951	3747	3278	4065	4045	3792	-253	0.5	0.0	1.8	0.6	0.4	-0.2
Portugal	PT	5510	5257	4863	3851	5003	5133	4552	4240	5091	851	28.9	32.4	17.4	9.5	26.6	17.1
Romania	RO	5238	4798	5882	5039	5044	3033	3276	3967	2221	-1746	28.3	1.1	9.0	10.7	0.5	-10.1
San Marino	SM	7540	6321	7296	5863	5860	5331	6220	6048	5067	-980	15.3	11.6	18.4	15.3	7.8	-7.5
Serbia (incl.	RS	5947	5239	6768	6378	6118	4001	5793	6844	4738	-2106	60.6	9.4	36.8	55.3	9.3	-46.0
Slovakia	SK	6141	6261	6098	5455	6348	4748	6051	6103	5116	-987	75.6	6.2	45.9	54.8	8.6	-46.2
Slovenia	SI	6242	7480	6671	5761	5775	5998	7062	7092	6540	-553	36.6	37.5	82.3	84.5	52.1	-32.4
Spain	ES	6139	5813	5992	5110	5983	6088	5858	5850	5895	45	57.7	50.0	46.7	48.1	51.7	3.6
Sweden	SE	2682	3635	1795	2387	2100	2025	2628	2233	2317	84	0	0	0	0	0	0
Switzerland	CH	5740	6321	5114	4619	5139	5127	5435	4990	4919	-72	14.3	12.9	14.3	10.9	12.3	1.5
United Kingdom	UK	1551	2676	1174	2044	1433	1072	1471	1183	1606	422	0	0	0	0	0.0	0.0
Total		**4706**	**5167**	**4411**	**4275**	**4275**	**3917**	**4414**	**4279**	**4089**	**-190**	**24.6**	**16.6**	**23.6**	**24.5**	**18.9**	**-5.7**
EU28		**4613**	**5128**	**4319**	**4178**	**4208**	**3888**	**4339**	**4154**	**4040**	**-114**	**23.6**	**16.7**	**23.6**	**22.8**	**18.5**	**-4.3**

We observe in 2013, compared to 2012, a slight European overall decrease (of just 0.9 %) in population exposed to ozone levels above 10 000 µg.m^{-3}.d, such that it leads to the percentage level of 2011.

In 2013 the total European population-weighted ozone concentration, in terms of SOMO35, was estimated to be 4089 µg.m^{-3}.d, which is less than in 2011 – 2012 and in 2005 - 2009, while more than in 2009.

6.2.3 Uncertainties

Uncertainty estimated by cross-validation

The basic uncertainty analysis is given by the cross-validation. In Table 6.5, the absolute mean uncertainty (RMSE) in 2013 was 1596 µg.m^{-3}.d for the rural areas and 1194 µg.m^{-3}.d for the urban areas, i.e. the least from the whole nine-year period (Horálek et al, 2014a and references cited therein). The relative mean uncertainty of the 2013 map of SOMO35 is 29.2 % for rural and 28.1 % for urban areas, which is for the urban area slightly less than in the years 2005 – 2012 and for the rural areas same as in 2012 and less than in all the previous years (Horálek et al., 2015). Table 7.7 summarises both the absolute and the relative uncertainties over these past nine years.

Figure 6.8 shows the cross-validation scatter plots for interpolated values at both rural and urban areas. R^2 for rural areas and urban areas in 2013 indicates that, respectively, about 61 % and 66 % of the variability is attributable to the interpolation. The corresponding values for the maps of the years 2005 – 2012 (see Table 7.7) show the results of 2013 are within the fluctuation of the previous years.

The scatter plots show again that in areas with high concentrations the interpolation methods tend to deliver underestimated predictions, although some overestimation or lower values of urban areas is also likely. For example, in urban areas (Figure 6.7, right panel) an observed value of 10 000 µg.m^{-3}.d is estimated in the interpolation as about 8 100 µg.m^{-3}.d. That is 19 % too low, leading in general to considerable underestimations at high SOMO35 values. Vice versa at low values an overestimation will occur, e.g. at a measured 2000 µg.m^{-3}.d the interpolation will predict some 2 800 µg.m^{-3}.d, which is about 38 % too high.

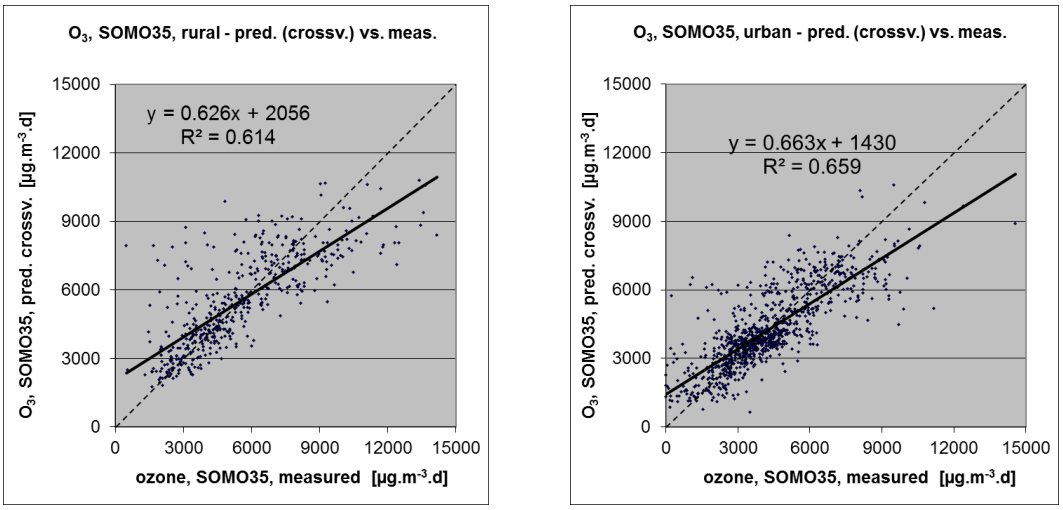

Figure 6.8 Correlation between cross-validation predicted values (y-axis) and measurements (x-axis) for the ozone indicator SOMO35 for rural (left) and urban (right) areas in 2013.

Comparison of point measurement values with the predicted grid value

Additional to the above point observation – point prediction cross-validation, a simple comparison was made between the point measurements and interpolated predicted grid values averaged in on a grid of 10x10 km resolution the separate rural and urban background maps. This point-grid comparison indicates to what extent the predicted value of a grid cell represents the corresponding measured values at stations located in that cell.

The comparison has been made primarily for the separate rural and separate urban background maps at 10x10 km resolution. (One can directly relate this comparison result to the cross-validation results of Figure 6.8.)

Next to this, the comparison has been done also for the final combined maps at 1x1 km resolution and for the spatial aggregated final maps at 10x10 km resolution. Figure 6.9 shows the scatterplots for these comparisons.

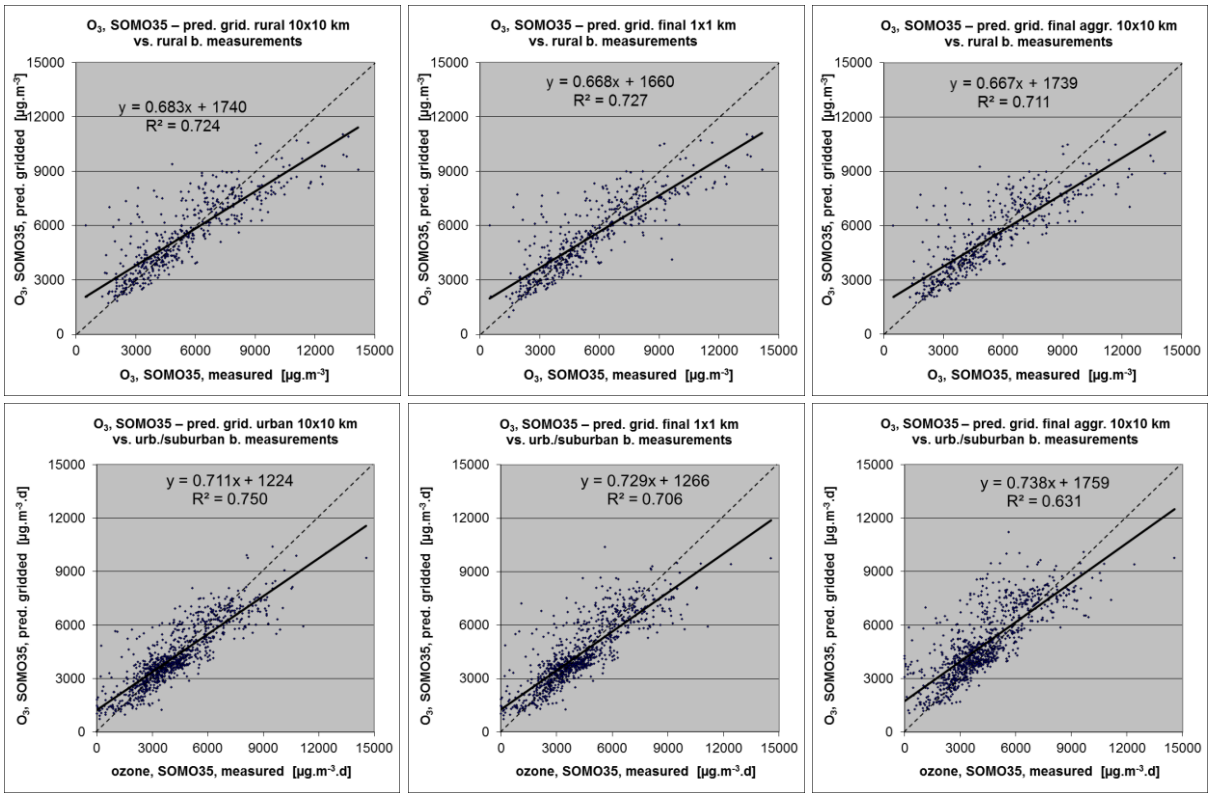

Figure 6.9 Correlation between predicted grid values from rural 10x10 km (upper left), urban 10x10 km (bottom left), final combined 1x1 km (upper and bottom middle) and final combined spatially aggregated 10x10 km (upper and bottom right) map (y-axis) versus measurements from rural (top), resp. urban/suburban (bottom) background stations (x-axis) for the ozone indicator SOMO35 for 2013.

The results of the point observation – point prediction cross-validation of Figure 6.8 and those of the point-grid validation for the separate rural and the separate urban background map, and for the final combined maps at both resolutions (Figure 6.4) are summarised in Table 6.8.

By the comparing the scatterplots and the statistical indicators for the separate rural and separate urban background map with the final combined maps in both resolutions, one can evaluate the level of representation of the rural resp. urban background areas in the final combined maps. The rural air quality is fairly well represented in both the 1x1 km and the aggregated 10x10 km final combined map. The urban air quality is quite well represented in the final combined 1x1 km map, but not in the aggregated final combined 10x10 km map, as one can deduce from the higher RMSE, the bias being further from zero and the lower R^2. Therefore, we present in Figure A1.5 of Annex 1 the 1x1 km urban background map in addition to the 10x10 km final combined map of Figure 6.6.

Table 6.8 shows a better correlated relationship (i.e. lower RMSE, higher R^2, smaller intercept, slope closer to 1) between station measurements and the interpolated values of the corresponding grid cells at both rural and urban background map areas than it does for the point cross-validation predictions. This is because the simple comparison between point measurements and the gridded interpolated values shows the uncertainty of predictions where there are actual station locations, while the point cross-validation prediction simulates the behaviour of the interpolation at point positions assuming no actual measurements would exist at these points within the area covered by measurements. The uncertainty at measurement locations is caused partly by the smoothing effect of the interpolation and partly by the spatial averaging of the values into 10x10 km grid cells. The degree of smoothing leading to

underestimation in areas with high values is weaker when measurements exist, than when no measurement exists. For example, in urban areas the predicted interpolation grid value in the separate urban background map will be about 8 600 µg.m^{-3}.d at a corresponding station point with an observed value of 10 000 µg.m^{-3}.d. This is an underestimation of about 14 %. It is less than the prediction underestimation of 19 % at the same point location, when leaving out this one actual measurement point and one does the interpolation without the station (see the previous subsection).

Table 6.8 Statistical indicators RMSE, bias, coefficient of determination R^2 and linear regression equation from the scatter plots for the predicted point values based on cross-validation and the predicted grid values from separate (rural resp. urban) 10x10 km, final combined 1x1 km and final combined spatially aggregated 10x10 km map versus the measured point values for rural (left) and urban (right) background stations for the ozone indicator SOMO35 of 2013.

	rural backgr. stations				urb./suburban backgr. stations			
	RMSE	bias	R^2	equation	RMSE	bias	R^2	equation
cross-valid. prediction, separate (r or ub) map	1596	13	0.614	y = 0.626x + 2056	1194	-5	0.667	y = 0.680x + 1374
grid prediction, 10x10 km separate (r or ub) map	1355	8	0.724	y = 0.683x + 1740	1028	-5	0.818	y = 0.763x + 1020
grid prediction, 1x1 km final merged map	1363	-157	0.73	y = 0.668x + 1660	1115	112	0.770	y = 0.780x + 1080
grid prediction, aggr. 10x10 km final merged map	1390	-81	0.71	y = 0.667x + 1739	1426	645	0.669	y = 0.793x + 1620

No Limit Value or Target Value is set for the WHO recommended ozone health indicator SOMO35, therefore no probability of exceedance map has been prepared.

6.3 AOT40 for crops and for forests

The ecosystem based accumulative ozone indicators described in this section are specifically prepared for calculation of EEA Core Set Indicator 005 (CSI005, http://themes.eea.europa.eu/indicators). For the estimation of the vegetation and forested area exposure to accumulated ozone the maps in this section are created on a grid of 2x2 km resolution, instead of the 10x10 km grid used for the human health indicators. This resolution is selected as a compromise between calculation time and accuracy in the impact assessment done for ozone within CSI005. It serves as a refinement of the exposure frequency distribution outcomes of the overlay with 100x100 m resolution CLC2006 land cover classes.

6.3.1 Concentration maps

The interpolated maps of AOT40 for crops and AOT40 for forests were created for rural areas only, combining AOT40 data derived from rural background station observations with supplementary data sources EMEP model output, altitude and surface solar radiation. Note that supplementary data sources are the same as for the human health related ozone indicators.

Table 6.9 presents the estimated parameters of the linear regression models and of the residual kriging, including their statistical indicators of the regression and kriging. The fit of the regression is expressed by adjusted R^2 and the standard error. The adjusted R^2 is 0.64 both for AOT40 for crops and for AOT40 for forests in 2013, which is the second better results in the nine-year period, see Horálek et al. (2015) and references cited therein. RMSE and bias are the cross-validation indicators, showing the quality of the resulting map. Section 5.3.3 discusses in more detail the RMSE analysis and comparison with results of 2005 – 2012.

Table 6.9 Parameters of the linear regression models (Eq2.1) and of the ordinary kriging (OK) variograms (nugget, sill, range) - and their statistics - of ozone indicators AOT40 for crops (left) and for forests (right) for 2013 in the rural areas as used for final mapping.

linear regr. model + OK on its residuals	AOT40 for crops parameter values	AOT40 for forests parameter values
c (constant)	-9135	-12519
a1 (EMEP model 2013)	0.87	0.70
a2 (altitude GTOPO)	3.66	6.92
a3 (s. solar radiation 2013)	1080.7	1610.5
adjusted R^2	**0.64**	**0.64**
standard error [µg.m^{-3}]	**5509**	**9729**
nugget	1.1E+07	2.4E+07
sill	2.2E+07	6.7E+07
range [km]	410	450
RMSE [µg.m^{-3}]	**5179**	**9257**
relative RMSE [%]	**34.6**	**34.7**
bias (MPE) [µg.m^{-3}]	**21**	**46**

Figure 6.10 presents the final map of AOT40 for *crops*. The areas and stations in the map that exceed the target value (TV) of 18 000 µg.m^{-3}.h are marked in red and dark red. Note that in Directive 2008/50/EC the target value is defined as 18 000 µg.m^{-3}.h *averaged over five years*.

As urban areas are considered not to represent agricultural areas, this map is applicable to rural areas only, and as such it is based on rural background station observations only. The highest AOT40 levels (red and dark red) can be found specifically in the southern, south-western and south-eastern regions of Europe. Compared to map of 2012 (Horálek et al., 2015) in general an increase in the extent of areas with the highest AOT40 levels can be seen in the Iberian Peninsula, while decreases are observed in the central Italy and Balkan.

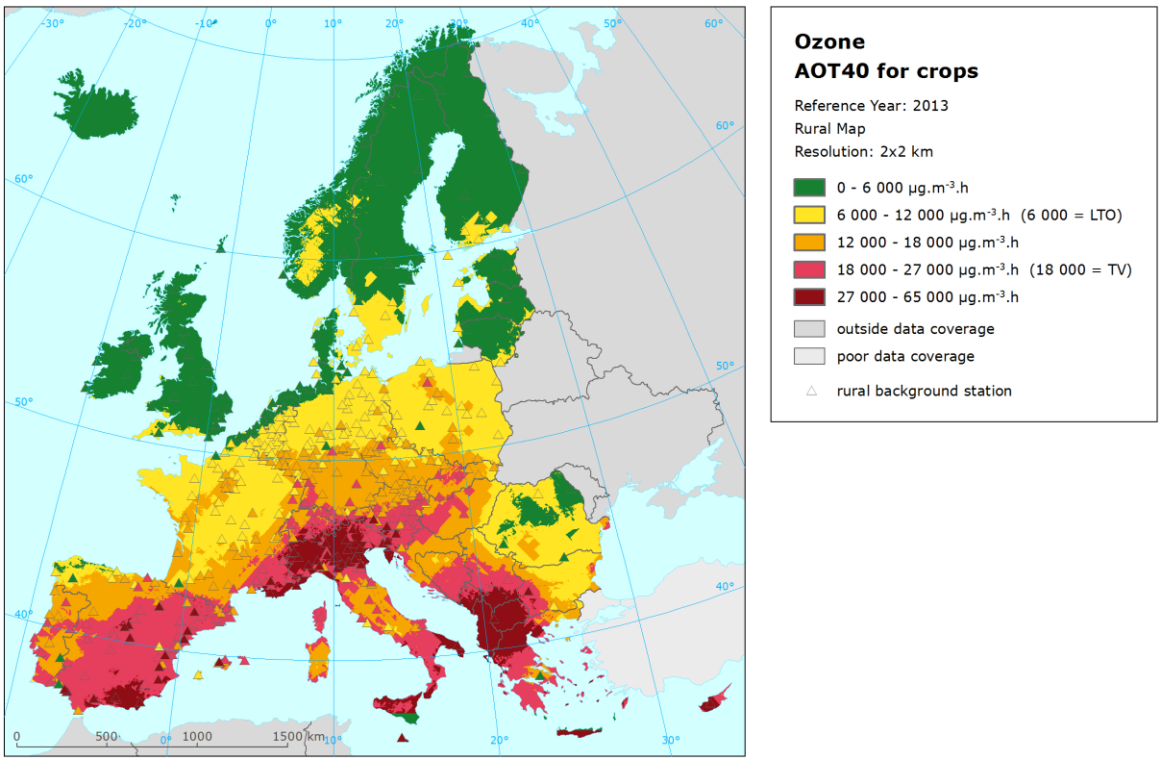

Figure 6.10 Rural concentration map of ozone vegetation indicator AOT40 for crops for the year 2013. Units: µg.m^{-3}.hours. Resolution: 2x2km.

Figure 6.11 presents the inter-annual difference between 2013 and 2012 for AOT40 for crops. Red areas show an increase of ozone concentration, while blue areas show a decrease. The highest increases are observed in Portugal, and the range of France, Germany, Switzerland, western Poland, Sweden, Finland, northern Norway, and in Albania and FYR of Macedonia. Contrary to that, considerable decreases are observed in central Italy, Poland, Latvia, Hungary, Slovakia and almost the whole region of south-eastern Europe. The only exceptions are just Albania and FYR of Macedonia – however, it should be noted that the increase in these countries is caused by just one station MK0042A with the extremely high concentration. In the case of the health related ozone indicators, this station does not have enough data and is not used in the mapping, leading to non-existence of such an increase of concentrations in the relevant difference maps, see Figures 6.2 and 6.7.

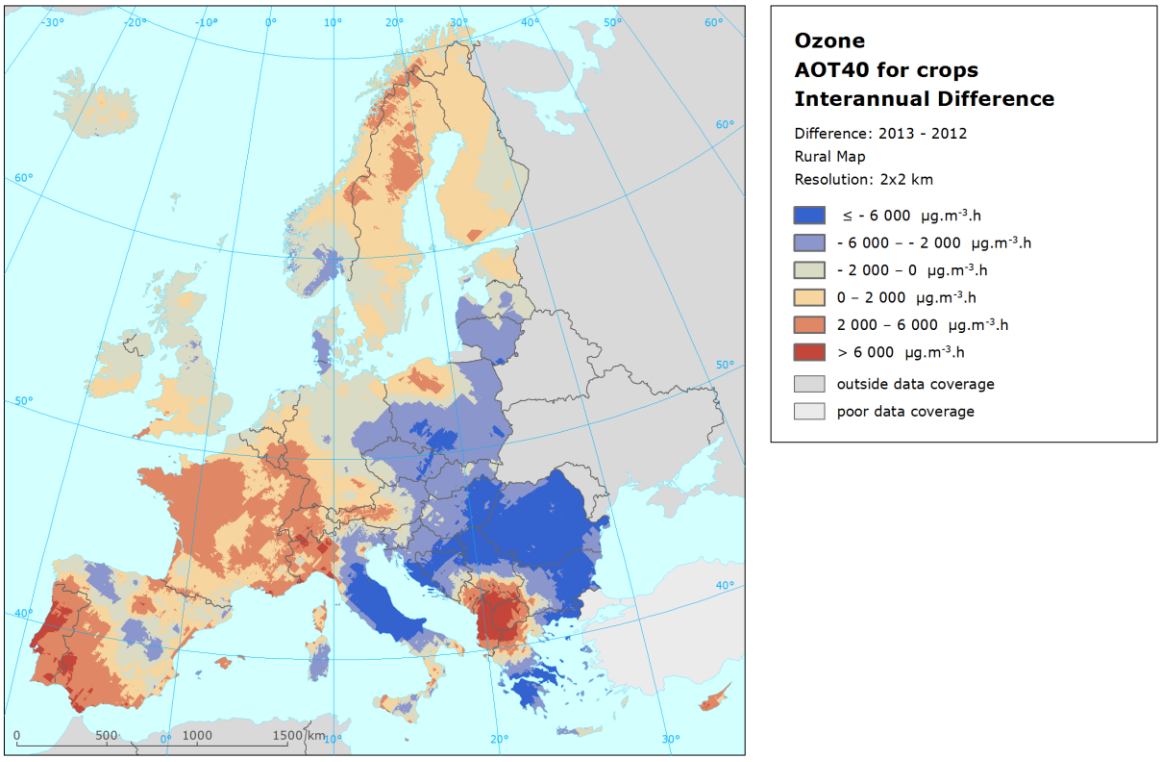

Figure 6.11 Inter-annual difference between mapped concentrations for 2013 and 2012 – ozone, AOT40 for crops. Units: µg.m^{-3}.hours.

Figure 6.12 presents the final map of AOT40 for forests. Like Figure 6.10, it concerns a map for rural areas as urban areas are considered as not forested. Therefore, the map is based on rural background station observations only, representing an indicator for vegetation exposure to ozone. For AOT40 for forests there is no TV defined, but there is a critical level established by UNECE (UNECE, 2004).

Figure 6.13 shows the inter-annual difference between 2013 and 2012 for AOT40 for forests. The main decrease is visible in Eastern Europe (Latvia, Lithuania, East Poland), Central Europe (Czech Republic, Hungary), the central part of Italy, and south-eastern Europe, specifically the most of the Balkan countries, Romania, Bulgaria, Greece. The increase is visible particularly in Portugal, and the range of France, Germany, Switzerland, Benelux, western Poland, Sweden and Norway. Next to this, strong increase can be seen in FYR of Macedonia and Albania, casing by the sole measuring station MK0042A with the extremely high concentration in the situation of the lack of other stations in these countries.

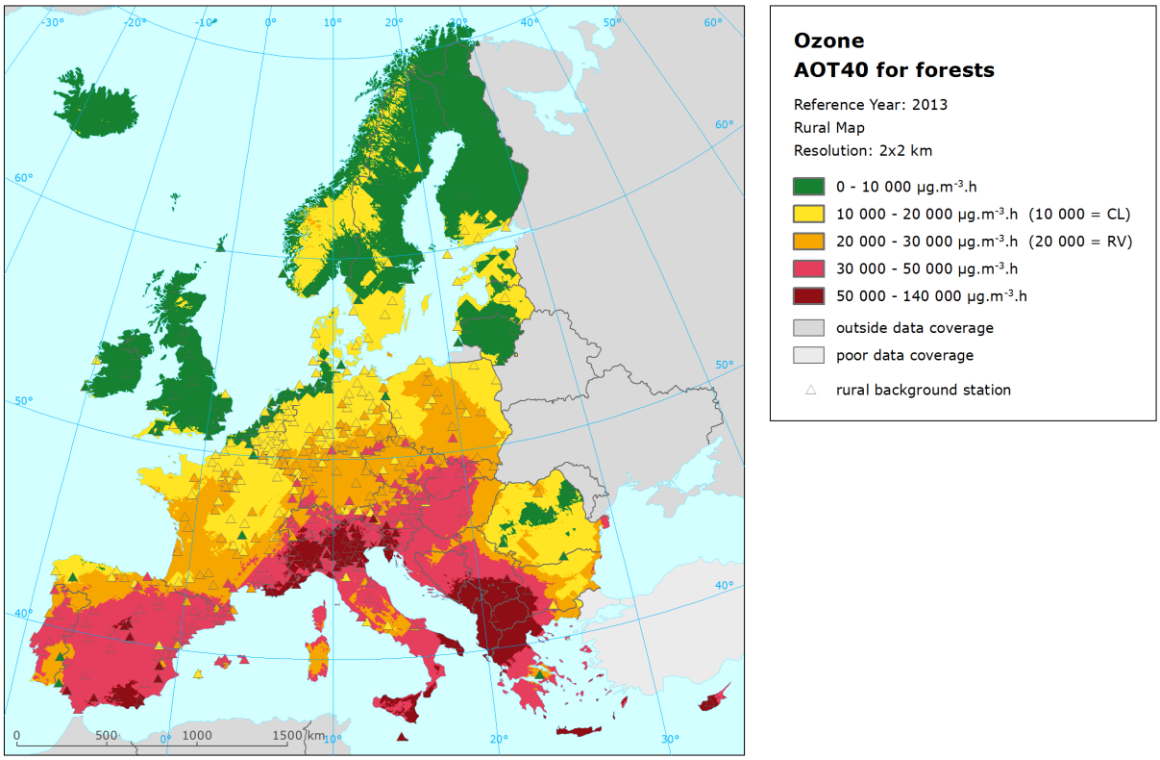

Figure 6.12 Rural concentration map of ozone vegetation indicator AOT40 for forests for the year 2013. Units: µg.m^{-3}.hours. Resolution: 2x2km.

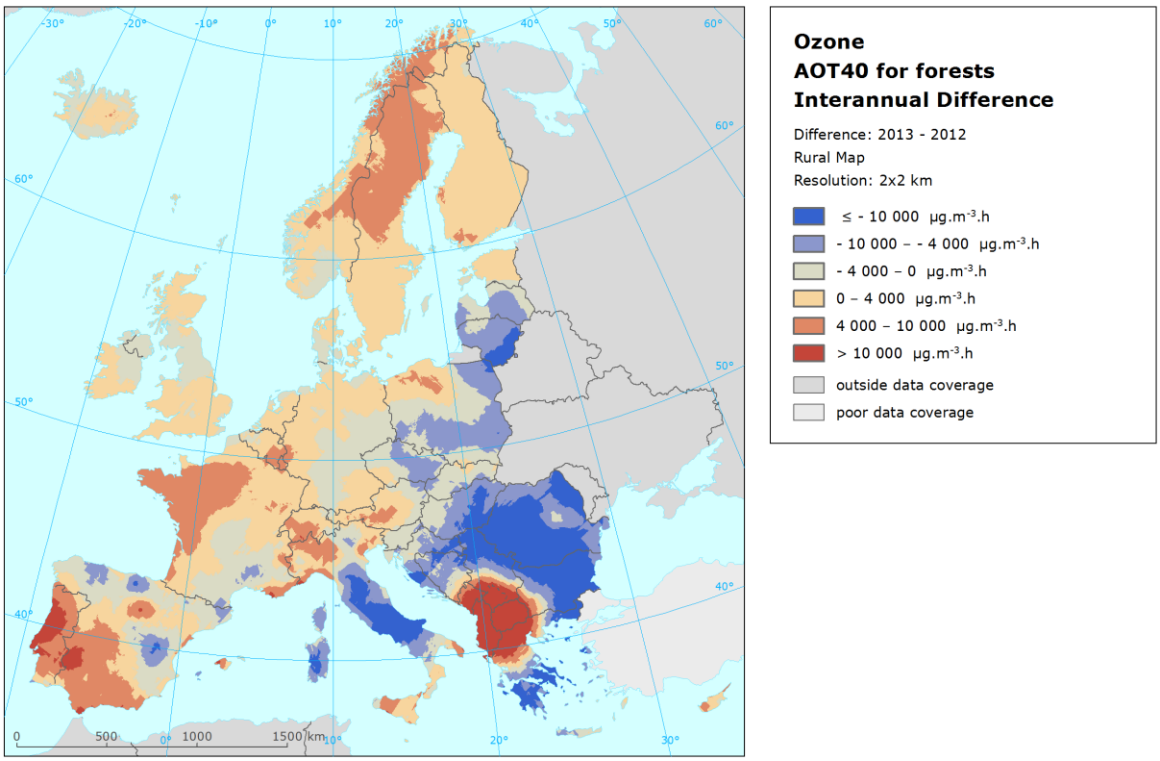

Figure 6.13 Inter-annual difference between mapped concentrations for 2013 and 2012 – ozone, AOT40 for forests. Units: µg.m^{-3}.hours. Resolution: 2x2km.

6.3.2 Vegetation exposure

Agricultural crops

The rural map with ozone indicator AOT40 for vegetation, i.e. agricultural crops, as given in Figure 6.10, has been combined with the land cover CLC2006 map. Following a similar procedure as described in Horálek et al. (2007) the exposure of agricultural areas, defined as the Corine Land Cover level-1 class *2 Agricultural areas* (encompassing the level-2 classes *2.1 Arable land, 2.2 Permanent crops, 2.3 Pastures* and *2.4 Heterogeneous agricultural areas)* has been calculated at the country-level.

Table 6.10 gives the absolute and relative agricultural area for each country and for four European regions where the target value (TV) and long-term objective (LTO) for ozone are exceeded. The frequency distribution of the agricultural area per country over the exposure classes is presented as well.

The table indicates the country grouping with corresponding colours of the region; *Northern Europe*: Sweden, Finland, Norway, Estonia, Lithuania, Latvia and Denmark. *North-western Europe*: United Kingdom, Ireland, Iceland, the Netherlands, Belgium, Luxembourg and France north of 45 degrees latitude. *Central and Eastern Europe*: Germany, Poland, Czech Republic, Slovakia, Hungary, Austria, Liechtenstein, Bulgaria and Romania. *Southern Europe*: Albania, Bosnia-Herzegovina, France south of 45 degrees latitude, Portugal, Spain, Italy, San Marino, Slovenia, Croatia, Greece, Cyprus, F.Y.R. of Macedonia, Montenegro, Serbia (including Kosovo under the UN Security Council Resolution 1244/99) and Malta.

Table 6.10 illustrates that in 2013, some 22 % of all European agricultural land was exposed to ozone exceeding the target value (TV) of 18 000 $\mu g.m^{-3}.h$. This is a decrease in the total area with agricultural crops above the TV (and as such considered to suffer from adverse effects to ozone exposure) compared to 2012 (30 %). It is slightly more than in 2010 – 2011 and less than in 2005 – 2009, see Table 6.12. Considering the long-term objective (LTO, 6 000 $\mu g.m^{-3}.h$) the area in excess is about 81 %, which is lower than in the most of the previous years, see Table 7.4. However, Iceland and Monaco were the only countries with ozone levels not being in excess of the LTO. In many countries of southern Europe, more than half of their total agricultural area experienced exposures above the less stringent TV.

Table 6.12 (left) presents for comparison the percentages of area in exceedance of the target value for the years 2005 – 2013. In southern Europe, about 63 % of the total agricultural area exceeded the target value in 2013. This is considerably more than in years 2007 – 2011 with 54 to 57 % but still substantially below the amount of 2006 (94 %). In northern Europe for the years 2005 and 2007 – 2013, no area was mapped in excess of the target value; only in 2006 almost 4 % of its area was in excess. In the north-western region the area exceeding the target value is still low with its 0.2 %, comparable to the levels of most of its previous years. For the central and eastern region, the total area where ozone exceeds the target value decreased considerably to some 5 % comparable to the levels of 2011.

Compared to 2006, the frequency distribution of agricultural areas over the exposure classes showed a clear shift towards lower exposures in 2007 leading to a decreased total area exceeded, towards a distribution more similar to that of 2005 (Horálek et al., 2008). In 2008, this tendency continued with an approximately similar area percentage in excess of the TV. However, a shift in area percentages with lower exposure levels in 2007 to somewhat higher levels in 2008 (but still below the target value) also occurred. Compared to 2007 – 2008, we observed in 2009 – 2010 an increased area with lower exposure level, leading to a lower TV exceedance. In 2011, this tendency seems to continue for most regions except for the southern European region where the areas with more elevated levels or areas in exceedances of the TV continue to exist or extended. In 2012 and 2013, this evolution seems to be continued rather unaltered.

Table 6.10 Agricultural area exposure and exceedance (Long Term Objective, LTO and Target Value, TV) for ozone, AOT40 for crops, year 2013.

Country	Agricultural Area, 2013					Percentage of agricultural area, 2013 [%]				
	total area	> LTO (6 mg.m^{-3}.h)		> TV (18 mg.m^{-3}.h)		< 6	6 - 12	12 - 18	18 - 27	> 27
	[km^2]	[km^2]	[%]	[km^2]	[%]	mg.m^{-3}.h	mg.m^{-3}.h	mg.m^{-3}.h	mg.m^{-3}.h	mg.m^{-3}.h
Albania	7877	7877	100	7877	100					100.0
Austria	27222	27222	100	9336	34.3			65.7	34.2	0.1
Belgium	17597	14309	81.3			18.7	68.5	12.8		
Bosnia-Herzegovina	18839	18839	100	8197	43.51		5.7	50.8	43.5	0.0
Bulgaria	57402	57402	100	6135	10.7		67.4	21.9	10.4	0.3
Croatia	22501	22501	100	7725	34.3		0.0	65.7	29.2	5.1
Cyprus	4290	4290	100	4250	99.1			0.9	47.7	51.4
Czech Republic	45117	45117	100	34	0.1		20.8	79.1	0.1	
Denmark (no Faroes)	32042	11751	36.7			63.3	36.6	0.0		
Estonia	14644	1724	11.8			88.2	11.8			
Finland	29023	5294	18.2			81.8	18.2			
France	327710	323038	98.6	14845	4.5	1.4	66.5	27.5	3.9	0.6
Germany	212177	193277	91.1	2858	1.3	8.9	54.2	35.5	1.3	
Greece (CLC2000)	51575	51575	100	41907	81.3		4.7	14.0	48.8	32.4
Hungary	62219	62219	100	13198	21.2		17.5	61.3	21.2	
Iceland	2378					100				
Ireland	46141	199	0.4			100	0.4			
Italy	156491	156491	100	118117	75.5		0.6	23.9	37.9	37.6
Latvia	28253	3644	12.9			87.1	12.9			
Liechtenstein	41	41	100	1.8	4.4			95.6	4.4	
Lithuania	39815	5133	13			87.1	12.9			
Luxembourg	1389	1389	100				41	58.8		
Macedonia, FYR of	9316	9316	100	9316	100				6.7	93.3
Malta	124	124	100	124	100					100
Monaco	0.00									
Montenegro	2298	2298	100	2298	100				48.7	51.3
Netherlands	24238	11750	48.5			51.5	48.5			
Norway	15673	193	1.2			98.8	1.2			
Poland	195798	195795	100	3	0.0	0.0	88.1	11.9	0.0	
Portugal	41909	41909	100	9424	22.5		0.8	76.7	22.5	
Romania	135293	98596	73	27	0.0	27.1	68.7	4.1	0.0	
San Marino	42	42	100	42	100				100.0	
Serbia (incl. Kosovo)	48639	48639	100	20562	42.3		15.7	42.0	31.8	10.5
Slovakia	23660	23660	100	3034	12.8		12.8	74.4	12.8	
Slovenia	7104	7104	100	7043	99.1			0.9	95.2	4.0
Spain	251578	249031	99.0	184431	73.3	1.0	4.3	21.4	68.8	4.5
Sweden	38647	14774	38.2			61.8	38.2			
Switzerland	11806	11806	100	4583	38.8			61.2	37.2	1.6
United Kingdom(& Man)	138874	12964	9.3			90.7	9.3			
Total	**2149741**	**1741333**	**81.0**	**475368**	**22.1**	**19.0**	**35.5**	**23.4**	**16.7**	**5.4**
EU-28	**2032833**	**1642283**	**80.8**	**422491**	**20.8**	**19.2**	**37.1**	**22.9**	**16.2**	**4.6**
France over 45N	259931	255258	98.2	952	0.4	1.8	77.2	20.6	0.4	0.0
France below 45N	67779	67779	100	13893	20.5	89.0	11.0			
Kosovo*	4438	4438	100	4438	100				5.3	94.7
Serbia (excl. Kosovo*)	44201	44201	100	16124	36.5		17.3	46.2	34.4	2.0

*) under the UN Security Council Resolution 1244/99

Northern	198097	42514	21.5	0	0
North-western	490547	295870	60.3	952	0.2
Central & Eastern	770734	715133	92.8	39211	5.1
Southern	690363	687816	99.6	435205	63.0
Total	**2149741**	**1741333**	**81.0**	**475368**	**22.1**

Note1: Countries not included due to lack of land cover data: Andorra, Turkey.
Note2: The percentage value "0.0" indicates an exposed agricultural area exists, but is small and estimated less than 0.05 %.
Empty cells mean: no agricultural area in exposure.

Forests

The rural map with ozone indicator AOT40 for forests, as given in Figure 6.9, was combined with the land cover CLC2000 map as done for crops. Following a similar procedure as described in Horálek et al. (2007) the exposure of forest areas, defined as CORINE Land Cover level-2 class *3.1 Forests* has been calculated at the country-level.

Table 6.11 gives the absolute and relative forest area where the *Critical Level* (*CL* of 10 000 $\mu g.m^{-3}.h$, as defined in the Mapping Manual, UNECE, 2004) in combination with the *Reporting Value* (RV of 20 000 $\mu g.m^{-3}.h$, as defined in Annex III of the former ozone directive 2002/3/EC) are exceeded. This is done for each country, for four European regions and for Europe as a whole. The table presents the frequency distribution of the forest area per country and over the exposure classes. The Reporting Value of the ozone directive was exceeded in 2013 at some 44 % of the total European forest area. Table 6.12 (right) presents for comparison the percentages of area that exceed the Reporting Value for the years 2005 – 2013. The area above the RV for 2013 is some 3 % lower than in 2012 (47 %) and also somewhat lower than the earlier mapping years 2007 – 2012 (48 – 50 %), while in 2006 it was almost 70 % and in 2005 about 60 %. This means that the area of forest exposed to levels above the accumulated ozone RV diminished and stabilised around 45 – 50 % in the period from 2007 to 2013, which is an area of around 10 – 15 percent points below that of 2005.

In 2005 about three-quarters of the European forested areas were exposed to exceedances of the Critical Level (CL) of 10 000 $\mu g.m^{-3}.h$, while in 2006 it was almost all forested areas. This extensive portion shrank in 2007 to 62 %, but in 2008 it increased to 80 %. In 2009 – 2013, the area reduced to a rather stable level ranging between 63 – 69 %, with 67 % in 2013 (Tables 6.11 and 7.4).

Like in 2010 – 2012, almost all European countries had their forests exposed to accumulated ozone concentrations above the CL in 2013. Many of those countries had forest areas experiencing exposures in excess of the less stringent RV. About the same set of countries do show in 2013 no RV exceedances like in 2010 – 2012, of which for some the area with concentrations above the CL has increased and for other it decreased. As in previous years, in 2013 the southern European region continued to have AOT40 levels such that all forested areas were exposed to exceedances of the CL and approximately all of the RV.

In 2013, about all forests of central and eastern regions are above the CL, and some 64 % above the RV. The central and eastern regions show, for the period of 2005 – 2013, a continued (close to) 100 % exceedance of the CL. The area with exceedances of the RV (Table 6.12) showed 96 % in 2005, a peak of almost 100 % in 2006, followed by a reduction to about 86 % in 2007 and a subsequent increase of about 10 % in 2008 to 95 %. In 2009, the area in excess of the RV was 88 %. In 2010, it is 76 % and in 2011 it increases to 90% with a decrease to some 82 % in 2012 and 64 % in 2013.

In the north-western region, the area exceeding the CL increased from 84 % in 2005 to practically the whole area (98 %) in 2006. In 2007, it dropped again to 78 %, but in 2008 it increased to almost all forested area (94 %). From 2009 to 2013, the percentages fluctuate between 80 – 82 %, i.e. close to the excess of 2007 (see Table 6.11 and Horálek et al., 2015). Concerning the north-western European forested area above the RV, there was a prominent drop from 69% in 2005 and 80% in 2006 to 28% in 2007 that continued in 2008 to 23 %, but increased again in 2009 to 30 % and to 60 % in 2010 and 2011. Then, it dropped to 20 % in 2012 and increased to 38 % in 2013.

Specifically in the northern region of Europe, the area in exceedance peaked considerably in 2006: the area above the CL enlarged from 40 % in 2005 to 100 % in 2006 and reduced thereafter to 12 % in 2007 and increased in 2008 to 51 %. In 2009, some 23 % of the northern European forest area exceeded the CL. In 2010, it was about 13 %, which increased in 2011 back to some 25 %, in 2012 downward back to some 17 % and in 2013 again upward back to 23 % (Table 6.11). The RV (Table 6.12) decreases in northern Europe from 23 % in 2006 (after an increase from none in 2005) to about none in 2007 – 2013.

Table 6.11 Forested area exposure and exceedance (critical level, CL and reporting value, RV) for ozone, AOT40 for forests, year 2013.

Country	Forested area, 2013					Percentage of forested area, 2013 [%]				
	total area	> CL (10 mg.m^{-3}.h)		> RV (20 mg.m^{-3}.h)		< 10	10 - 20	20 - 30	30 - 50	> 50
	[km^2]	[km^2]	[%]	[km^2]	[%]	mg.m^{-3}.h	mg.m^{-3}.h	mg.m^{-3}.h	mg.m^{-3}.h	mg.m^{-3}.h
Albania	7589	7589	100	7589	100					100
Austria	37223	37223	100	37186	100		0.1	22.8	76.7	0.4
Belgium	6092	5975	98.1	1465	24.1	1.9	74.0	24.1		
Bosnia-Herzegovina	22804	22804	100	22804	100			6.2	83.5	10.3
Bulgaria	34635	34635	100	28543	82.4		17.6	36.5	33.1	12.8
Croatia	20094	20094	100	20094	100			3.7	87.3	9.1
Cyprus	1535	1535	100	1535	100				6.7	93.3
Czech Republic	26092	26092	100	26092	100			83.0	17.0	
Denmark (no Faroes)	3731	3633	97.4	94	2.5	2.6	94.9	2.5		
Estonia	20559	14431	70.2			29.8	70.2			
Finland	194003	17821	9.2			90.8	9.2			
France	141881	141688	100	96383	67.9	0.1	31.9	49.7	15.4	2.9
Germany	104143	103217	99.1	64401	61.8	0.9	37.3	58.8	3.1	
Greece (CLC2000)	23562	23562	100	23477	100		0.4	10.8	46.6	42.2
Hungary	17520	17520	100	17437	100		0.5	16.9	82.6	
Iceland	318					100.0				
Ireland	2835	27	0.9			99.1	0.9			
Italy	78246	78246	100	78184	100		0.1	10.8	58.5	30.6
Latvia	26158	14365	54.9			45.1	54.9			
Liechtenstein	85	85	100	85	100			25.7	74.3	
Lithuania	18728	1426	7.6			92.4	7.6			
Luxembourg	931	931	100	589	63		36.7	63.3		
Macedonia, FYR of	8232	8232	100	8232	100					100
Malta	2	2	100	2	100					100
Monaco	0.44	0.44	100	0.44	100				84.1	15.9
Montenegro	5738	5738	100	5738	100					100
Netherlands	3100	2478	79.9			20.1	79.9			
Norway	103846	26357	25.4	3	0.0	74.6	25.4	0.0		
Poland	93919	93919	100	50756	54.0		46.0	51.2	2.9	
Portugal	20132	20132	100	20100	99.8		0.2	30.9	69.0	
Romania	69989	61861	88.4	7603	10.9	11.6	77.5	10.7	0.1	
San Marino	6	6	100	6	100				100.0	
Serbia (incl. Kosovo)	26875	26875	100	26567	99		1.1	8.8	41.8	48.2
Slovakia	19683	19683	100	19683	100			19.6	80.4	
Slovenia	11471	11471	100	11471	100				65.8	34.2
Spain	90274	90029	100	81054	89.8	0.3	9.9	20.1	65.8	3.8
Sweden	243521	66624	27.4	0.2	0.0	72.6	27.4	0.0		
Switzerland	12530	12530	100	12530	100			37.6	55.3	7.1
United Kingd. (& Man)	20056	1122	5.6			89.0	11.0			
Total	**1518137**	**1019956**	**67.2**	**669703**	**44.1**	**32.8**	**23.1**	**18.7**	**19.4**	**6.0**
EU-28	**1330115**	**909741**	**68.4**	**586150**	**44.1**	**31.6**	**24.3**	**20.7**	**19.4**	**4.0**
France over 45N	88005	87812	99.8	43673	49.6	0.2	50.2	45.5	4.1	0.1
France below 45N	53876	53876	100	52709	97.8	89.0	11.0			
Kosovo*	4292	4292	100	4292	100					100
Serbia (excl.Kosovo)*	22583	22583	100	22275	98.6		1.4	10.5	49.8	38.4

*) under the UN Security Council Resolution 1244/99

Northern	610546	144657	23.7	97	0.0
North-western	121336	98344	81.1	45728	37.7
Central & Eastern	415821	406765	97.8	264317	63.6
Southern	370434	370189	99.9	359561	97.1
Total	**1518137**	**1019956**	**67.2**	**669703**	**44.1**

Note1: Countries not included due to lack of land cover data: Andorra, Turkey.
Note2: The percentage value "0.0" indicates an exposed forested area exists, but is small and estimated less than 0.05 %.
Empty cells mean: no forested area in exposure.

Table 6.12 Evolution of percentage agricultural area above target value for AOT40 for crops (left) and percentage forested area above reporting value for AOT40 for forests (right) in the years 2005-2013.

Country		AOT40 for crops										AOT40 for forests									
		Agricultural area above TV [%]										Forested area above RV [%]									
		2005	2006	2007	2008	2009	2010	2011	2012	2013	diff. '13 - '12	2005	2006	2007	2008	2009	2010	2011	2012	2012	diff. '13 - '12
Albania	AL	100	100	100	87.3	100	4.0	100	100	100	0	100	100	100	100	100	100	100	100	100	0
Austria	AT	98.6	100	81.8	67.3	4.0	40.9	32.5	59.5	34.3	-25.2	100	100	100	100	100	99.7	99.7	99.8	99.9	0.1
Belgium	BE	6.4	98.0	0	0	0	0	0	0	0	0	74.3	99.8	7.9	0	0	33.7	35.8	0	24.1	24.1
Bosnia-Herzegovina	BA	78.1	62.7	100	80.0	90.3	46.2	51.2	99.98	43.5	-56.5	100	100	100	100	100	100	100	100	100	0
Bulgaria	BG	99.0	44.5	99.6	2.4	64.4	4.6	10.5	31.3	10.7	-20.6	100	100	100	100	100	98.1	100	100	82.4	-17.6
Croatia	HR	74.1	82.2	100	95.8	85.5	62.0	68.6	99.6	34.3	-65.3	100	100	100	100	100	100	100	100	100	0
Cyprus	CY	100	99.0	100	0.0	100	87.2	90.6	88.0	99.1	11.0	100	100	100	100	100	100	100	100	100	0
Czech Republic	CZ	81.4	100	83.0	99.0	0.0	8.0	4.8	24.7	0.1	-24.6	100	100	100	100	100	96.4	99.7	100	100	0
Denmark	DK	0	5.3	0	0	0	0	0	0	0	0	5.9	91.7	0.9	1.7	1.7	0	0.9	0.2	2.5	2.3
Estonia	EE	0	0	0	0	0	0	0	0	0	0	0.0	52.6	0	0	0	0	0	0	0	0
Finland	FI	0	0	0	0	0	0	0	0	0	0	0.0	2.1	0	0	0	0	0	0	0	0
France	FR	33.7	78.0	3.4	10.2	10.2	11.9	6.5	3.8	4.5	0.8	92.6	97.0	50.9	48.0	52.2	85.3	85.3	51.0	67.9	16.9
Germany	DE	33.9	94.7	3.6	62	0.0	24.4	0.3	0.3	1.3	1.0	88.6	99.8	76.9	92.8	81.0	84.0	85.1	59.6	61.8	2.3
Greece	GR	100	95.2	97.4	79.0	95.2	44.1	77.6	96.7	81.3	-15.4	100	100	100	100	100	100	100	100	99.6	-0.4
Hungary	HU	75.2	93.4	100	82.8	83.6	7.2	15.3	89.0	21.2	-67.8	100	100	100	100	100	92.6	99.95	100	99.5	-0.5
Iceland	IS	*no data*		0	0	0	0	0	0	0	0	*no data*		0	0	0	0	0.0	0	0	0
Ireland	IE	0	0	0	0	0	0	0	0	0	0	0	0	0	0	0	0	0.0	0	0	0
Italy	IT	99.7	100.0	84.0	83.8	91.2	67.9	80.7	96.7	75.5	-21.2	100	100	100	100	100	100	100	100	99.9	-0.1
Latvia	LV	0	0	0	0	0	0	0	0	0	0	0.0	39.9	0	0	0	0	0.2	0.0	0	0.0
Liechtenstein	LI	100	100	7.7	100	0	100	100	6.5	4.4	-2.1	100	100	100	100	100	100	100	100	100	0
Lithuania	LT	0	0	0	0	0	0	0	0	0	0	0.3	55.1	0	0	0	0	0	24.6	0	-24.6
Luxembourg	LU	95.6	100	0	0	0	26.8	0	0	0	0	100	100	64.8	7.4	100	94.9	82.0	0	63.3	63.3
Macedonia, FYR of	MK	100	100	100	99.8	100	1.3	72.1	100	100	0.0	100	100	100	100	100	100	100	100	100	0
Malta	MT	100	99	99.1	100	100	100	100	100	100	0	100	100	100	100	100	100	100	100	100	0
Monaco	MC		100	92.3	0	100	100	0	0	0	0		100	100	100	100	100	100	100	100	0
Montenegro	ME	*no data*		100	94.2	100	26.4	83.3	100	100	0.0	*no data*		100	100	100	100	100	100	100	0
Netherlands	NL	0	53.3	0	0	0	0	0	0	0	0	0	87.7	0	0	0	0	0	0	0	0
Norway	NO	*no data*		0	0	0	0	0	0	0	0	*no data*		0.2	0.0	0	0	0	4.0	0.0	-4.0
Poland	PL	6.0	94.4	21.2	38.9	0	0	0.6	4.0	0.0	-4.0	96	100	65.3	81.7	70.0	27.3	73.2	71.3	54.0	-17.2
Portugal	PT	98.7	87.7	0	2	0	41.5	4.2	1.0	22.5	21.4	100	100	91.1	89.1	95.7	99.7	89.1	71.6	99.8	28.2
Romania	RO	49.4	10.4	97.0	9.9	21.5	0	0.0	22.3	0.0	-22.3	100	98.8	100	99.6	100	80.8	96.0	88.9	10.9	-78.0
San Marino	SM	100	100	100	100	100	100	100	100	100	0	100	100	100	100	100	100	100	100	100	0
Serbia (incl.Kosovo)	RS	*no data*		100	67.4	100	2.9	24.1	2.9	42.3	39.4	*no data*		100	100	100	100	100	100	99	-1.1
Slovakia	SK	76.4	99.1	99.7	78.7	58.4	0.2	25.4	74.6	12.8	-61.8	100	100	100	100	100	90.8	99.8	100	100	0.0
Slovenia	SI	86.6	100	100	95.6	73.1	100	100	100	99	-1	100	100	100	100	100	100	100	100	100	0
Spain	ES	98.7	93.3	27.2	58.5	35.1	60.7	48.4	61.0	73.3	12.3	100.0	99.4	94.3	89.8	88.4	93.3	93.1	89.5	89.8	0.3
Sweden	SE	0	12.6	0	0	0	0	0	0	0	0	0.2	31.2	0.0	0	0	0	0	0	0	0
Switzerland	CH	*no data*			67.4	10.0	98.1	29.2	14.5	38.8	24.3	*no data*			100	99.9	100	100	98.9	100	1.1
United Kingdom	UK	0	14.4	0	0	0	0	0	0	0	0	0.0	11.0	0	0	0	0	0	0	0	0
Total		**48.5**	**69.1**	**35.7**	**37.8**	**26.0**	**21.3**	**19.2**	**30.0**	**22.1**	**-7.9**	**59.1**	**69.4**	**48.4**	**50.2**	**49.2**	**49.3**	**53.0**	**47.2**	**44.1**	**-3.1**
EU-28		**47.8**	**68.9**	**33.3**	**36.3**	**23.3**	**21.4**	**18.3**	**27.4**	**20.8**	**-6.7**	**57.9**	**68.5**	**49.4**	**51.0**	**49.9**	**49.9**	**54.2**	**47.6**	**44.1**	**-3.6**
Northern		0	3.6	0	0	0	0	0	0	0	0	0.2	22.9	0.0	0	0.0	0	0.0	0.8	0.0	-0.7
North-western		11.2	49.4	0.1	2.0	2.0	33.0	1.1	0.1	0.2	0.1	69.3	79.8	27.8	23.3	29.9	59.7	59.6	19.9	37.7	17.8
Central & eastern		44.1	76.8	50.3	47.2	17.4	11.0	4.9	20.6	5.1	-15.5	96.1	99.7	86.1	94.0	88.5	75.4	89.5	81.5	63.6	-17.9
Southern		96.2	93.9	55.3	63.5	60.4	56.8	53.6	70.5	63.0	-7.4	100.0	99.7	94.2	93.1	92.8	97.8	97.2	94.4	97.1	2.7

Note: Lack of land cover data in 2006: CH, IS, ME, NO, RS; in 2007: CH.

In comparison with 2006, the frequency distribution of the whole European forested area over the exposure classes shows for 2007 a clear shift to lower exposures. In 2008 a shift was observed of areas exposed in 2007 to the highest exposure class to its neighbouring lower class interval and for the areas exposed in 2007 to the lowest exposure class to its neighbouring higher class interval. In 2009 and 2010 the distribution showed similarity with that of 2007. In 2011 a light shift to the higher classes is observed,

most prominently in the central and eastern European regions. In 2012 the overall distribution looks very familiar to that of the years 2009, while in 2013 to that of the year 2011.

The total area with AOT40 for forests levels below the CL diminished by 18 % in 2008 (20 %) compared to 2007 (38 %) but increased again in 2009 up to 33 % and in 2010 to 37 %. In 2011 it is 32% and in 2012 about 35 %. In 2013 it is with 33 % in the same range as in the years 2007 and 2009 – 2012 with percentages between 33 – 38 %. The total forested area exposed to levels below the RV fluctuated in the period 2007 – 2013 around a value of some 50 %.

6.3.3 Uncertainties

Uncertainty estimated by cross-validation

In Table 6.9 the absolute mean uncertainty (RMSE) obtained by cross-validation is 5509 µg.m^{-3}.h for the AOT40 for crops and 9729 µg.m^{-3}.h for the AOT40 for forests. It indicates that the year 2013 has the absolute mean uncertainty values in quite similar levels as in its previous five year (see Table 7.7). The relative mean uncertainties of the 2013 maps are for both vegetation indicator type some 35 %. For crops, that is more than in 2012 (33 %), 2010 (31 %), 2008 (31 %) and 2006 (30 %), while same as in 2011 (35 %) and less than in 2009 (38 %), 2007 (40 %) and 2005 (41 %). For forests, the relative RMSE is more than in the year 2006 and in the period 2008 – 2012 and less than in the years 2005 and 2007. Table 7.7 summarises both the absolute and the relative uncertainties over these past nine years.

Figure 6.14 shows the cross-validation scatter plots of the AOT40 for both crops and forests. R^2 indicates that for both indicators about 68 % of the variability is attributable to the interpolation. The corresponding values for the previous seven years one find in Table 7.7 and demonstrate a somewhat increased level of interpolation performance in the period 2009 – 2013 compared to its previous years.

The cross-validation scatter plots show again that in areas with higher accumulated ozone concentrations the interpolation methods tend to deliver underestimated predicted values. For example, in agricultural areas (Figure 6.14, left panel) an observed value of 30 000 µg.m^{-3}.h is estimated in the interpolation as about 26 000 µg.m^{-3}.h, i.e. an underestimation of about 15 %. In addition, an overestimation at the lower end of predicted values occurred. One could reduce this under- and overestimation by extending the number of measurement stations and by optimising the spatial distribution of those stations, specifically in areas with elevated values.

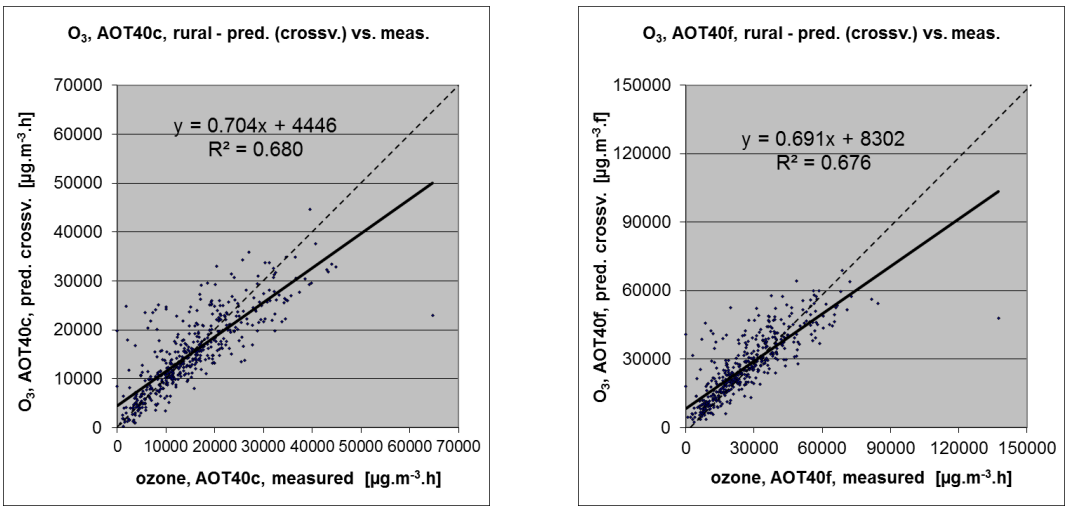

Figure 6.14 Correlation between cross-validation predicted values (y-axis) and measurements (x-axis) for the ozone indicators AOT40 for crops (left) and AOT40 for forests (right) for rural areas in 2013.

Comparison of point measurement values with the predicted grid value

In addition to the above point observation – point prediction cross-validation, a simple comparison was made between the point measurements and interpolated predicted grid values on the grid of 2x2 km resolution. The results of the cross-validation compared to the gridded validation are summarised in Table 6.13. The table shows for both receptors a better correlation between the station measurements and the averaged interpolated predicted values of the corresponding grid cells, case ii), than it does at the point cross-validation predictions, case i), of Figure 6.14. Case ii) represents the uncertainty of the predicted gridded interpolation map at the actual station locations (points) themselves, whereas the point cross-validation prediction of case i) simulates the behaviour of the interpolation at point positions assuming no actual measurements would exist at these points within the area covered by measurements. The uncertainty at measurement locations has partly its cause in the smoothing effect of interpolation and partly in the spatial averaging of the values in the 2x2 km grid cells. In such situations, the degree of smoothing leading to underestimation at areas with high values appears to be smaller than when there would be no measurement present in such areas. For example, in agricultural areas a predicted interpolation grid value will be about 28 000 $\mu g.m^{-3}.h$ at a corresponding station point with an observed value of 30 000 $\mu g.m^{-3}.h$. This is an underestimation of about 6 %. Nevertheless, it is less than the prediction underestimation of 15 % at the same point location, when leaving out this one actual measurement point from the interpolation (see the previous subsection).

Table 6.13 Statistical indicators RMSE, bias, coefficient of determination R^2 and linear regression equation from the scatter plots for (i) the predicted point values based on cross-validation and (ii) aggregation into 2x2 km grid cells versus the measured point values for ozone indicators AOT40 for crops (left) and AOT40 for forests (right) for rural areas in 2013.

	AOT40 for crops				AOT40 for forests			
	RMSE	bias	R^2	equation	RMSE	bias	R^2	equation
(i) cross-validation prediction, rural map	5179	21	0.68	y = 0.704x + 4446	9257	46	0.68	y = 0.691x + 8302
(ii) grid prediction, 2x2 km rural map	3426	3	0.86	y = 0.809x + 3868	5356	4	0.90	y = 0.828x + 4588

The AOT40 for crops with a target value of 18 000 $\mu g.m^{-3}.h$ would allow us to prepare a probability of exceedance map. However, we limited the preparation of such maps to the human health related indicators, thus not involving the accumulative ozone indicators used in the EEA CSI005 (itself not demanding such maps).

7 Concluding exposure and uncertainty estimates

Mapping and exposure results

This paper presents the interpolated maps for 2013 on the PM_{10}, $PM_{2.5}$ and ozone human health related air pollution indicators, together with their frequency distribution of the estimated population exposures and exceedances. It concerns the annual average and the 36th highest daily mean for PM_{10}, annual average for $PM_{2.5}$, and the 26th highest daily maximum 8-hour value and the SOMO35 for ozone. Interpolated maps on the vegetation/ecosystem based ozone indicators AOT40 for crops and AOT40 for forests are additionally presented, including their frequency distribution of estimated land area exposures and exceedances. A mapping approach similar to previous years (De Smet et al. 2011 and references cited therein, Denby et al. 2011c) on observational data was used. For the fourths time, inter-annual difference maps are presented.

Human health PM_{10} indicators

Table 7.1 summarises for both *human health PM_{10} indicators* the average concentration the European inhabitant is exposed to, i.e. the population-weighted concentration and the number of Europeans exposed to PM_{10} concentrations above their limit values (LV) for the years 2005 to 2013. The table presents the results obtained from both the 1x1 km resolution grid as tested with the 2006 data in Horálek et al (2010), recomputed for 2005 and 2007 and implemented fully on the 2008 data and onwards.

Table 7.1 Population-weighted concentration and the percentage of the total European population exposed to concentrations above limit value (LV) for the human health PM_{10} indicators annual average and 36th highest daily mean for 2005 to 2013.

PM10		2005	2006	2007	2008	2009	2010	2011	2012	2013
Annual average										
Population-weighted concentration (µg.m-3)	1x1 merger	28.0	28.5	26.2	24.8	24.6	24.3	22.1	22.7	22.2
Population exposed > LV (40 µg.m-3) (% of total)	1x1 merger	13.3	10.3	6.8	5.8	6.0	5.2	2.5	3.4	2.6
36th highest daily mean										
Population-weighted concentration (µg.m-3)	1x1 merger	46.8	47.8	44.1	41.3	41.2	41.9	39.0	39.7	38.6
Population exposed > LV (40 µg.m-3) (% of total)	1x1 merger	34.3	35.7	26.2	19.4	16.5	20.6	15.8	16.5	16.4

The population exposed to *annual mean* concentrations of PM_{10} above the limit value of 40 µg.m^{-3} is at least 2.6 % of the total population in 2013, somewhat less than in 2012. Furthermore, it is estimated that European inhabitants living in background (neither hot-spot nor industrial) areas – without regard to urban or rural – are exposed on average to the annual mean PM_{10} concentration of about 22 µg.m^{-3}. In comparison with the previous eight years, the number of people living in the areas above the LV tends not to go down further. However, it is not possible to talk about a trend when taking into account (i) the meteorologically induced variations and (ii) the uncertainties involved in the interpolation and (iii) station densities and their spatial distributions over the European regions. Longer time series, reduced uncertainties and improved spatial coverages will be needed before any conclusions on a possible trend can be drawn. Next to this, we should bear in mind that different trends in various parts of Europe may take place. Moreover, if we do a trend-like analysis it should be based on pop-weighted concentrations as this is more robust than the fraction exposed.

In 2013 at least some 16 % of the European population lived in areas where the PM_{10} limit value of 50 µg.m^{-3} for the *36th highest daily mean* is exceeded, being the same as in 2012. When comparison this quantity with those of the previous years of the given limited time series, one may conclude that it fits within the fluctuation of the past five years. The overall European population-weighted concentration of the 36th highest daily mean for the background areas is estimated to be at least 39 µg.m^{-3}, which fits in the range we observed over the past three years.

Comparing the observed (and also predicted) exceedances for both PM_{10} indicators, one may conclude that the daily limit value is more stringent throughout the years.

Human health $PM_{2.5}$ indicator

Table 7.2 summarises for *human health $PM_{2.5}$ indicator* (annual average) the population-weighted concentration and the number of Europeans exposed to $PM_{2.5}$ concentrations above its target value (TV) for the years 2007 to 2013 (without 2009, for which nor the map nor the population exposure were prepared).

Table 7.2 Population-weighted concentration and the percentage of the total European population exposed to concentrations above target value (TV) for the human health $PM_{2.5}$ indicator annual average for 2007 to 2013.

PM2.5		2007	2008	2009	2010	2011	2012	2013
Annual average								
Population-weighted concentration (µg.m-3)	1x1 merger	16.3	16.3	not	16.8	15.9	15.6	15.3
Population exposed > TV (25 µg.m-3) (% of total)	1x1 merger	7.8	7.6	mapped	8.3	6.2	9.0	5.8

The proportion exposed to annual mean concentrations of $PM_{2.5}$ above the target value of 25 $\mu g.m^{-3}$ is about 6 % of the total population in 2013, which is about similar like in 2011 and lower than in other years of the limited time series considered. Furthermore, it is estimated that European inhabitants living in background (neither hot-spot nor industrial) areas – without regard to urban or rural – are exposed on average to the annual mean $PM_{2.5}$ concentration of about 15 $\mu g.m^{-3}$.

In comparison with the previous years, both the population-weighted concentration and the number of people living in the areas above the TV seems slightly to decrease.

Health related ozone indicators

Table 7.3 summarises the levels of both *human health ozone indicators* that European inhabitants are exposed to, i.e. population-weighted concentrations. Furthermore, it presents the number of Europeans exposed to concentrations above the target value (TV) of the 26th highest daily maximum 8-hour mean and above a level of 6 000 $\mu g.m^{-3}.d$ for the SOMO35 for the years 2005 to 2013.

Table 7.3 Population-weighted concentration and the percentage of the total European population exposed to concentrations above the target value (TV) or the indicative chosen threshold for the human health ozone indicators 26th highest daily maximum 8-hour average and SOMO35 for2005 to 2013.

Ozone		2005	2006	2007	2008	2009	2010	2011	2012	2013
26th highest daily max. 8-hr average										
Population-weighted concentration (µg.m-3)	1x1 merger	112.1	118.2	110.7	109.8	108.1	106.8	108.9	107.9	108.3
Population exposed > TV (120 µg.m-3) (% of total)	1x1 merger	31.6	51.4	27.1	15.0	16.0	16.3	16.5	20.7	15.0
SOMO35										
Population-weighted concentration (µg.m-3.d)	1x1 merger	4706	5167	4411	4275	4275	3917	4414	4279	4088
Population exposed > 6 mg.m-3.d (% of total)	1x1 merger	27.0	29.5	28.1	19.6	24.6	16.6	23.6	24.5	18.8

The table presents the results obtained with the 1x1 km merging resolution as tested on the 2006 data in Horálek et al (2010), recomputed for 2005 and 2007 and implemented fully on the 2008 data and onwards.

For the ozone indicator *26th highest daily maximum 8-hour mean* it is estimated that at least 15 % of the population lived in 2013 in areas above the ozone target value (TV) of 120 $\mu g.m^{-3}$, which is lower than in its four previous years. The overall European population-weighted ozone concentration in terms of the 26th highest daily maximum 8-hour mean in the background areas is estimated at about 108 $\mu g.m^{-3}$, which is within the range of values of the four earlier years of the recorded time series. Examining the time series 2005 – 2013, one could conclude that 2006 is an exceptional year with elevated ozone concentrations, leading to increased exposure levels compared to the other eight years. Additionally, the

population exposed to ozone level above the target value is in the period 2008 – 2013 lower than in the preceding period of 2005 – 2007.

A similar tendency is observed for the *SOMO35*: In 2006 – 2007 almost one-third of the population lived in areas where a level of 6 000 µg.m^{-3}.d$^{(*)}$ was exceeded, with the highest level in 2006. In the period of 2008 – 2013 it fluctuates between about one-fifth to a quarter of the population. The population-weighted SOMO35 concentrations shows a quite similar kind of pattern over time.

(*) Note that the 6 000 µg.m^{-3}.d does not represent a health-related legally binding 'threshold'. In this and previous papers it concerns a somewhat arbitrarily chosen threshold to facilitate the discussion of the observed distributions of SOMO35 levels in their spatial and temporal context. For motivation of this choice, see Section 6.2.2.

Agricultural and forest ozone indicators

Exposure indicators describing the *agricultural and forest areas exposed to accumulated ozone* concentrations above defined thresholds are summarised in Table 7.4. Those thresholds are the target value (TV) of 18 000 µg.m^{-3}.h and the long-term objective (LTO) of 6 000 µg.m^{-3}.h for the AOT40 for crops, and the Reporting Value (RV) of 20 000 µg.m^{-3}.h and the Critical Level (CL) of 10 000 µg.m^{-3}.h for the AOT40 for forests.

Table 7.4 Percentages of the total European agricultural and forest area exposed to ozone concentrations above their thresholds: target value (TV) and long-term objective (LTO) for AOT40 for crops, and Critical Level (CL) and Reporting Value (RV) for AOT40 for forests for2005 to 2013.

Ozone		2005	2006	2007	2008	2009	2010	2011	2012	2013
AOT40 for crops										
Agricultural area % > TV (18 mg.m^{-3}.h)	(% of total)	48.5	69.1	35.7	37.8	26.0	21.3	19.2	30.0	22.1
Agricultural area % > LTO (6 mg.m^{-3}.h)	(% of total)	88.8	97.6	77.5	95.5	81.0	85.4	87.9	86.4	81.0
AOT40 for forests										
Forest area exposed > RV (20 mg.m^{-3}.h)	(% of total)	59.1	69.4	48.4	50.2	49.2	49.3	53.0	47.2	44.1
Forest area exposed > CL (10 mg.m^{-3}.h)	(% of total)	76.4	99.8	62.1	79.6	67.4	63.4	68.6	65.0	67.2

In 2013, at least 22 % of all agricultural land (*crops*) was exposed to accumulated ozone concentrations (AOT40) exceeding the target value (TV) and 81 % was exposed to levels in excess of the long-term objective (LTO). Compared the last nine years one could conclude that 2006 was a year with elevated ozone concentrations, leading to increased exposure levels above the target value. One the one hand, from 2007 and onward the total area exceeding the TV reduced continuously. On the other hand, the percentage of the total area exposed to levels above the LTO is in 2007 lowest compared to all the other years of the time series 2005 – 2013, and in the period 2008 – 2013 it ranges between 81 – 88 %, not demonstrating the same reduction as observed at the TV exceedance.

For the ozone indicator AOT40 for *forests* the level of 20 000 µg.m^{-3}.h (Reporting Value, RV) was in 2013 exceeded in about 44 % of the European forest area, which is the lowest of the whole time series and clearly below the percentages of the years 2005 and 2006. The forest area exceeding the Critical Level (CL) was in 2013 about 67 %, which is within the range of exceedances between 62 – 67 % as observed for the years 2007 and 2009 – 2012 and well below the exceedances of 2005 and 2008 (with 76 – 80 %), and 2006 when all forest area was exceeded.

The temporal pattern of the AOT40 for forests exceedances shows some similarity with those of the AOT40 for crops, despite their different definitions. This annual variability is, however, heavily dependent on meteorological variability.

Uncertainty results

Next to the creation of European wide interpolated air pollutant maps and exposure tables, we evaluated the uncertainty of the presented concentration maps and maps with estimated probability of threshold exceedance for the human health indicators. As the same method and data sources have been applied over the years 2005 to 2013, a change in uncertainty is in principle related to the data content itself.

However, for the 2008 data we implemented for the first time an increased resolution (from a 10x10 km into 1x1 km grid field) at the merging of the separate human health indicator interpolated maps (on 10x10 km grid) into one combined final 1x1 km gridded indicator map. The merging made use of the 1x1 km population density map. (The subsequent exposure estimates however, have been based on the 10x10 km grid fields aggregated from the 1x1 km grids of the merging result). The increased merging resolution should in principle improve the accuracy in the concentration maps, including the subsequent exposure estimates. Denby et al. (2009) discusses a diversity of uncertainty factors potentially involved, including their possible levels of influence. More background information on causes of uncertainties and their assessment can be found in Malherbe et al (2012). The paper recommends options to reduce uncertainties systematically. Horálek et al. (2010) explored specific options to reduce interpolation uncertainty related to the spatial resolutions applied at the different process steps of the mapping method. This paper concludes and justifies the implementation of the increased merging grid as the most significant uncertainty reduction measure, against the least additional computational demands. For further reading on the sub-grid variability and its influence to the exposure estimates, see Denby et al. (2011a).

Table 7.5 summarises the absolute and relative mean interpolation uncertainties, and additionally also R^2 from cross-validation scatterplot for the PM_{10} maps for the nine-year sequence. In the year 2013, both absolute and relative uncertainty results show the lowest levels compared to all previous years, for both PM_{10} indicators. The low uncertainty levels in the urban areas in 2013 are influenced by the lack of Turkish urban background stations in this year. The results from the Turkish urban background stations were reported since 2008 to 2012, but not in 2013.

Table 7.5 Absolute mean uncertainty (RMSE, $\mu g.m^{-3}$), relative mean uncertainty (RMSE relative to mean indicator value, in %) and R^2 from cross-validation scatterplot for the total European rural and urban areas for PM_{10} annual average and the 36th highest daily average for the years 2005 – 2013.

PM10			2005	2006	2007	2008	2009	2010	2011	2012	2013
Annual average											
rural areas	abs. mean uncertainty	RMSE [µg.m^{-3}]	5.5	5.8	4.6	5.0	4.6	4.5	4.1	3.8	3.4
	rel. mean uncertainty	RRMSE [%]	*25.9*	*26.6*	*23.5*	*27.2*	*23.9*	*22.7*	*21.1*	*21.4*	*19.6*
	coeff. of determination	R^2	*0.52*	*0.52*	*0.59*	*0.48*	*0.54*	*0.62*	*0.68*	*0.67*	*0.70*
urban areas	abs. mean uncertainty	RMSE [µg.m^{-3}]	5.5	6.1	5.0	6.3	6.7	6.6	6.1	6.1	4.3
	rel. mean uncertainty	RRMSE [%]	*20.0*	*20.9*	*18.4*	*22.4*	*23.0*	*22.5*	*20.7*	*22.1*	*17.3*
	coeff. of determination	R^2	*0.71*	*0.69*	*0.66*	*0.82*	*0.73*	*0.75*	*0.77*	*0.76*	*0.74*
36th max. daily average											
rural areas	abs. mean uncertainty	RMSE [µg.m^{-3}]	9.7	9.9	8.0	8.8	8.0	8.6	8.4	7.7	6.4
	rel. mean uncertainty	RRMSE [%]	*26.3*	*26.6*	*23.5*	*28.2*	*24.1*	*24.4*	*23.5*	*24.5*	*21.0*
	coeff. of determination	R^2	*0.55*	*0.56*	*0.60*	*0.52*	*0.56*	*0.64*	*0.66*	*0.64*	*0.69*
urban areas	abs. mean uncertainty	RMSE [µg.m^{-3}]	9.9	11.7	9.1	12.7	13.2	12.2	13.0	11.9	8.4
	rel. mean uncertainty	RRMSE [%]	*21.4*	*23.5*	*19.6*	*24.4*	*26.7*	*23.7*	*24.3*	*24.5*	*19.2*
	coeff. of determination	R^2	*0.75*	*0.65*	*0.65*	*0.79*	*0.72*	*0.77*	*0.75*	*0.75*	*0.75*

Table 7.6 presents the uncertainty results for $PM_{2.5}$ maps for the years 2007 – 2013 (excluding the 'non-mapped' year 2009). Both absolute and relative uncertainties show for 2013 better results than in 2012, quite similar results as in 2010 – 2011, and better results than in 2007 – 2008.

Table 7.6 Absolute and relative mean uncertainty and R^2 from cross-validation scatterplot for the total European rural and urban areas for $PM_{2.5}$ annual average, for the years 2007 – 2013.

PM2.5			2007	2008	2009	2010	2011	2012	2013
Annual average									
rural areas	abs. mean uncertainty	RMSE [µg.m^{-3}]	3.3	3.5	not mapped	3.4	2.8	3.0	2.7
	rel. mean uncertainty	RRMSE [%]	*27.4*	*29.8*		*25.0*	*16.8*	*24.9*	*22.1*
	coeff. of determination	R^2				*0.74*	*0.82*	*0.78*	*0.78*
urban areas	abs. mean uncertainty	RMSE [µg.m^{-3}]	4.1	3.6	not mapped	3.1	3.2	3.3	2.9
	rel. mean uncertainty	RRMSE [%]	*23.7*	*20.0*		*16.8*	*16.7*	*18.7*	*17.5*
	coeff. of determination	R^2				*0.81*	*0.80*	*0.78*	*0.78*

The mean interpolation uncertainty of the ozone maps presented in Table 7.7 decreased slightly for the health-related indicators in 2013, compared to previous year 2012. For the vegetation-related indicators, the interpolation uncertainties of the 2013 maps increased slightly, compared to 2012. For all the indicators, the uncertainty results of 2013 maps fit within the fluctuation of the previous five years.

Table 7.7 Absolute and relative mean uncertainty and R^2 from cross-validation scatterplot for the total European areas for ozone the 26th highest daily maximum 8-hour average, SOMO35, AOT40 for crops and for forests, for the years 2005 – 2013.

Ozone			2005	2006	2007	2008	2009	2010	2011	2012	2013
26th highest daily max. 8-hr average											
rural areas	abs. mean uncertainty	RMSE [µg.m^{-3}]	12.3	11.2	8.8	8.7	8.2	8.9	8.4	8.5	8.3
	rel. mean uncertainty	RRMSE [%]	*10.3*	*8.9*	*7.5*	*7.6*	*7.2*	*7.7*	*7.2*	*7.4*	*7.2*
	coeff. of determination	R^2	*0.51*	*0.49*	*0.71*	*0.56*	*0.69*	*0.68*	*0.67*	*0.71*	*0.67*
urban areas	abs. mean uncertainty	RMSE [µg.m^{-3}]	10.0	10.2	8.9	8.8	9.3	9.2	9.1	9.1	9.0
	rel. mean uncertainty	RRMSE [%]	*8.9*	*8.4*	*7.9*	*7.9*	*8.4*	*8.2*	*8.1*	*8.3*	*8.0*
	coeff. of determination	R^2	*0.50*	*0.53*	*0.66*	*0.61*	*0.64*	*0.71*	*0.66*	*0.70*	*0.68*
SOMO35											
rural areas	abs. mean uncertainty	RMSE [µg.m^{-3}.d]	2 173	2 077	1 801	1 609	1 635	1 608	1 747	1 633	1 596
	rel. mean uncertainty	RRMSE [%]	*35.5*	*31.6*	*33.3*	*30.7*	*29.7*	*29.6*	*29.6*	*29.2*	*29.2*
	coeff. of determination	R^2	*0.55*	*0.47*	*0.63*	*0.63*	*0.63*	*0.62*	*0.63*	*0.68*	*0.61*
urban areas	abs. mean uncertainty	RMSE [µg.m^{-3}.d]	1 459	1 472	1 260	1 293	1 475	1 278	1 374	1 362	1 194
	rel. mean uncertainty	RRMSE [%]	*32.0*	*29.2*	*29.5*	*31.3*	*33.1*	*29.6*	*29.7*	*31.7*	*28.1*
	coeff. of determination	R^2	*0.58*	*0.49*	*0.67*	*0.54*	*0.62*	*0.65*	*0.66*	*0.67*	*0.66*
AOT40 for crops											
rural areas	abs. mean uncertainty	RMSE [µg.m^{-3}.h]	7 677	7 674	5 876	5 283	5 138	5 198	5 263	5 062	5 179
	rel. mean uncertainty	RRMSE [%]	*40.7*	*29.6*	*39.6*	*31.3*	*37.7*	*30.8*	*34.9*	*32.9*	*34.6*
	coeff. of determination	R^2	*0.58*	*0.53*	*0.63*	*0.53*	*0.69*	*0.67*	*0.62*	*0.70*	*0.68*
AOT40 for forests											
rural areas	abs. mean uncertainty	RMSE [µg.m^{-3}.h]	12 474	11 990	10 190	8 750	9 304	8 384	9 341	8 847	9 257
	rel. mean uncertainty	RRMSE [%]	*41.5*	*33.6*	*37.1*	*34.0*	*33.9*	*31.4*	*32.7*	*32.8*	*34.7*
	coeff. of determination	R^2	*0.55*	*0.49*	*0.67*	*0.56*	*0.68*	*0.69*	*0.67*	*0.70*	*0.68*

The scatter plots of the interpolation results versus the measurements show that for both the PM_{10} and the ozone indicators, in areas with high values, an underestimation of the predicted values occurs. This also leads to a considerable underestimation at locations without measurements and at areas with the higher concentrations. This effect occurs most prominently for the ozone indicators. We expect that the underestimation would reduce when an improved fit of the linear regression with (other) supplementary data could be obtained. For example, in the near future more contributions from satellite imagery data and interpretation techniques could be expected. An option is to extend the number of measurement stations and/or using additional mobile stations. Another possibility is the use of more advanced chemical transport model. For further reading on this subject, we refer to Denby et al. (2009), Gräler et al. (2013), Schneider et al. (2012) and Horálek et al (2014b).

Probability of exceedance

Maps with the probability of exceedance of Limit Values and Target Value have been prepared for the human health indicators of PM_{10}, $PM_{2.5}$, and ozone.

These probability maps, with a class distribution as defined in Table 4.5, are derived from combining the indicator map and its uncertainty map following the same method throughout the years 2005 to 2013. The differences in the maps between years depend on annual fluctuations in concentration levels, supplementary data and their involved uncertainties (Denby et al. 2009, Gräler et al. 2012, 2013). Some disruption or 'jump' could be expected between the data of 2005 – 2007 and 2008 – 2012. This would be caused by the increased merging resolution applied for the first time on the 2008 data. As Horálek et al. (2010) indicated, it should improve the population exposure estimates, specifically for population living in urban areas (that profit most of this methodological refinement). Nevertheless, as the maps are spatially merged into 10x10 km grid resolution, the influence of the urban pollution into the final map is smaller than was in the methodology used until 2007. Thus, it is needed to bear in mind that the spatial average of a 10x10 km grid cell can show low probability of exceedance even though some smaller (e.g. urban) areas inside such a grid cell would show high probability of exceedance (in case of using a finer grid cell resolution).

In 2013 for the annual average PM_{10}, the patterns in the spatial distribution of the different probability of exceedance (PoE) classes over Europe were somewhat reduced to those of 2012. The Po Valley in Italy shows a considerable reduced probability of exceedance compared to 2012. The region of southern Poland – north-eastern Czech Republic shows in 2013 smaller area with the highest PoE compared to 2012. In south-eastern Europe, only somewhat elevated PoE do show up at a few cities. In comparison with 2012, their number has reduced considerably. In other parts of Europe there exists just little likelihood of exceedance.

The 36th highest daily means of PM_{10} do show a decrease in the spatial extents and PoE levels throughout south-eastern Europe, in comparison with 2012. The Po Valley in northern Italy has slightly reduced PoE pattern compared to 2012. Throughout the years 2009 – 2013, areas with continued increased PoE levels do occur in southern Poland and north-eastern Czech Republic. Northern Serbia, southern Romania, and the centre of Bulgaria show throughout the years 2010 – 2013 areas with continued high PoE levels, however the extent of these areas was reduced. The increased levels of PoE area around Almería, southern Spain, has slightly reduced in 2013 compared to the year 2012.

PoE map for $PM_{2.5}$ shows the highest probability of TV exceedance in the Po Valley in northern Italy, the region of southern Poland – north-eastern Czech Republic, the cities in the central part of Poland, and big cities in south-eastern Europe. In comparison with 2012, the reduction of the areas with elevated levels of PoE took place in all these areas.

In the case of ozone, one can conclude that in the central Italy and south-eastern Europe, the PoE decreased considerably in its level in 2013 compared to 2012. In some areas north of the Alps the levels of PoE increased somewhat, as well as in the Iberian Peninsula. This is in agreement with the inter-annual general increase of the ozone concentrations in the northwest of Europe and their general decrease in the southeast of Europe. The inter-annual change of the ozone concentrations in the years 2012 and 2013 in these regions show in general the opposite effect than in the years 2011 and 2012.

References

Cressie N (1993). Statistics for spatial data. Wiley series, New York.

Danielson JJ, Gesch DB (2011). Global multi-resolution terrain elevation data 2010 (GMTED2010): U.S. Geological Survey Open-File Report 2011–1073. https://lta.cr.usgs.gov/GMTED2010

Denby B, Schaap M, Segers A, Builtjes P, Horálek J (2008). Comparison of two data assimilation methods for assessing PM_{10} exceedances on the European scale. Atmospheric Environment 42, 7122–7134.

Denby B, De Leeuw F, De Smet P, Horálek J (2009). Sources of uncertainty and their assessment in spatial mapping. ETC/ACC Technical Paper 2008/20. http://acm.eionet.europa.eu/reports/ETCACC_TP_2008_20_spatialAQ_uncertainties

Denby B, Cassiani M, de Smet P, de Leeuw F, Horálek J (2011a). Sub-grid variability and its impact on European wide air quality exposure assessment. Atmospheric Environment 45, 4220-4229.

Denby B, Gola G, De Leeuw F, De Smet P, Horálek J (2011b). Calculation of pseudo $PM_{2.5}$ annual mean concentrations in Europe based on annual mean PM10 concentrations and other supplementary data. ETC/ACC Technical Paper 2010/9. http://acm.eionet.europa.eu/reports/ETCACC_TP_2010_9_pseudo_PM2.5_stations

Denby B, Horálek J, de Smet P, de Leeuw F (2011c). Mapping annual mean $PM_{2.5}$ concentrations in Europe: application of pseudo $PM_{2.5}$ station data. ETC/ACM Technical Paper 2011/5. http://acm.eionet.europa.eu/reports/ETCACM_TP_2011_5_spatialPM2.5mapping

De Leeuw F (2012). AirBase: a valuable tool in air quality assessments at a European and local level. ETC/ACM Technical Paper 2012/4. http://acm.eionet.europa.eu/reports/ETCACM_TP_2012_4_AirBase_AQassessment

De Smet P, Horálek J, Coňková M, Kurfürst P, de Leeuw F, Denby B (2009). European air quality maps of ozone and PM_{10} for 2006 and their uncertainty analysis. ETC/ACC Technical Paper 2008/8. http://acm.eionet.europa.eu/reports/ETCACC_TP_2008_8_spatAQmaps_2006

De Smet P, Horálek J, Coňková M, Kurfürst P, de Leeuw F, Denby B (2010). European air quality maps of ozone and PM_{10} for 2007 and their uncertainty analysis. ETC/ACC Technical Paper 2009/9. http://acm.eionet.europa.eu/reports/ETCACC_TP_2009_9_spatAQmaps_2007

De Smet P, Horálek J, Coňková M, Kurfürst P, de Leeuw F, Denby B (2011). European air quality maps of ozone and PM_{10} for 2008 and their uncertainty analysis. ETC/ACC Technical Paper 2010/10. http://acm.eionet.europa.eu/reports/ETCACC_TP_2010_10_spatAQmaps_2008

De Smet P, Horálek J, Schreiberová M, Kurfürst P, de Leeuw F (2012). European air quality maps of ozone and PM_{10} for 2009 and their uncertainty analysis. ETC/ACM Technical Paper 2011/11. http://acm.eionet.europa.eu/reports/ETCACM_TP_2011_11_spatAQmaps_2009

EC (2008). Directive 2008/50/EC of the European Parliament and of the Council of 21 May 2008 on ambient air quality and cleaner air for Europe. OJ L 152, 11.06.2008, 1-44. http://eur-lex.europa.eu/LexUriServ/LexUriServ.do?uri=OJ:L:2008:152:0001:0044:EN:PDF

ECMWF: Meteorological Archival and Retrieval System (MARS). http://www.ecmwf.int/

EEA (2008). ORNL Landscan 2008 Global Population Data conversion into EEA ETRS89-LAEA5210 1km grid (eea_r_3035_1_km_landscan-eurmed_2008, by Hermann Peifer of EEA).

EEA (2011). Guide for EEA map layout. EEA operational guidelines. August 2011, version 4. http://www.eionet.europa.eu/gis/docs/GISguide_v4_EEA_Layout_for_map_production.pdf

EEA (2013a). Corine land cover 2000 (CLC2000) raster data. 100x100m gridded version 17 (12/2013). http://www.eea.europa.eu/data-and-maps/data/corine-land-cover-2000-raster-3

EEA (2013b). Corine land cover 2006 (CLC2006) raster data. 100x100m gridded version 17 (12/2013) http://www.eea.europa.eu/data-and-maps/data/corine-land-cover-2006-raster-3

EEA (2015a). Air Quality e-Reporting. Air quality database. http://www.eea.europa.eu/data-and-maps/data/aqereporting

EEA (2015b). Air quality in Europe – 2015 report. EEA Report 5/2015. http://acm.eionet.europa.eu/reports/EEA_Rep_5_2015_AQinEurope

Eurostat (2014). GEOSTAT 2011 grid dataset. Population distribution dataset. http://ec.europa.eu/eurostat/web/gisco/geodata/reference-data/population-distribution-demography

Eurostat (2015). Total population for European states for 2013. http://epp.eurostat.ec.europa.eu/tgm/table.do?tab=table&language=en&pcode=tps00001&tableSelection=1&footnotes=yes&labeling=labels&plugin=1

EMEP (2014). Transboundary particular matter, photo-oxidants, acidifying and eutrophying components. EMEP Report 1/2014. http://emep.int/publ/reports/2014/EMEP_Status_Report_1_2014.pdf

EMEP (2015). Transboundary particular matter, photo-oxidants, acidifying and eutrophying components. Status Report 1/2015, August 2015, 228 pp. http://emep.int/publ/reports/2015/EMEP_Status_Report_1_2015.pdf

Gräler B, Gerharz L, Pebesma E (2012). Spatio-temporal analysis and interpolation of PM_{10} measurements in Europe. ETC/ACM Technical Paper 2011/10. http://acm.eionet.europa.eu/reports/ETCACM_TP_2011_10_spatio-temp_AQinterpolation

Gräler B, Rehr M, Gerharz L, Pebesma E (2013). Spatio-temporal analysis and interpolation of PM10 measurements in Europe for 2009. ETC/ACM Technical Paper 2012/8. http://acm.eionet.europa.eu/reports/ETCACM_2012_8_spatio-temp_PM10analyses

Horálek J, Kurfürst P, Denby B, de Smet P, de Leeuw F, Brabec M, Fiala J (2005). Interpolation and assimilation methods for European scale air quality assessment and mapping. Part II: Development and testing new methodologies. ETC/ACC Technical paper 2005/8. http://acm.eionet.europa.eu/docs/ETCACC_TechnPaper_2005_8_SpatAQ_Part_II.pdf

Horálek J, Denby B, de Smet P, de Leeuw F, Kurfürst P, Swart R, van Noije T (2007). Spatial mapping of air quality for European scale assessment. ETC/ACC Technical paper 2006/6. http://acm.eionet.europa.eu/reports/ETCACC_TechnPaper_2006_6_Spat_AQ

Horálek J, de Smet P, de Leeuw F, Denby B, Kurfürst P, Swart R (2008). European air quality maps for 2005 including uncertainty analysis. ETC/ACC Technical paper 2007/7. http://acm.eionet.europa.eu/reports/ETCACC_TP_2007_7_spatAQmaps_ann_interpol

Horálek J, de Smet P, de Leeuw F, Coňková M, Denby B, Kurfürst P (2010). Methodological improvements on interpolating European air quality maps. ETC/ACC Technical Paper 2009/16. http://acm.eionet.europa.eu/reports/ETCACC_TP_2009_16_Improv_SpatAQmapping

Horálek J, de Smet P, Corbet L, Kurfürst P, de Leeuw F (2013). European air quality maps of PM and ozone for 2010 and their uncertainty. ETC/ACM Technical Paper 2012/12. http://acm.eionet.europa.eu/reports/ETCACM_TP_2012_12_spatAQmaps_2010

Horálek J, de Smet P, Kurfürst P, de Leeuw F, Benešová N (2014a). European air quality maps of PM and ozone for 2011 and their uncertainty. ETC/ACM Technical Paper 2013/13. http://acm.eionet.europa.eu/reports/ETCACM_TP_2013_13_spatAQmaps_2011

Horálek J, Tarrasón L, de Smet P, Malherbe L, Schneider P, Ung A, Corbet L, Denby B (2014b). Evaluation of Copernicus MACC-II ensemble products in the ETC/ACM spatial air quality mapping. ETC/ACM Technical Paper 2013/9. http://acm.eionet.europa.eu/reports/ETCACM_TP_2013_9_AQmaps_with_MACCproducts

Horálek J, de Smet P, Kurfürst P, de Leeuw F, Benešová N (2015). European air quality maps of PM and ozone for 2012 and their uncertainty. ETC/ACM Technical Paper 2014/4. http://acm.eionet.europa.eu/reports/ETCACM_TP_2014_4_spatAQmaps_2012

Horálek J, Benešová N, de Smet P (2016). Application of FAIRMODE Delta tool to evaluate interpolated European air quality maps for 2012. ETC/ACM Technical Paper 2015/2. http://acm.eionet.europa.eu/reports/ETCACM_TP_2015_2_Delta_Evaluation_AQMaps2012

JRC (2009). Population density disaggregated with Corine land cover 2000. 100x100 m grid resolution, EEA version popu01clcv5.tif of 24 Sep 2009. http://www.eea.europa.eu/data-and-maps/data/population-density-disaggregated-with-corine-land-cover-2000-2

Malherbe L, Ung A, Colette A, Debry E (2012). Formulation and quantification of uncertainties in air quality mapping. ETC/ACM Technical Paper 2001/9. http://air-climate.eionet.europa.eu/reports/ETCACM_TP_2011_9_AQmapping_uncertainties

Mareckova K, Wankmüller R, Moosman L, Pinterits M, Tista M (2014). Inventory Review 2014. Review of emission data reported under the LRTAP Convention and NEC Directive. Stage 1 and 2 review & Status of gridded and LPS data. EEA/CEIP Technical Report 1/2014. http://www.ceip.at/fileadmin/inhalte/emep/pdf/2014/DP-143_InventoryReport_2014_forWeb.pdf

Mareckova K, Wankmüller R, Pinterits M, Ullrich B (2015). Inventory Review 2015. Review of emission data reported under the LRTAP Convention and NEC Directive. Stage 1 and 2 review & Status of gridded and LPS data. EEA/CEIP Technical Report 1/2015. www.ceip.at/fileadmin/inhalte/emep/pdf/2015/DP0146_InventoryReport_2015_forWeb.pdf

NILU (2015). EBAS, database of atmospheric chemical composition and physical properties (NILU, Norway). http://ebas.nilu.no/

ORNL (2008). ORNL LandScan high resolution global population data set. http://www.ornl.gov/sci/landscan/landscan_documentation.shtml

Schneider P, Tarrasón L, Guerreiro C, (2012), The potential of GMES satellite data for mapping nitrogen dioxide at the European scale, ETC/ACM Technical Paper 2012/9. acm.eionet.europa.eu/reports/ETCACM_TP_2012_9_GMESsatdata_NOx_Euromap

Simpson D, Benedictow A, Berge H, Bergström R, Emberson LD, Fagerli H, Hayman GD, Gauss M, Jonson JE, Jenkin ME, Nyíri A, Richter C, Semeena VS, Tsyro S, Tuovinen J-P, Valdebenito A, Wind P (2012). The EMEP MSC-W chemical transport model – technical description. Atmospheric Chemistry and Physics, 12, 7825–7865, doi:10.5194/acp-12-7825-2012.

Simpson D, Schulz M, Semeena VS, Tsyro S, Valdebenito Á, Wind P, Steensen BM (2013). EMEP model development and performance changes. Simpson D, Tsyro S, Wind P, Steensen BM (2013). EMEP model development. In: Transboundary acidification, eutrophication and ground level ozone in Europe in 2011, EMEP Report 1/2013. http://emep.int/publ/reports/2013/EMEP_status_report_1_2013.pdf

UNECE (2004). Manual on methodologies and criteria for modelling and mapping critical loads and levels and air pollution effects, risks and trends. UNECE Convention on Long-range Transboundary Air Pollution. http://www.icpmapping.org/Mapping_Manual

UN (2015). World Population Prospects, the 2015 Revision. United Nations. Department of Economic and Social Affairs, Population Division. http://esa.un.org/unpd/wpp/Download/Standard/Population/

WHO (2005). WHO Air quality guidelines for particulate matters, ozone, nitrogen dioxide and sulphur dioxide. Global update 2005. http://www.who.int/phe/health_topics/outdoorair/outdoorair_aqg/en/index.html

Annex 1 Urban background maps

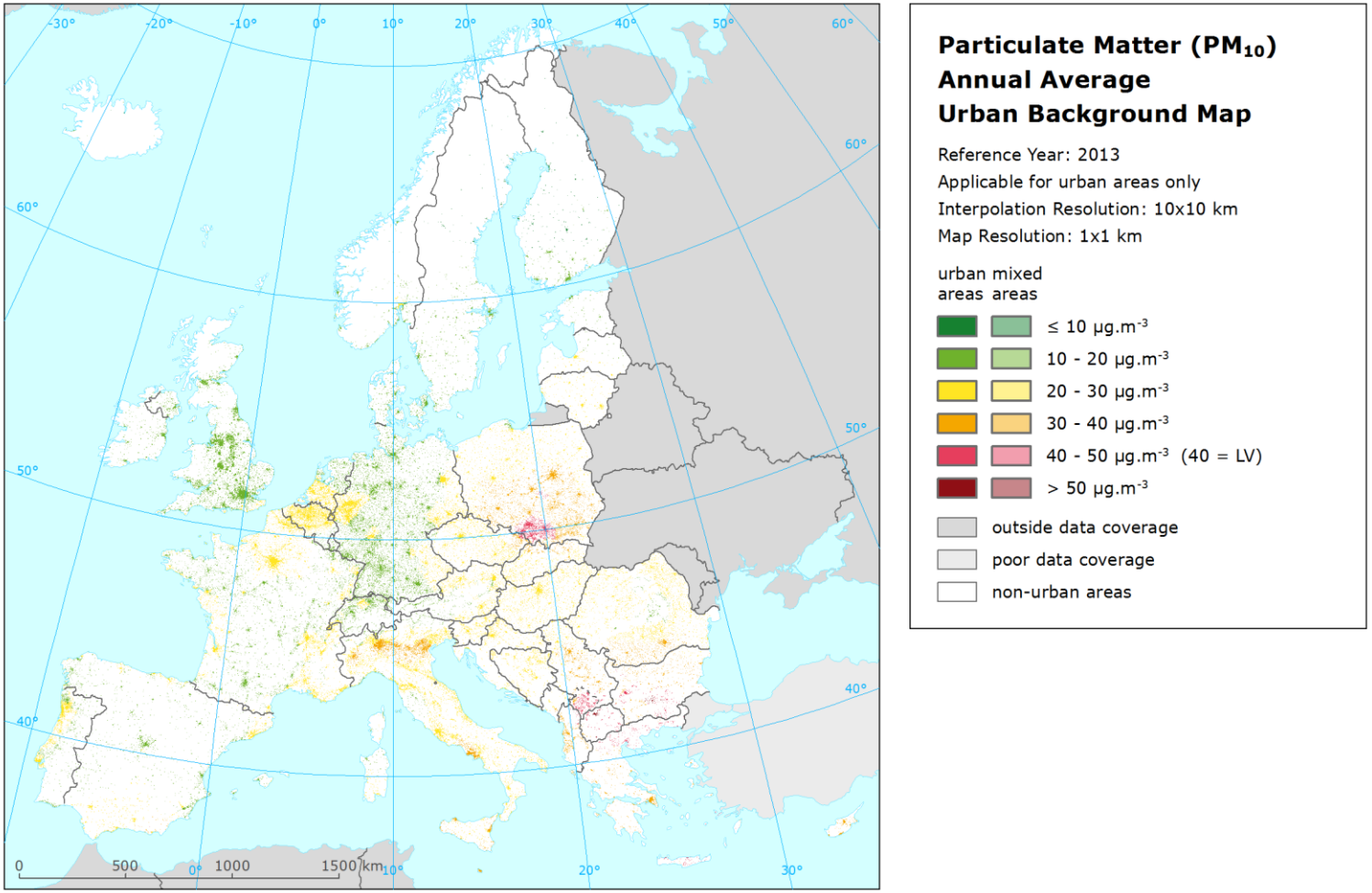

Figure A1.1 Urban background concentration map of PM_{10} – annual average, year 2013. Spatial interpolated concentration field (10x10 km grid resolution) in urban areas (1x1 km grid resolution). Units: µg.m^{-3}. Applicable for urban areas only.

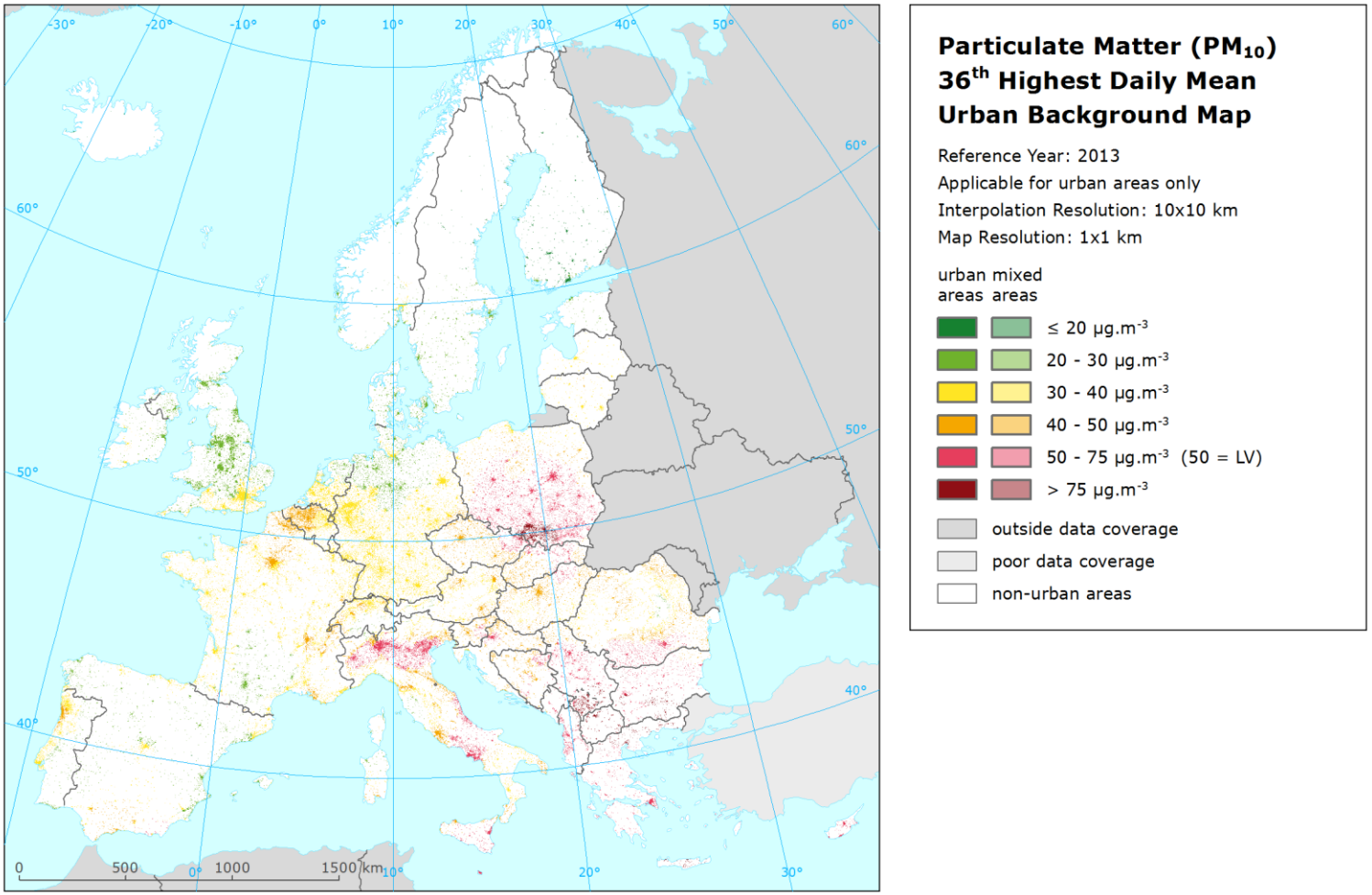

Figure A1.2 Urban background concentration map of PM_{10} – 36th highest daily average value, year 2013. Spatial interpolated concentration field (10x10 km grid resolution) in urban areas (1x1 km grid resolution). Units: µg.m^{-3}. Applicable for urban areas only.

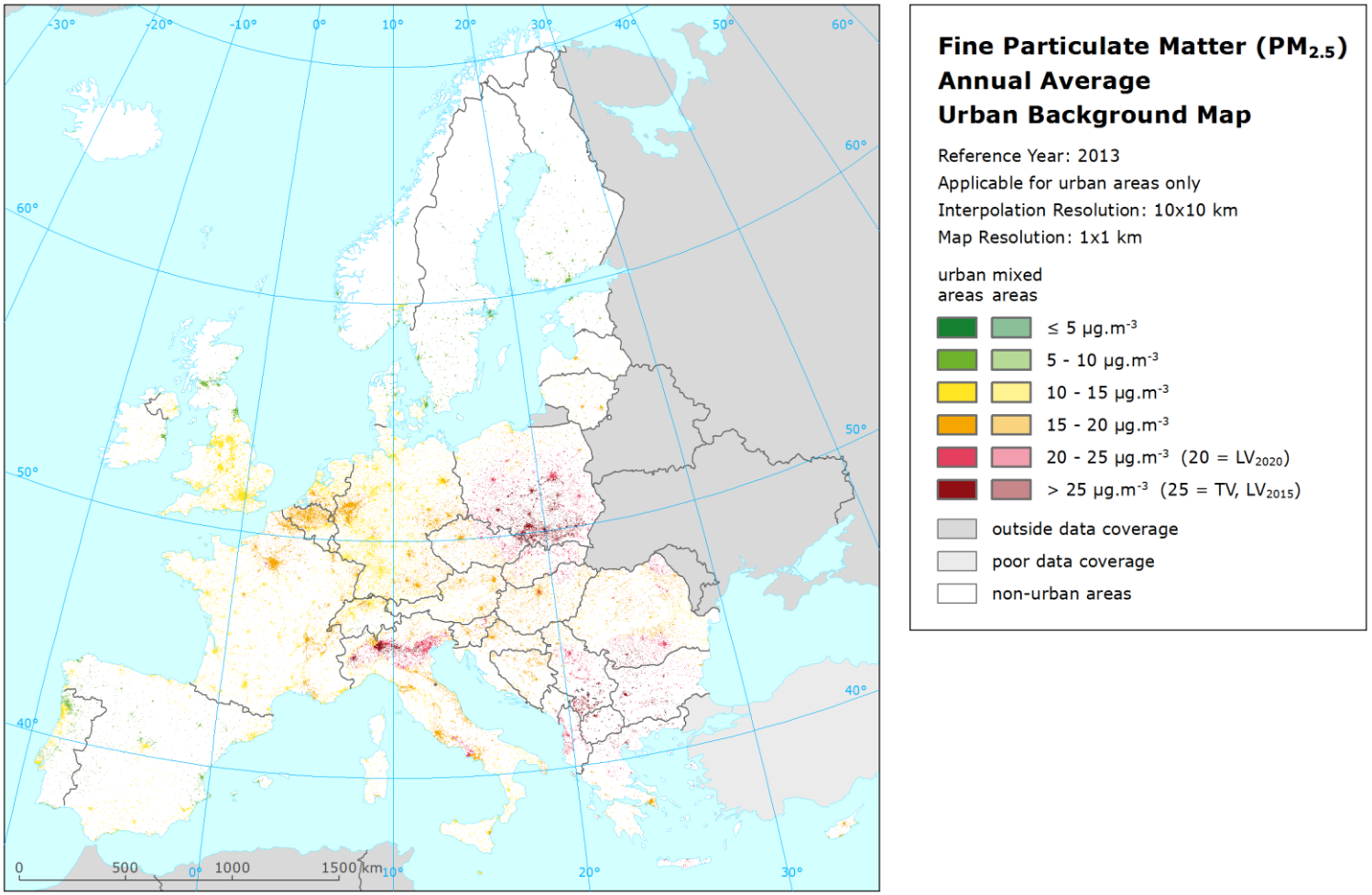

Figure A1.3 Urban background concentration map of $PM_{2.5}$ – annual average, year 2013. Spatial interpolated concentration field (10x10 km grid resolution) in urban areas (1x1 km grid resolution). Units: µg.m^{-3}. Applicable for urban areas only.

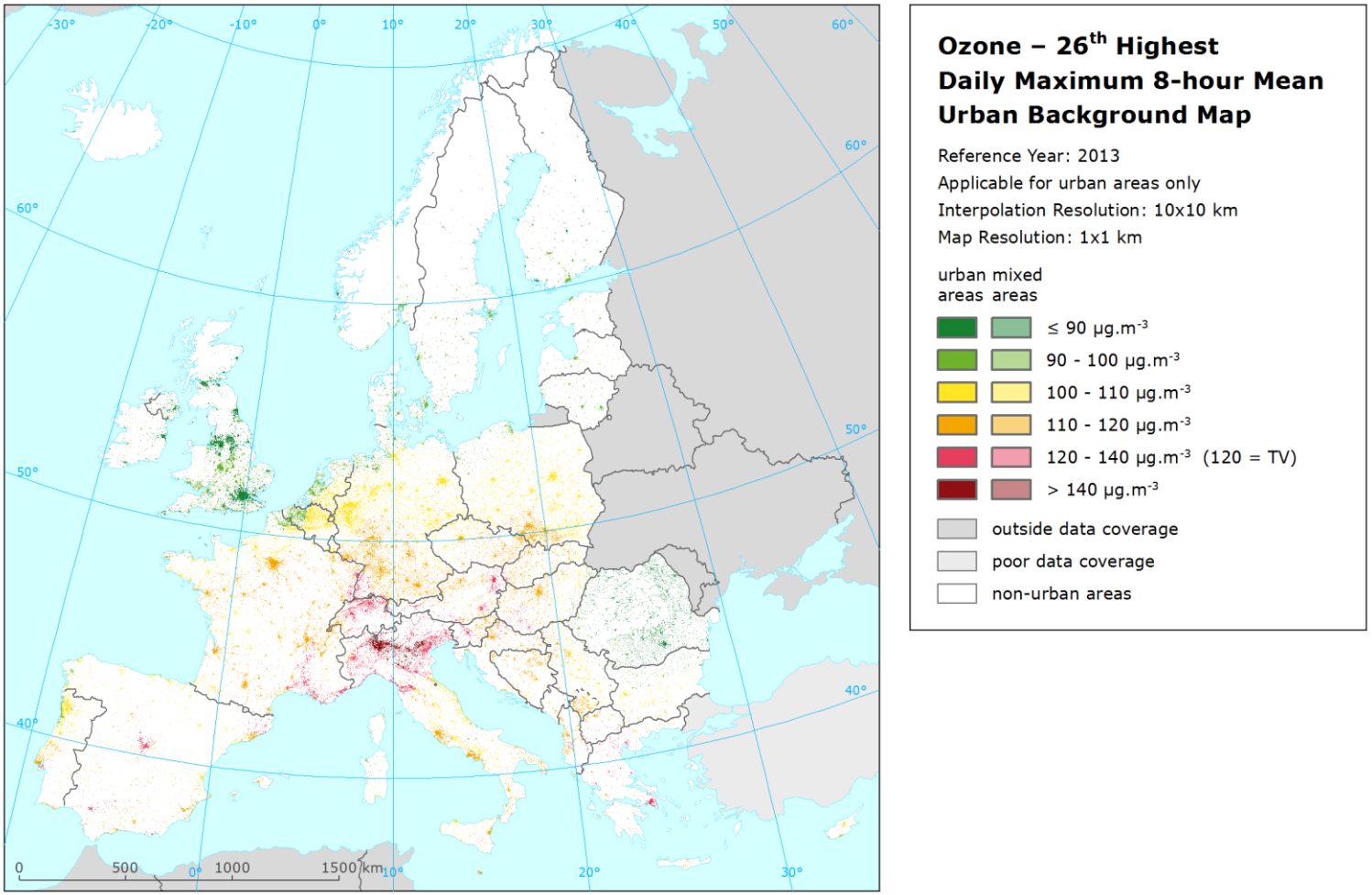

Figure A1.4 Urban background concentration map of ozone health indicator 26th highest daily maximum 8-hour value, year 2013. Spatial interpolated concentration field (10x10 km grid resolution) in urban areas (1x1 km grid resolution). Units: µg.m-3. Applicable for urban areas only.

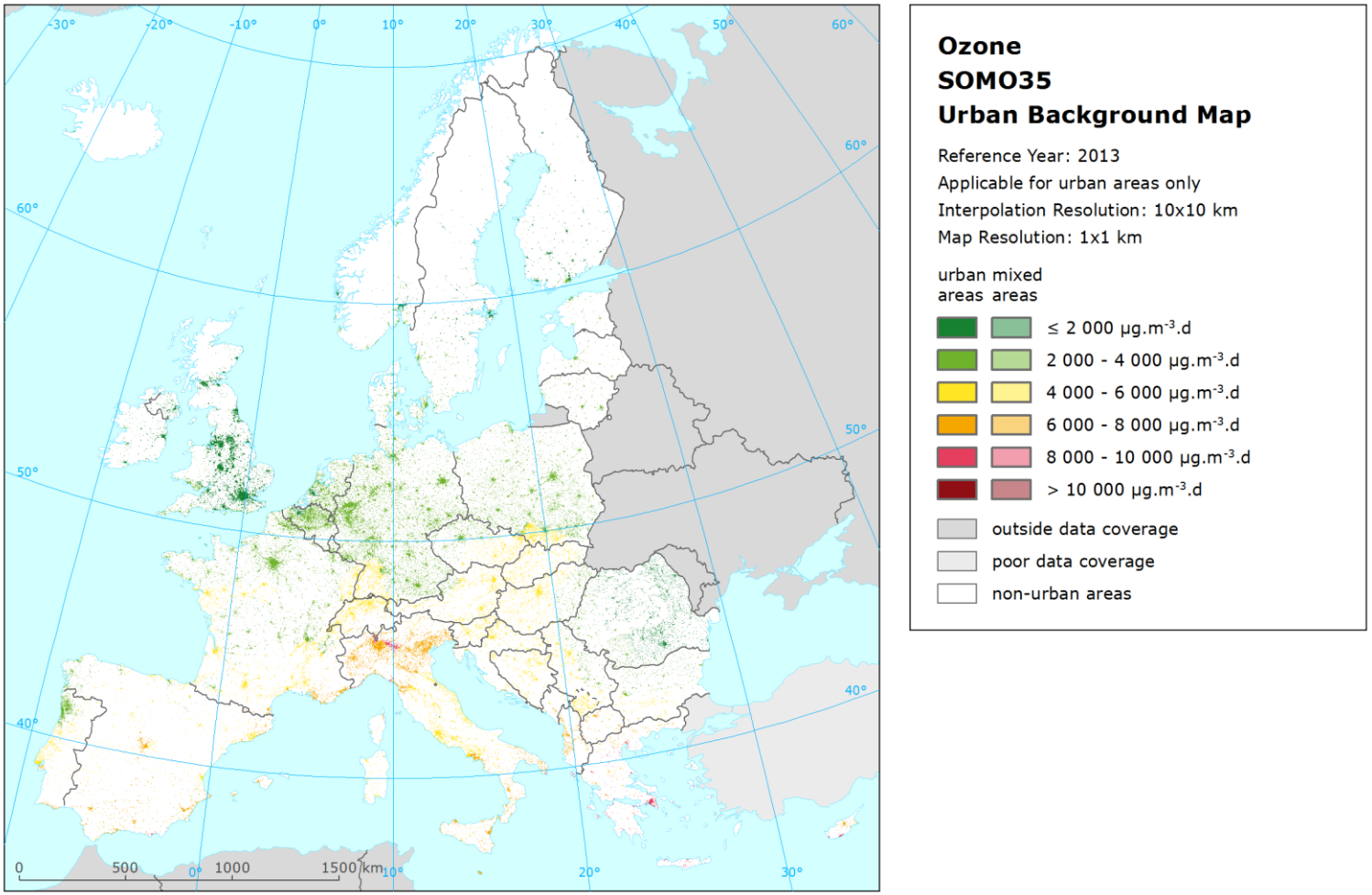

Figure A1.5 Urban background concentration map of ozone health indicator SOMO35, year 2013. Spatial interpolated concentration field (10x10 km grid resolution) in urban areas (1x1 km grid resolution). Units: µg.m^{-3}.days. Applicable for urban areas only.

Annex 2 Percentile maps

In the dealing with the annual indicator data, the missing daily data should be taken into account. As stated in Section 3.1, the stations with annual data coverage of at least 75 percent are used in the mapping. The data coverage of less than 100 percent will result in an additional uncertainty. How large this uncertainty is, depend on the kind of indicator.

For different indicators, different ways how to treat with the missing data are used. In the case of the annual average, no correction can be applied. In the cases of and SOMO35 and AOT40 indicators, the correction for the missing data is routinely applied, see Section 3.1. For the x-th highest values (i.e. for the PM_{10} indicator 36th highest daily mean and for the ozone indicator 26th highest daily maximum 8-hour mean), no correction is applied so far. Nevertheless, this leads in general into the underestimation of the indicators. The simplest way how to correct the indicator values is to use the percentiles instead of the x-th highest values, i.e. 90.4th percentile of the daily values in the case of PM_{10} and 93.2nd percentile of the daily maximum 8-hour means in the case of ozone.

Using a Monte Carlo approach it has been shown that by randomly creating missing values in a complete time series (data coverage is 100%) the additional uncertainty related to the incomplete time series is substantially smaller when using percentile values than if using the x-th highest value (de Leeuw, 2012).

In a formal sense, one should distinguish between a normal and a leap year, which should lead into 90.41st against 90.44th percentile for PM_{10} and 93.15th against 93.17th percentile for ozone. However when the AQ Directive (EU, 2008) mentions the 90.4th percentile, it makes no distinction between a normal and a leap year and it gives the percentile with one decimal. According to this rounding rule there is no difference between the two cases.

Throughout the years, the maps and tables of PM_{10} indicator 36th highest daily value and ozone indicator 26th highest daily maximum 8-hour average has been constructed, without any correction for the missing values. In this Annex, the maps and tables for percentile values are presented.

For future, it is possible to routinely construct just the maps of percentiles, instead of the x-th highest values. The advantage of such maps is the more realistic concentration level. The disadvantage is that the time series like in Tables 4.8 and 6.3 could not be constructed. (Unless the percentile maps and tables for recent years are constructed.)

A2.1 PM_{10} – 90.4th percentile of daily means

Figure A2.1 presents the combined final map for the PM_{10} indicator 90.4th percentile of daily means. Table A2.1 presents the estimated parameters of the linear regression models and of the residual kriging.

Table A2.1 Parameters of the linear regression models (Eq. 2.2) and of the ordinary kriging (OK) variograms (nugget, sill, range) – and their statistics – of PM_{10} indicator 90.4th percentile of daily means for 2013 in rural (left) and urban (right) areas as used for the combined final map.

linear regr. model + OK of its residuals	rural areas parameter values	urban areas parameter values
c (constant)	2.25	2.08
a1 (log. EMEP model 2013)	0.565	0.55
a2 (altitude GTOPO)	-0.00048	
a3 (wind speed 2013)	-0.106	
a4 (s. solar radiation 2013)	*non signif.*	
adjusted R^2	**0.50**	**0.23**
standard error [µg.m^{-3}]	**0.27**	**0.31**
nugget	0.033	0.013
sill	0.061	0.071
range [km]	460	520
RMSE [µg.m^{-3}]	**6.47**	**8.63**
Relative RMSE [%]	**21.0**	**19.5**
bias (MPE) [µg.m^{-3}]	**0.01**	**-0.07**

The parameters including the statistical indicators of both the regression and the kriging are quite similar like presented in Table 4.6.

If compared the final map of Figure A2.1 with Figure 4.6 (showing the map for the 36th highest daily mean), one can see slightly higher concentration level for the percentile values. The difference of the two maps would show the level of improvement if the percentiles values are used.

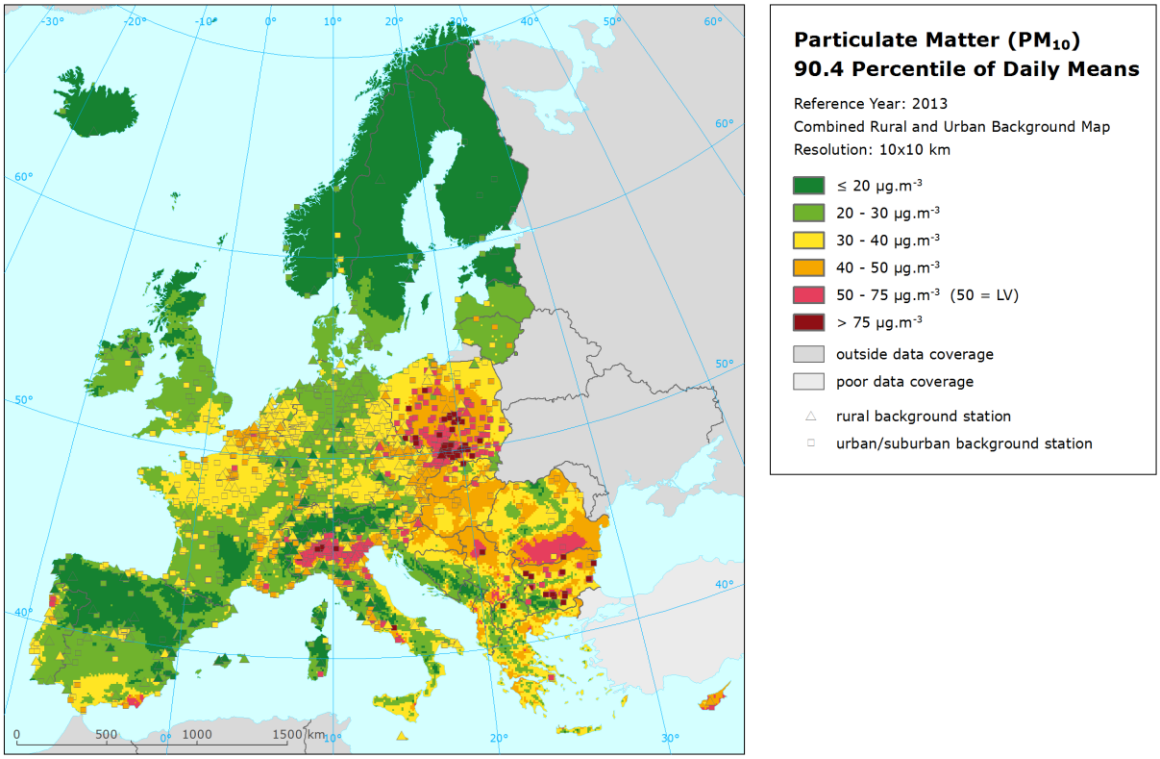

Figure A2.1 Combined rural and urban concentration map of PM_{10} – 90.4th percentile of daily average values in the year 2013. Spatial interpolated concentration field (10x10 km grid resolution, excluding Turkey due to lack of air quality data) and the measured values in the measuring points. Units: µg.m^{-3}.

Table A2.2 gives, for the PM_{10} indicator 90.4th percentile of daily means, the population frequency distribution for a limited number of exposure classes, as well as the population-weighted concentration for individual countries and for Europe as a whole. This table improves the exposure table constructed for the indicator 36th highest daily mean (see Table 4.7).

It has been estimated that in 2013 about 17 % of the European population lived in areas where the 90.4th percentile of PM_{10} daily means exceeded the limit value of 50 µg.m^{-3}. The European-wide population-weighted concentration of the 90.4th percentile of daily means is estimated for the year 2013 at 39.4 µg.m^{-3}. Compared to the results presented in Table 6.2 (16 % and 38.6 µg.m^{-3}), one can see slightly higher results for the percentile values. The difference between the results presented in Tables A2.2 and 4.7 shows the level of improvement if the 90.4th percentile values are used instead of the 36th highest daily means.

Table A2.2 Population exposure and population-weighted concentration – PM_{10}, 90.4th percentile of daily average values for the year 2013. Resolution: 1x1 km.

Country		Population	PM_{10}, 90.4th percentile od daily means, exposed population [%]						Pop. weighted conc.
			< LV				> LV		
			< 20	20 - 30	30 - 40	40 - 50	50 - 75	> 75	
		[inhbs . 1000]	µg.m^{-3}	µg.m^{-3}	µg.m^{-3}	µg.m^{-3}	µg.m^{-3}	µg.m^{-3}	[µg.m^{-3}]
Albania	AL	2 899	0.0	3.0	9.0	9.8	71.9	6.3	61.4
Andorra	AD	76	0.4	0.8	1.0	97.7			47.6
Austria	AT	8 452	1.8	9.5	50.9	37.8			37.0
Belgium	BE	11 162		1.6	26.6	71.8			41.2
Bosnia & Herzegovina	BA	3 836	0.9	7.8	17.8	51.1	22.3		44.2
Bulgaria	BG	7 285	0.1	1.6	4.4	10.2	58.2	25.6	67.9
Croatia	HR	4 262	0.1	5.5	15.0	55.5	23.8		44.6
Cyprus	CY	866			0.8	21.0	78.2		56.9
Czech Republic	CZ	10 516		1.1	14.4	65.4	15.9	3.3	46.9
Denmark	DK	5 603	0.4	96.6	2.8	0.2			26.7
Estonia	EE	1 320	23.0	77.0					22.6
Finland	FI	5 427	70.8	29.2					18.0
France (metropolitan)	FR	63 652	0.9	14.8	49.0	35.3	0.1	0.0	36.9
Germany	DE	80 524	0.0	22.2	77.1	0.7			32.9
Greece	GR	11 004	0.0	1.0	6.3	6.7	63.2	22.9	61.2
Hungary	HU	9 909			13.5	78.9	7.6		44.6
Iceland	IS	322	23.7	75.2	1.1				20.1
Ireland	IE	4 591	1.9	78.8	19.3	0.0			26.3
Italy	IT	59 685	0.5	5.7	18.0	27.8	48.0	0.1	49.7
Latvia	LV	2 024	0.8	27.9	71.1	0.2			33.0
Liechtenstein	LI	37	1.4	8.5	90.0				32.4
Lithuania	LT	2 972		22.1	73.5	4.4			34.1
Luxembourg	LU	537		17.9	82.1				31.5
Macedonia, FYROM of	MK	2 062	0.0	0.9	2.0	1.5	4.4	91.2	93.1
Malta	MT	421			1.3	1	97.6		62.2
Monaco	MC	38			100.0				39.0
Montenegro	ME	621	3.3	10.0	7.4	5.6	73.4	0.3	53.6
Netherlands	NL	16 780		9.2	89.1	2			34.2
Norway	NO	5 051	34.2	38.3	27.5	0.0			23.7
Poland	PL	38 063	0.0	0.3	17.8	23.1	45.1	13.8	55.4
Portugal (excl. Az., Mad.)	PT	9 977	2.5	23.7	54.4	17.7	1.8		34.5
Romania	RO	20 020	0.0	1.7	27.2	42.1	28.8	0.2	45.4
San Marino	SM	34		3.7	15.8	80			40.2
Serbia (incl. Kosovo*)	RS	8 997	0.0	1.5	5.7	18.1	56.2	18.4	61.3
Slovakia	SK	5 411	0.0	0.3	5.4	65.3	29.0	0.0	47.5
Slovenia	SI	2 059	0.0	4.7	26.9	62.3	6.2		42.2
Spain (excl. Canarias)	ES	44 623	2.7	40.6	44.2	11.4	1.1	0.0	30.7
Sweden	SE	9 556	21.5	78.4	0.1				22.5
Switzerland	CH	8 039	1.9	10.1	62.1	25.9			36.5
United Kingdom (& dep.)	UK	63 905	0.5	56.9	42.5	0.1			29.0
Total		**532 614**	**2.1**	**21.6**	**39.3**	**19.7**	**14.7**	**2.6**	**39.4**
			82.7				**17.3**		
EU-28		**500 603**	**1.8**	**22.3**	**40.1**	**19.8**	**14.0**	**2.0**	**38.8**
			84.0				**16.0**		
Kosovo*	KS	1 816	0.0	0.9	7.1	5.6	16.6	69.8	80.9
Serbia (excl. Kosovo*)	RS	7 182	0.0	1.6	5.4	21.2	65.9	5.9	56.6

*) under the UN Security Council Resolution 1244/99

Note1: Turkey is not included in the calculation due to lacking air quality data in rural areas.
Note2: The percentage value "0.0" indicates an exposed population exists, but is small and estimated less than 0.05 %. Empty cells mean: no population in exposure.

A2.2 Ozone – 93.2nd percentile of daily maximum 8-hour means

Figure A2.2 presents the combined final map for the ozone indicator 93.2nd percentile of daily maximum 8-hour means as a result of combining the separate rural and urban interpolated map. Table A2.3 presents the estimated parameters of the linear regression models and of the residual kriging, including the statistical indicators of both the regression and the kriging. The parameters used are quite similar like presented in Table 6.1. If compared the final map of Figure A2.2 with Figure 6.1 (showing the 26th highest daily maximum 8-hour value), one can see slightly higher concentration level for the percentile values. The difference of the two maps would show the level of improvement if the percentiles are used.

Table A2.3 Parameters of the linear regression models (Eq. 2.2) and of the ordinary kriging (OK) variograms (nugget, sill, range) – and their statistics – of ozone indicator 93.2nd percentile of daily maximum 8-hour means for 2013 in the rural (left) and urban (right) areas as used for the combined final map.

linear regr. model + OK on its residuals	rural areas parameter values	urban areas parameter values
c (constant)	1.3	34.1
a1 (EMEP model 2013)	0.98	0.77
a2 (altitude GTOPO)	0.0036	
a3 (wind speed 2013)		-2.67
a4 (s. solar radiation 2013)	0.53	0.11
adjusted R^2	**0.58**	**0.49**
standard error [µg.m^{-3}]	**9.43**	**11.50**
nugget	51	55
sill	82	94
range [km]	320	300
RMSE [µg.m^{-3}]	**8.47**	**9.07**
realtive RMSE [%]	**7.3**	**8.1**
bias (MPE) [µg.m^{-3}]	**0.14**	**-0.04**

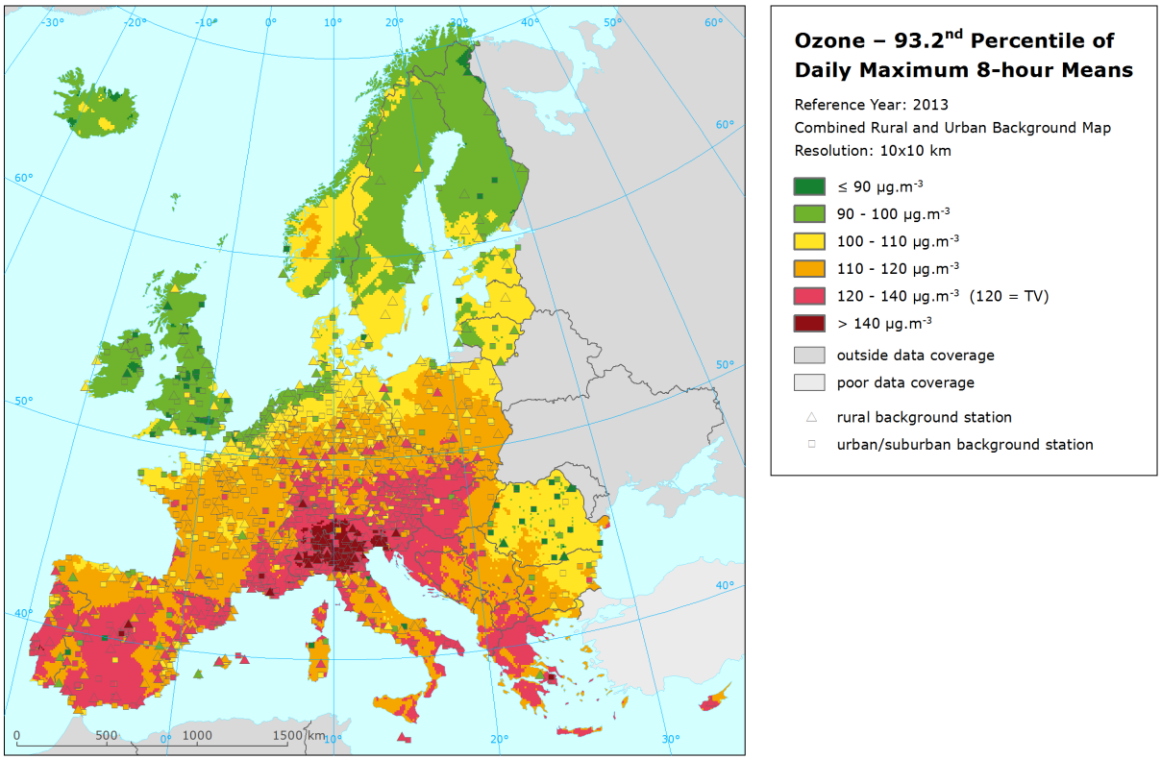

Figure A2.2 Combined rural and urban concentration map of ozone health indicator 93.2nd percentile of daily maximum 8-hour values for the year 2013. Its target value is 120 µg.m^{-3}. Resolution: 10x10 km. Units: µg.m^{-3}.

Table A2.4 gives the exposure table for the percentile parameter. This table improves Table 6.2.

Table A2.4 Population exposure and population weighted concentration – ozone, 93.2nd percentile of daily maximum 8-hour means for the year 2013.

Country		Population	O3, 93.2nd percentile of daily maximum 8-h means, exposed						Population-weighted conc.
			< TV				> TV		
		[inhbs . 1000]	< 90 µg.m^{-3}	90 - 100 µg.m^{-3}	100 - 110 µg.m^{-3}	110 - 120 µg.m^{-3}	120 - 140 µg.m^{-3}	> 140 µg.m^{-3}	[µg.m^{-3}]
Albania	AL	2 899				77.6	22.4		117.8
Andorra	AD	76					100		122.4
Austria	AT	8 452				29.1	70.9	0.0	121.4
Belgium	BE	11 162	0.1	23.3	73.0	3.6			102.5
Bosnia & Herzegovina	BA	3 836			8.1	78.9	13.0		116.2
Bulgaria	BG	7 285	6.2	19.8	59.0	14.9	0.1		103.5
Croatia	HR	4 262			4.0	53.2	42.5	0.3	119.4
Cyprus	CY	866			48.7	44.5	6.8		110.9
Czech Republic	CZ	10 516			14.7	81.4	3.8		113.9
Denmark	DK	5 603	0.8	81.0	18.0	0.2			96.7
Estonia	EE	1 320	1.3	78.6	20.1				97.6
Finland	FI	5 427	26.1	68.1	5.8				92.6
France (metropolitan)	FR	63 652		4.6	16.8	66.3	12.1	0.1	113.2
Germany	DE	80 524		5.1	48.5	42.1	4.3		110.2
Greece	GR	11 004			4.1	25.8	70.1		123.5
Hungary	HU	9 909		3.8	17.6	61.8	16.7		113.9
Iceland	IS	322	84.77	15.2	0.0				87.8
Ireland	IE	4 591	39.2	60.2	0.6				91.6
Italy	IT	59 685		1.1	14.3	35.1	26.2	23.3	126.1
Latvia	LV	2 024	2.4	66.1	31.5				98.0
Liechtenstein	LI	37					100.0		124.8
Lithuania	LT	2 972		74.6	25.4				98.8
Luxembourg	LU	537			72.9	27.1			109.5
Macedonia, FYROM of	MK	2 062			0.1	73.6	26.3		118.1
Malta	MT	421				98.2	1.8		112.0
Monaco	MC	38					100.0		122.5
Montenegro	ME	621			2.7	95.4	1.9		113.2
Netherlands	NL	16 780		58.2	40.3	1.5			99.5
Norway	NO	5 051	12.3	80.9	6.7	0.1			94.5
Poland	PL	38 063		4.6	53.1	41.8	0.5		109.4
Portugal (excl. Az., Mad.)	PT	9 977		9.2	28.0	33.0	29.5	0.2	113.5
Romania	RO	20 020	64.6	19.9	13.4	2.1			86.5
San Marino	SM	34			77.5	17.8	4.7		110.7
Serbia (incl. Kosovo*)	RS	8 997		2.8	37.4	57.5	2.3		110.5
Slovakia	SK	5 411			4.4	73.3	22.3		117.4
Slovenia	SI	2 059				21.0	78.5	0.5	125.5
Spain (excl. Canarias)	ES	44 623		0.8	25.8	47.0	26.5		114.9
Sweden	SE	9 556	9.0	80.5	10.3	0.1			94.8
Switzerland	CH	8 039				16.1	79.8	4.1	124.2
United Kingdom (& dep.)	UK	63 905	55.7	43.8	0.5	0.0	0.0	0.0	89.7
Total		**532 614**	**10.2**	**15.8**	**24.1**	**34.0**	**13.2**	**2.7**	**108.9**
			26.0		**58.1**		**15.9**		
EU-28		**500 603**	**10.6**	**16.0**	**24.8**	**33.4**	**12.4**	**2.8**	**108.6**
			26.6		**58.2**		**15.2**		
Kosovo*	KS	1 816	0.0	0.0	19.5	75.3	5.2	0.0	113.6
Serbia (excl. Kosovo*)	RS	7 182	0.0	3.4	41.7	53.2	1.6	0.0	109.7

*) under the UN Security Council Resolution 1244/99

Note1: Turkey is not included in the calculation due to lack of air quality data.
Note2: The percentage value "0.0" indicates an exposed population exists, but is small and estimated less than 0.05 %.
Empty cells mean: no population in exposure.

Annex 3 Analysis of maps using EMEP model Y-1 results with Y-2 emissions

A3.1 Introduction

According to current mapping procedure (Horálek et al., 2015) the interpolated maps for year Y-2 are available by end of November of year Y. Typically, the critical factor on its timing is the availability of the formal EMEP model results for year Y-2 by September of year Y only. This is systematically too late to deliver the interpolated AQ maps timely for inclusion in EEA's latest (i.e. year Y) Air Quality report. AQ measurement e-reporting data on year Y-2 is expected to be available in March of the year Y. If the modelling data would be available at that date for inclusion in the interpolated maps, then the Y-2 interpolated maps could be produced timely, i.e. June of year Y, for inclusion in the EEA AQ report in year Y.

Since 2014, the EMEP model has been available in two variants:

(1) EMEP modelling results for the year Y-2, based on both meteorology and emissions of Y-2;

(2) EMEP modelling results for Y-1, based on meteorology of Y-1 and emissions of Y-2.

Both variants are delivered simultaneously with the publishing of the annual EMEP Status Report in August, which describes both variants (EMEP, 2015).

The aim of this annex is to examine whether the quality of Y-1 interpolated maps using EMEP modelling results for Y-1 (based on both meteorological data and emissions data of year Y-1) is comparable to Y-1 interpolated maps using EMEP modelling results for Y-1 based on meteorology of Y-1, but with the one year older emissions of Y-2.

If the quality of the maps based on EMEP model with emissions of Y-2 prove to be as adequate, then these maps could be routinely produced with this variant of the EMEP model. It would facilitate a timely availability of interpolated maps against comparable quality compared to the maps based on the formal UNECE rubber stamped Y-2 EMEP model results.

The performance analysis is executed for PM_{10} annual average and for ozone indicator 26th highest daily maximum 8-hour value.

A3.2 EMEP model versions

The comparative performance analyses we execute on the year Y = 2014, which means that Y-1 = 2013 and Y - 2 = 2012.

The following two versions of EMEP model results for 2013 were used: the EMEP model output for 2013 based on meteorology of 2013 and emissions of 2013; the EMEP model output for 2013 based on meteorology of 2013 and emissions of 2012. For details, see EMEP (2015) and Section 3.2.

Figures A3.1 and A3.2 present the two modelling results.

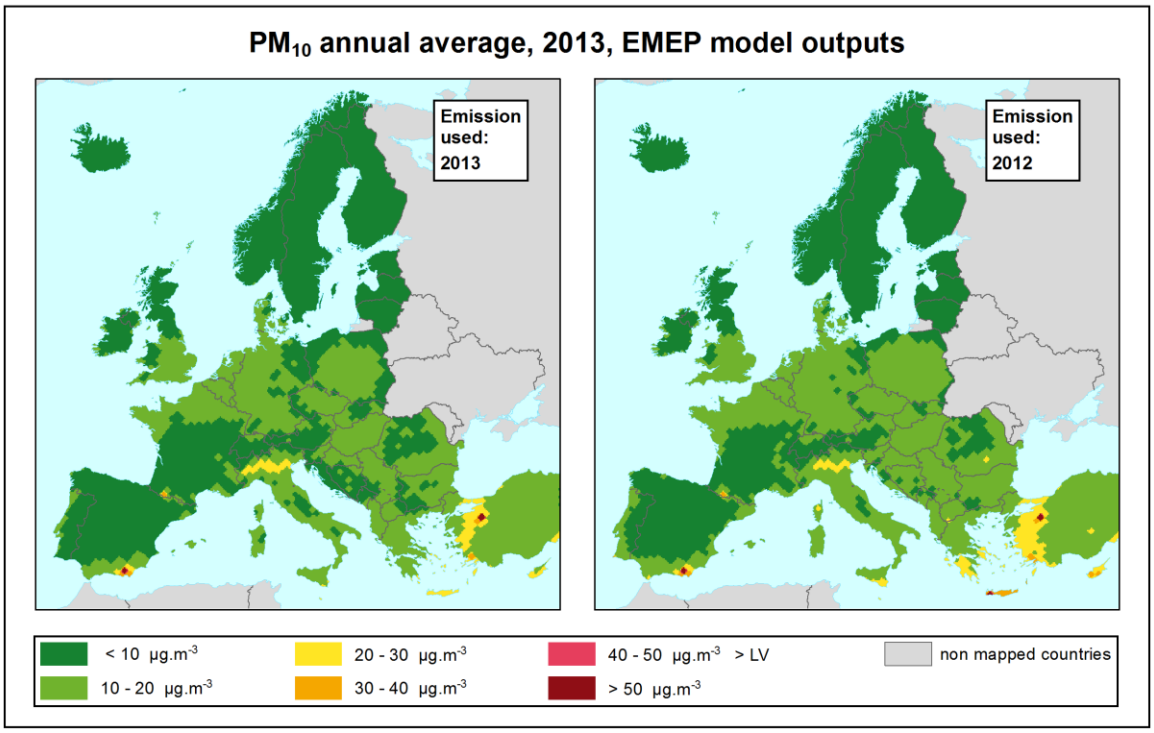

Figure A3.1 EMEP model 2013 output based on meteorology of 2013 and emissions of 2013 (left), and of emissions of 2012 (right), PM_{10} annual average, year 2013. Original model resolution: 50 x 50 km. Map resolution: 10 x 10 km. Units: µg.m^{-3}.

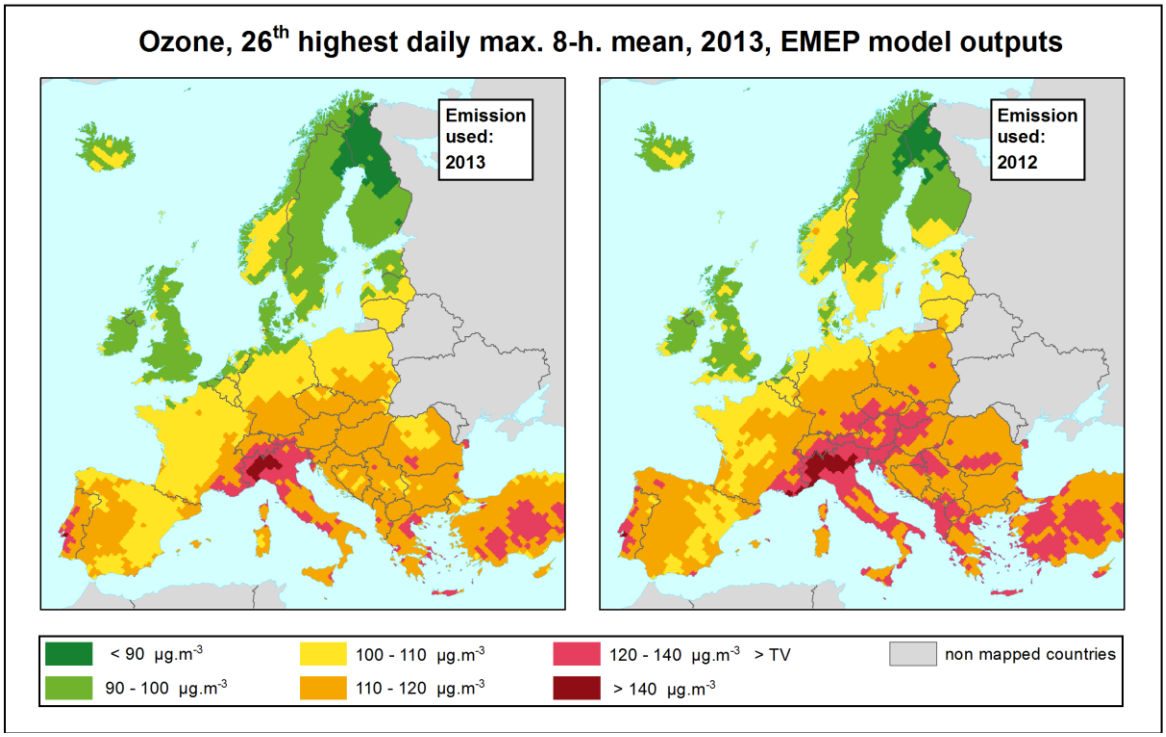

Figure A3.2 EMEP model 2013 output based on meteorology of 2013 and on emissions of 2013 (left), and emissions of 2012 (right), ozone indicator 26th highest daily maximum 8-hour value, year 2013. Original model resolution: 50 x 50 km. Map resolution: 10 x 10 km. Units: µg.m^{-3}.

Figure A3.3 presents the difference between the two variants of the model, for both PM_{10} and ozone.

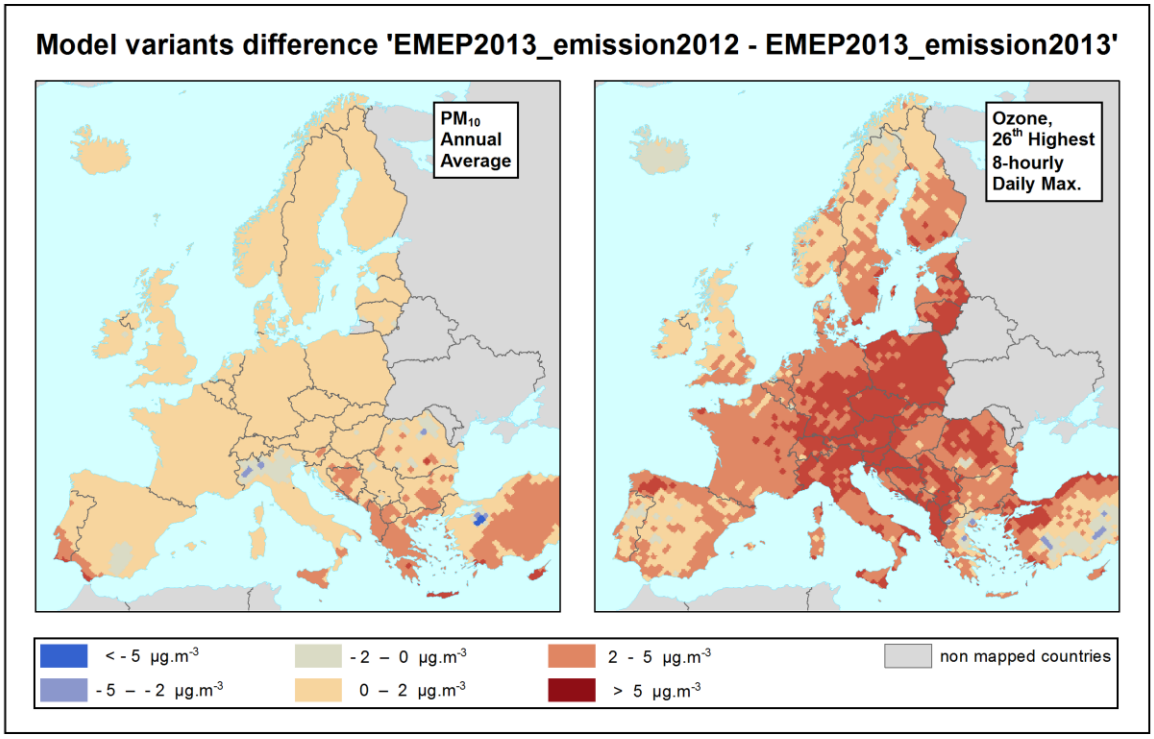

Figure A3.3 Difference between two variants of the EMEP 2013 model output, i.e. difference between the 2013 model results based on emissions of 2012 and on emissions of 2013, for PM_{10} annual average (left) and ozone indicator 26th highest daily maximum 8-hour value (right), year 2013. Original model resolution: 50 x 50 km. Map resolution: 10 x 10 km. Units: µg.m^{-3}.

As can be seen, the concentration level of the difference in the model results is somewhat different for ozone indicator. Nevertheless, the absolute concentration level of the model output does not play an important role in the mapping procedure, see Horálek et al. (2014). The spatial distribution of the model results is much more important.

A3.3 Comparison of the interpolated maps using different model versions

The interpolated maps have been constructed as usually, but using two different model versions, as described in Section A3.2.

A3.3.1 PM_{10} – annual average

Table A3.1 presents the parameters of the linear regression model and the residual kriging, for both the variants of the map. Comparing the results, one can see very similar parameters for both the mapping variants. Using the cross-validation results (see the yellow highlighted rows), one can directly compare the uncertainty of both interpolated maps. One can see they deliver at both cases almost identical results.

Table A3.1 Parameters of the linear regression models (Eq. 2.2) and of the ordinary kriging (OK) variograms (nugget, sill, range) – and their statistics – of PM_{10} indicator annual average for 2013 in rural and urban areas as used for the combined final map, for maps using two different variants of the EMEP model.

linear regr. model + OK of its residuals	Map using EMEP with 2013 meterology and 2013 emissions		Map using EMEP with 2013 meterology and 2012 emissions	
	rural areas	urban areas	rural areas	urban areas
	parameter value	parameter value	parameter value	parameter value
c (constant)	2.12	1.91	2.01	1.69
a1 (log. EMEP model 2013)	0.522	0.52	0.564	0.59
a2 (altitude GTOPO)	-0.00054		-0.00054	
a3 (wind speed 2013)	-0.102		-0.107	
a4 (s. solar radiation 2013)	*non signif.*		*non signif.*	
adjusted R^2	**0.53**	**0.25**	**0.53**	**0.29**
standard error [µg.m^{-3}]	**0.27**	**0.27**	**0.27**	**0.27**
nugget	0.037	0.014	0.035	0.013
sill	0.060	0.063	0.060	0.059
range [km]	480	740	480	690
RMSE [µg.m^{-3}]	**3.4**	**4.3**	**3.4**	**4.3**
Relative RMSE [%]	**19.6**	**17.3**	**19.8**	**17.3**
Bias (MPE) [µg.m^{-3}]	**0.0**	**0.0**	**0.0**	**0.0**

Table A3.2 presents the linear regression equation and R^2 from the cross-validation scatterplot. Again, one can see very similar results.

Table A3.2 Linear regression equation and coefficient of determination R^2 from the scatter plots of the predicted point values based on cross-validation versus the measured point values for PM_{10} indicator annual average for rural and urban areas of 2013 for two variant of the mapping results, i.e. using 2013 or 2012 emission..

	rural areas		urban areas	
	equation	R^2	equation	R^2
EMEP model with 2013 emission used in mapping	y = 0.669x + 5.7	0.699	y = 0.754x + 6.1	0.743
EMEP model with 2012 emission used in mapping	y = 0.674x + 5.6	0.693	y = 0.759x + 5.9	0.742

Figure A3.4 shows the final mapping results, for both variants. The geographical distribution of the concentrations seems very similar, with few differences in the places with the low density of the measurement (e.g. some limited areas in Balkan).

Then, the difference map was prepared, in order to better visualize the differences of both the maps, see Figure A3.5.

Next to the maps, the exposure table was prepared, see Table A3.3. This table can be directly compared with the Table 4.2. Doing so, one can conclude that for the most of the countries, the difference is smaller than 0.5 µg.m^{-3}. For three countries (Greece, FYR of Macedonia and Montenegro), the difference is in the range of 0.5 – 1 µg.m^{-3}, two countries (Cyprus and Bosnia-Herzegovina) show the difference in the range of 1 – 2 µg.m^{-3}, and two countries (Albania and Malta) have the difference in the range of 2 – 4 µg.m^{-3}. In all of these seven countries, there is a small density of the monitoring stations.

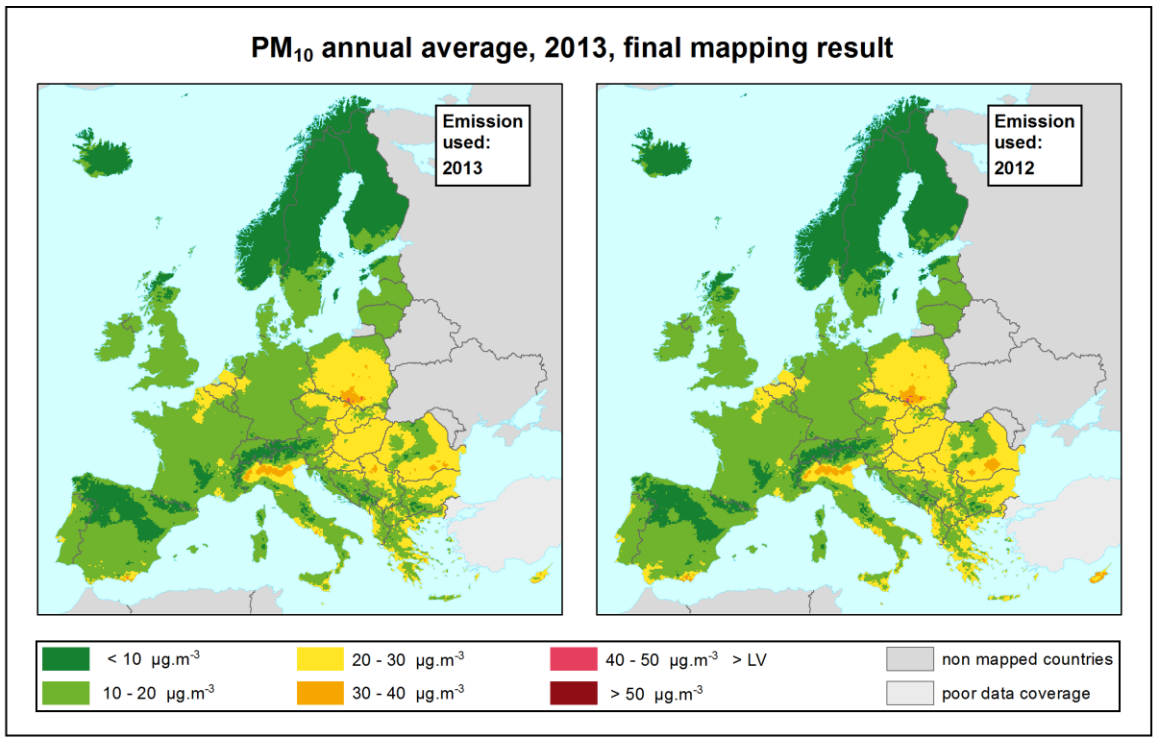

Figure A3.4 Combined rural and urban concentration map of PM_{10} – annual average, year 2013. Spatial interpolated concentration field using EMEP model 2013 output based on emissions of 2013 (left) and on emissions of 2012 (right), PM_{10} annual average, year 2013. Resolution: 10 x 10 km. Units: $\mu g.m^{-3}$.

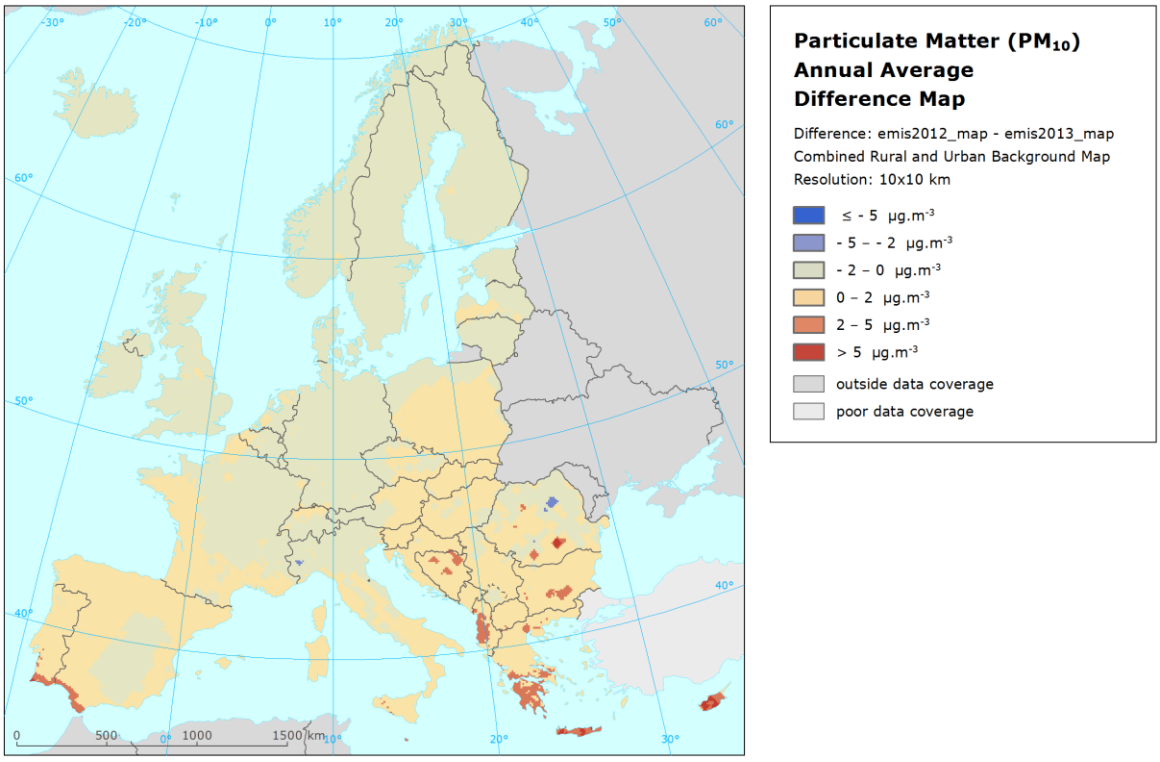

Figure A3.5 Difference between the interpolated mapping results using EMEP model output based on emissions of 2012 and emissions of 2013 – PM_{10}, annual average. Resolution: 10x10 km. Units: $\mu g.m^{-3}$.

Table A3.3 Population exposure and population-weighted concentration – PM_{10}, annual average, year 2013. Spatial interpolated concentration field using EMEP model 2013 output based on emissions of 2012. Resolution: 1x1 km.

Country		Population	PM_{10} annual average, exposed population [%]						Population weighted conc. [µg.m^{-3}]
			< LV				> LV		
		[inhbs . 1000]	< 10 µg.m^{-3}	10 - 20 µg.m^{-3}	20 - 30 µg.m^{-3}	30 - 40 µg.m^{-3}	40 - 45 µg.m^{-3}	> 45 µg.m^{-3}	
Albania	AL	2 899	0.0	5.8	16.5	72.7	5.1		34.7
Andorra	AD	76	0.7	1.2	98.2				24.6
Austria	AT	8 452	1.6	39.7	58.7				20.2
Belgium	BE	11 162		6.6	93.4				23.6
Bosnia & Herzegovina	BA	3 836	0.1	15.0	70.5	14.4			24.9
Bulgaria	BG	7 285	0.0	3.3	16.6	44.9	28.0	7.2	36.7
Croatia	HR	4 262	0.0	9.9	89.8	0.3			23.7
Cyprus	CY	866			5.8	82.3	11.9		37.4
Czech Republic	CZ	10 516		8.9	79.6	8.4	3.1		25.6
Denmark	DK	5 603	0.1	99.7	0.3				16.2
Estonia	EE	1 320	6.2	93.8					13.4
Finland	FI	5 427	42.2	57.8					10.4
France (metropolitan)	FR	63 652	0.4	43.8	55.6	0.2			20.7
Germany	DE	80 524	0.0	70.4	29.6				19.0
Greece	GR	11 004		1.9	12.9	65.8	16.9	2.5	35.2
Hungary	HU	9 909		0.1	98.0	2.0			25.3
Iceland	IS	322	15.6	84.4					11.5
Ireland	IE	4 591	0.1	99.6	0.3				14.9
Italy	IT	59 685	0.3	11.3	55.6	32.9			27.0
Latvia	LV	2 024	0.0	38.6	61.4				19.8
Liechtenstein	LI	37	1.4	98.6					15.2
Lithuania	LT	2 972		30.5	69.5				20.3
Luxembourg	LU	537		100.0					18.7
Macedonia, FYROM of	MK	2 062	0.0	1.7	3.8	11.0	48.3	35.2	45.2
Malta	MT	421			1.9	21	77.0		39.5
Monaco	MC	38			100.0				23.1
Montenegro	ME	621	1.4	16.0	41.6	40.9			28.0
Netherlands	NL	16 780		28.7	71.3				20.7
Norway	NO	5 051	29.2	51.9	18.9				13.8
Poland	PL	38 063		6.2	45.4	34.8	13.5		30.5
Portugal (excl. Az., Mad.)	PT	9 977	0.5	41.8	57.7				20.5
Romania	RO	20 020	0.0	12.5	65.8	21.7			25.9
San Marino	SM	34		13.1	86.9				22.1
Serbia (incl. Kosovo*)	RS	8 997	0.0	4.2	36.2	47.0	12.6	0.1	31.4
Slovakia	SK	5 411		1.5	78.5	20.0	0.0		26.9
Slovenia	SI	2 059	0.0	16.4	83.6				23.2
Spain (excl. Canarias)	ES	44 623	1.4	60.1	37.1	1.4	0.1		19.1
Sweden	SE	9 556	16.6	83.4					13.0
Switzerland	CH	8 039	2.2	72.2	25.6				18.3
United Kingdom (& dep.)	UK	63 905	0.1	96.7	3.2				17.0
Total		**532 614**	**1.3**	**44.0**	**41.0**	**11.1**	**2.3**	**0.3**	**22.3**
			45.3				**2.6**		
EU-28		**500 603**	**1.0**	**44.8**	**41.6**	**10.3**	**2.0**	**0.2**	**22.1**
			45.9				**2.1**		
Kosovo*	KS	1 816	0.0	5.1	15.1	20.4	59.0	0.4	37.9
Serbia (excl. Kosovo*)	RS	7 182	0.0	4.0	41.3	53.5	1.2	0.0	29.9

*) under the UN Security Council Resolution 1244/99

Note1: Turkey is not included in the calculation due to lacking air quality data.
Note2: The percentage value "0.0" indicates an exposed population exists, but is small and estimated less than 0.05 %. Empty cells mean: no population in exposure.

A3.3.2. Ozone – 26th highest daily 8-hourly maximum

Like at PM_{10}, the parameters of the linear regression model and the residual kriging are presented also for the ozone indicator map, see Table A3.4. In most cases, the parameter values at both model variants are very similar, with few exceptions. The comparison of uncertainty results of the maps, each using one of the model variants and separately produced for urban and rural areas do show almost identical results.

Table A3.4 Parameters of the linear regression models (Eq. 2.2) and of the ordinary kriging (OK) variograms (nugget, sill, range) – and their statistics – of ozone indicator 26th highest daily maximum 8-hour mean for 2013 in rural and urban areas as used for the combined final map, for maps using two variants of the EMEP model.

linear regr. model + OK of its residuals	Map using EMEP with 2013meterology and 2013 emissions		Map using EMEP with 2013 meterology and 2012 emissions	
	rural areas	urban areas	rural areas	urban areas
	parameter value	parameter value	parameter value	parameter value
c (constant)	2.4	35.0	5.2	34.45
a1 (log. EMEP model 2013)	0.97	0.76	0.87	0.70
a2 (altitude GTOPO)	0.0038		0.0036	
a3 (wind speed 2013)		-2.73		-2.45
a4 (s. solar radiation 2013)	0.49	0.10	0.85	0.43
adjusted R^2	**0.58**	**0.48**	**0.60**	**0.49**
standard error [µg.m^{-3}]	**9.4**	**11.5**	**9.1**	**11.5**
nugget	50	54	48	54
sill	81	93	77	91
range [km]	320	310	320	310
RMSE [µg.m^{-3}]	**8.3**	**9.0**	**8.3**	**8.9**
Relative RMSE [%]	**7.2**	**8.0**	**7.2**	**8.0**
Bias (MPE) [µg.m^{-3}]	**0.1**	**0.0**	**0.1**	**0.0**

Almost identical results are also visible for the parameter values of the cross-validation scatter plot, see Table A3.5.

Table A3.5 Linear regression equation and coefficient of determination R^2 from the scatter plots of the predicted point values based on cross-validation versus the measured point values for PM_{10} indicator annual average for rural and urban areas of 2013 for two variant of the mapping results, i.e. using 2013 or 2012 emissions.

	rural areas		urban areas	
	equation	R^2	equation	R^2
EMEP model with 2013 emission used in mapping	y = 0.691x + 36.1	0.668	y = 0.698x + 33.8	0.683
EMEP model with 2012 emission used in mapping	y = 0.694x + 35.6	0.671	y = 0.698x + 33.8	0.684

Figure A3.6 shows the final mapping results, for both variants. One can see a quite similar geographical distribution of the concentration levels over Europe. Next to this, one can observe that the concentrations are of a similar level of magnitude in the two maps, with no regard to the different level of the concentration levels of the two variants of the EMEP model, see Figure A3.2. Again, it is confirmed that the mapping methodology is driven primarily by the observations.

Next to this, we present the difference map in Figure A3.7. As one can observe, the main differences occur in areas lacking stations.

Finally, the exposure table was prepared, see Table A3.6. This table can be directly compared with the Table 6.2.

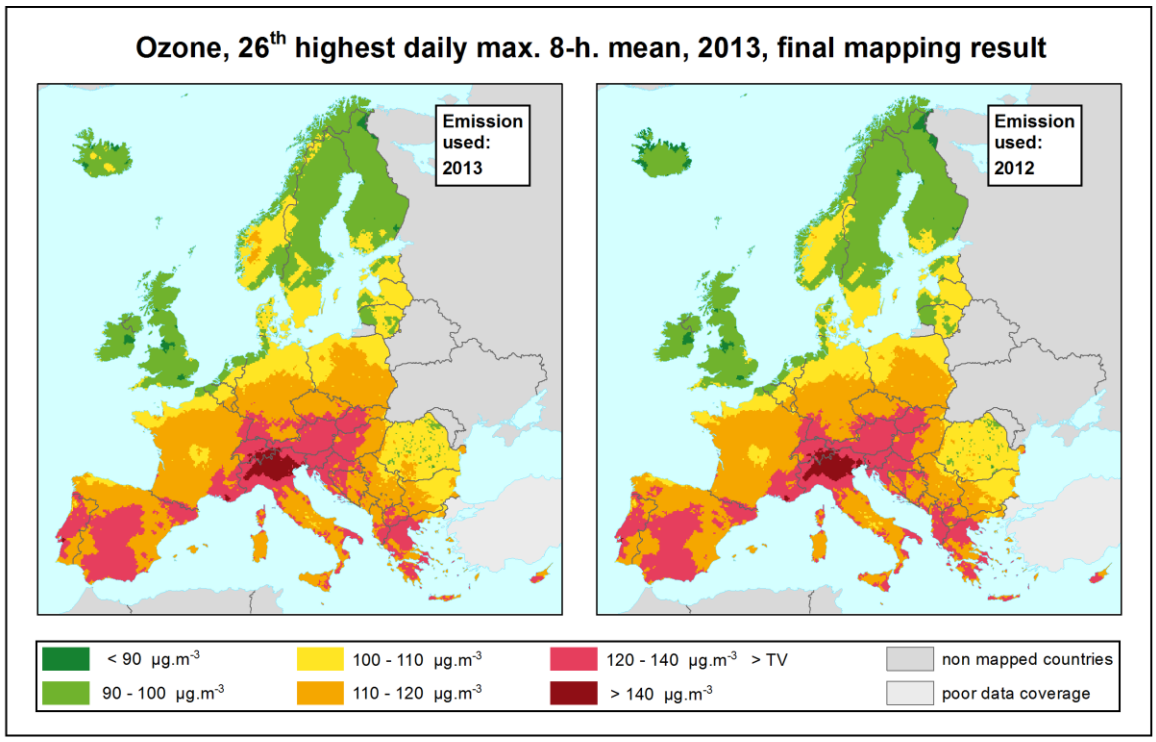

Figure A3.6 Combined rural and urban interpolated concentration map of ozone indicator 26th highest daily maximum 8-hour value, year 2013. Spatial interpolated concentration field using EMEP model output based on emissions of 2013 (left) and on emissions of 2012 (right). Resolution: 10 x 10 km. Units: µg.m-3.

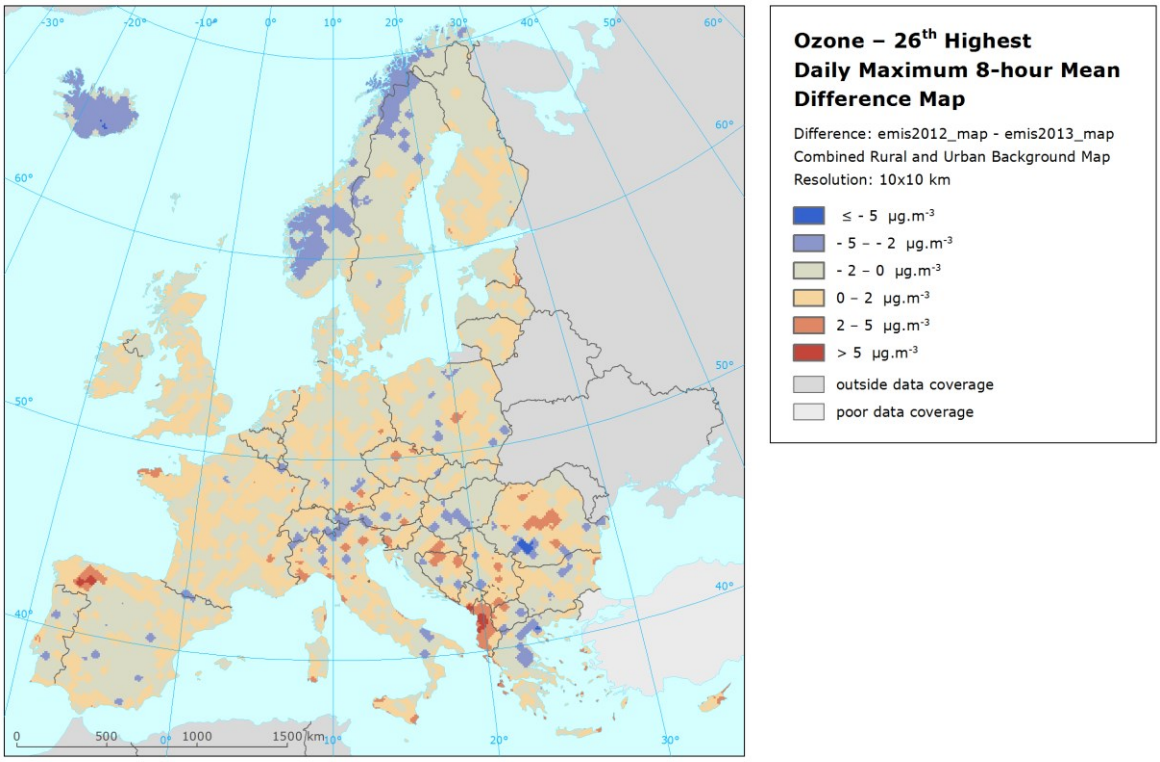

Figure A3.7 Difference between the interpolated mapping results using EMEP 2013 model output based on emissions of 2012 and on emissions of 2013 – ozone, 26th highest daily maximum 8-hour value. Resolution: 10x10 km. Units: µg.m-3.

Table A3.6 Population exposure and population weighted concentration – ozone, 26th highest daily maximum 8-hour mean for the year 2013. Spatial interpolated concentration field using EMEP model output based on emissions of 2012.

Country		Population	Ozone, 26th highest dmax. 8-h, exposed population [%]						Population-weighted conc.
			< TV				> TV		
		[inhbs . 1000]	< 90 µg.m^{-3}	90 - 100 µg.m^{-3}	100 - 110 µg.m^{-3}	110 - 120 µg.m^{-3}	120 - 140 µg.m^{-3}	> 140 µg.m^{-3}	[µg.m^{-3}]
Albania	AL	2 899				29.6	70.4		121.4
Andorra	AD	76					100		120.7
Austria	AT	8 452				28.7	71.3	0.0	120.9
Belgium	BE	11 162	0.1	24.0	73.6	2.4			101.7
Bosnia & Herzegovina	BA	3 836			10.7	71.4	17.9		116.3
Bulgaria	BG	7 285	6.2	21.0	60.8	12.0	0.0		103.0
Croatia	HR	4 262			4.0	63.2	32.7	0.0	118.8
Cyprus	CY	866			24.9	68.4	6.7		112.5
Czech Republic	CZ	10 516			19.7	77.2	3.1		113.6
Denmark	DK	5 603	0.8	84.3	14.7	0.2			96.3
Estonia	EE	1 320	2.0	80.8	17.2				97.0
Finland	FI	5 427	29.5	64.8	5.8				92.1
France (metropolitan)	FR	63 652		5.4	22.7	59.9	11.9	0.0	112.7
Germany	DE	80 524		4.9	51.3	39.5	4.2		109.9
Greece	GR	11 004			2.9	29.3	67.8		122.8
Hungary	HU	9 909	0.0	5.0	19.4	63.1	12.5		112.6
Iceland	IS	322	89.71	10.3					85.4
Ireland	IE	4 591	43.8	55.7	0.5				91.4
Italy	IT	59 685		1.2	16.3	34.7	25.5	22.3	125.3
Latvia	LV	2 024	7.0	72.6	20.5				97.1
Liechtenstein	LI	37					100.0		123.9
Lithuania	LT	2 972		84.9	15.1				98.0
Luxembourg	LU	537			86.3	13.7			107.3
Macedonia, FYROM of	MK	2 062			3.8	67.3	28.9		118.0
Malta	MT	421				98.2	1.8		112.1
Monaco	MC	38					100.0		121.9
Montenegro	ME	621			5.3	88.6	6.0		114.3
Netherlands	NL	16 780		59.6	40.3	0.1			98.8
Norway	NO	5 051	15.7	80.0	4.3				93.3
Poland	PL	38 063		5.6	56.2	38.2	0.0		108.6
Portugal (excl. Az., Mad.)	PT	9 977		11.4	28.2	41.6	18.7	0.2	112.4
Romania	RO	20 020	68.9	17.0	13.3	0.8			85.3
San Marino	SM	34			26.8	67.9	5.3		111.6
Serbia (incl. Kosovo*)	RS	8 997		2.9	41.8	53.2	2.0		110.1
Slovakia	SK	5 411			6.5	75.6	17.9		116.4
Slovenia	SI	2 059				21.8	78.0	0.2	125.1
Spain (excl. Canarias)	ES	44 623		0.7	27.5	46.3	25.4		114.4
Sweden	SE	9 556	10.1	80.7	9.1	0.1			94.3
Switzerland	CH	8 039				20.3	75.9	3.9	124.0
United Kingdom (& dep.)	UK	63 905	61.4	38.1	0.5	0.0			89.3
Total		**532 614**	**11.1**	**15.4**	**25.9**	**32.3**	**12.8**	**2.6**	**108.3**
			26.5		**58.1**		**15.3**		
EU-28		**500 603**	**11.6**	**15.5**	**26.6**	**31.9**	**11.6**	**2.7**	**108.0**
			27.1		**58.6**		**14.3**		
Kosovo*	KS	1 816			19.4	73.7	6.8		113.9
Serbia (excl. Kosovo*)	RS	7 182		3.7	47.3	48.3	0.8		109.1

*) under the UN Security Council Resolution 1244/99

Note1: Turkey is not included in the calculation due to lack of air quality data.
Note2: The percentage value "0.0" indicates an exposed population exists, but is small and estimated less than 0.05 %. Empty cells mean: no population in exposure.

If compared Tables 6.2 and A3.6, one can conclude that, the difference is smaller than 1 $\mu g.m^{-3}$. For five countries (Iceland, Luxembourg, Andorra, San Marino and Montenegro), the difference is in the range of 1– 2 $\mu g.m^{-3}$, two countries (Cyprus and Albania) show the difference in the range of 1 – 2 $\mu g.m^{-3}$, and two countries (Albania and Malta) has the difference in the range of 2 – 4 $\mu g.m^{-3}$. In all of these seven countries, there is a small density of the monitoring stations.

A3.4 Conclusion

We constructed for both the PM_{10} annual average and the ozone 26th highest daily maximum 8-hour value a difference map of the interpolated maps using different EMEP model results. The first interpolated map is based on EMEP Y-1 modelling results using both meteorological data and emission data of Y-1, where Y-1 = 2013. The second map is based on EMEP Y-1 modelling results using again meteorological data of Y-1, but emission data Y-2 (i.e. the emissions of its previous year, being Y-2 = 2012).

The interpolated mapping results for 2013 using the EMEP model with 2013 or using 2012 emissions are very similar. The same is true also for the exposure tables. Therefore, we recommend to use in the future the EMEP model for Y-1 based on meteorological data of Y-1 with emissions data of Y-2, in order to enable the earlier delivery of the maps, such that they can be included in the state of the art EEA air pollution reports.

It should be noted that the MSC-W team prepares an improvement of the EMEP model: next to the model in 50x50 km grid resolution, the model in a 10°x10° (i.e. cca 10x10 km) grid resolution is presented, see EMEP (2015).

The increased resolution is very desirable for the mapping procedure. It would be very useful if the EMEP model in 10°x10° resolution is calculated in the variant "Y-1 with the emission of Y-2" as well. According to the EMEP team, this has not been decided yet.